ELECTRO–THERMAL SIMULATION OF MOSA AND DERIVATION OF THERMAL EQUIVALENT TEST SECTIONS

by

LIYING HUANG

A Thesis
Submitted to the Faculty of Graduate Studies
in Partial Fulfillment of the Requirements
for the Degree of

Master of Science

Department of Electrical and Computer Engineering
University of Manitoba
Winnipeg, Manitoba

ISBN 0-315-81721-6

Name ____________________

Dissertation Abstracts International is arranged by broad, general subject categories. Please select the one subject which most nearly describes the content of your dissertation. Enter the corresponding four-digit code in the spaces provided.

ELECTRICAL ENGINEERING — 0544 — U·M·I

SUBJECT TERM — SUBJECT CODE

Subject Categories

THE HUMANITIES AND SOCIAL SCIENCES

COMMUNICATIONS AND THE ARTS
Architecture 0729
Art History 0377
Cinema 0900
Dance 0378
Fine Arts 0357
Information Science 0723
Journalism 0391
Library Science 0399
Mass Communications 0708
Music 0413
Speech Communication 0459
Theater 0465

EDUCATION
General 0515
Administration 0514
Adult and Continuing 0516
Agricultural 0517
Art 0273
Bilingual and Multicultural 0282
Business 0688
Community College 0275
Curriculum and Instruction 0727
Early Childhood 0518
Elementary 0524
Finance 0277
Guidance and Counseling 0519
Health 0680
Higher 0745
History of 0520
Home Economics 0278
Industrial 0521
Language and Literature 0279
Mathematics 0280
Music 0522
Philosophy of 0998
Physical 0523
Psychology 0525
Reading 0535
Religious 0527
Sciences 0714
Secondary 0533
Social Sciences 0534
Sociology of 0340
Special 0529
Teacher Training 0530
Technology 0710
Tests and Measurements 0288
Vocational 0747

LANGUAGE, LITERATURE AND LINGUISTICS
Language
- General 0679
- Ancient 0289
- Linguistics 0290
- Modern 0291

Literature
- General 0401
- Classical 0294
- Comparative 0295
- Medieval 0297
- Modern 0298
- African 0316
- American 0591
- Asian 0305
- Canadian (English) 0352
- Canadian (French) 0355
- English 0593
- Germanic 0311
- Latin American 0312
- Middle Eastern 0315
- Romance 0313
- Slavic and East European 0314

PHILOSOPHY, RELIGION AND THEOLOGY
Philosophy 0422
Religion
- General 0318
- Biblical Studies 0321
- Clergy 0319
- History of 0320
- Philosophy of 0322

Theology 0469

SOCIAL SCIENCES
American Studies 0323
Anthropology
- Archaeology 0324
- Cultural 0326
- Physical 0327

Business Administration
- General 0310
- Accounting 0272
- Banking 0770
- Management 0454
- Marketing 0338

Canadian Studies 0385
Economics
- General 0501
- Agricultural 0503
- Commerce-Business 0505
- Finance 0508
- History 0509
- Labor 0510
- Theory 0511

Folklore 0358
Geography 0366
Gerontology 0351
History
- General 0578
- Ancient 0579
- Medieval 0581
- Modern 0582
- Black 0328
- African 0331
- Asia, Australia and Oceania 0332
- Canadian 0334
- European 0335
- Latin American 0336
- Middle Eastern 0333
- United States 0337

History of Science 0585
Law 0398
Political Science
- General 0615
- International Law and Relations 0616
- Public Administration 0617

Recreation 0814
Social Work 0452
Sociology
- General 0626
- Criminology and Penology 0627
- Demography 0938
- Ethnic and Racial Studies 0631
- Individual and Family Studies 0628
- Industrial and Labor Relations 0629
- Public and Social Welfare 0630
- Social Structure and Development 0700
- Theory and Methods 0344

Transportation 0709
Urban and Regional Planning 0999
Women's Studies 0453

THE SCIENCES AND ENGINEERING

BIOLOGICAL SCIENCES
Agriculture
- General 0473
- Agronomy 0285
- Animal Culture and Nutrition 0475
- Animal Pathology 0476
- Food Science and Technology 0359
- Forestry and Wildlife 0478
- Plant Culture 0479
- Plant Pathology 0480
- Plant Physiology 0817
- Range Management 0777
- Wood Technology 0746

Biology
- General 0306
- Anatomy 0287
- Biostatistics 0308
- Botany 0309
- Cell 0379
- Ecology 0329
- Entomology 0353
- Genetics 0369
- Limnology 0793
- Microbiology 0410
- Molecular 0307
- Neuroscience 0317
- Oceanography 0416
- Physiology 0433
- Radiation 0821
- Veterinary Science 0778
- Zoology 0472

Biophysics
- General 0786
- Medical 0760

EARTH SCIENCES
Biogeochemistry 0425
Geochemistry 0996
Geodesy 0370
Geology 0372
Geophysics 0373
Hydrology 0388
Mineralogy 0411
Paleobotany 0345
Paleoecology 0426
Paleontology 0418
Paleozoology 0985
Palynology 0427
Physical Geography 0368
Physical Oceanography 0415

HEALTH AND ENVIRONMENTAL SCIENCES
Environmental Sciences 0768
Health Sciences
- General 0566
- Audiology 0300
- Chemotherapy 0992
- Dentistry 0567
- Education 0350
- Hospital Management 0769
- Human Development 0758
- Immunology 0982
- Medicine and Surgery 0564
- Mental Health 0347
- Nursing 0569
- Nutrition 0570
- Obstetrics and Gynecology 0380
- Occupational Health and Therapy 0354
- Ophthalmology 0381
- Pathology 0571
- Pharmacology 0419
- Pharmacy 0572
- Physical Therapy 0382
- Public Health 0573
- Radiology 0574
- Recreation 0575
- Speech Pathology 0460
- Toxicology 0383

Home Economics 0386

PHYSICAL SCIENCES
Pure Sciences

Chemistry
- General 0485
- Agricultural 0749
- Analytical 0486
- Biochemistry 0487
- Inorganic 0488
- Nuclear 0738
- Organic 0490
- Pharmaceutical 0491
- Physical 0494
- Polymer 0495
- Radiation 0754

Mathematics 0405
Physics
- General 0605
- Acoustics 0986
- Astronomy and Astrophysics 0606
- Atmospheric Science 0608
- Atomic 0748
- Electronics and Electricity 0607
- Elementary Particles and High Energy 0798
- Fluid and Plasma 0759
- Molecular 0609
- Nuclear 0610
- Optics 0752
- Radiation 0756
- Solid State 0611

Statistics 0463

Applied Sciences

Applied Mechanics 0346
Computer Science 0984

Engineering
- General 0537
- Aerospace 0538
- Agricultural 0539
- Automotive 0540
- Biomedical 0541
- Chemical 0542
- Civil 0543
- X Electronics and Electrical 0544
- Heat and Thermodynamics 0348
- Hydraulic 0545
- Industrial 0546
- Marine 0547
- Materials Science 0794
- Mechanical 0548
- Metallurgy 0743
- Mining 0551
- Nuclear 0552
- Packaging 0549
- Petroleum 0765
- Sanitary and Municipal 0554
- System Science 0790

Geotechnology 0428
Operations Research 0796
Plastics Technology 0795
Textile Technology 0994

PSYCHOLOGY
General 0621
Behavioral 0384
Clinical 0622
Developmental 0620
Experimental 0623
Industrial 0624
Personality 0625
Physiological 0989
Psychobiology 0349
Psychometrics 0632
Social 0451

Nom ______________________________

Dissertation Abstracts International est organisé en catégories de sujets. Veuillez s.v.p. choisir le sujet qui décrit le mieux votre thèse et inscrivez le code numérique approprié dans l'espace réservé ci-dessous.

______________________________ [ ][ ][ ][ ] U·M·I

SUJET — CODE DE SUJET

Catégories par sujets

HUMANITÉS ET SCIENCES SOCIALES

COMMUNICATIONS ET LES ARTS

Architecture 0729
Beaux-arts 0357
Bibliothéconomie 0399
Cinéma 0900
Communication verbale 0459
Communications 0708
Danse 0378
Histoire de l'art 0377
Journalisme 0391
Musique 0413
Sciences de l'information 0723
Théâtre 0465

ÉDUCATION

Généralités 515
Administration 0514
Art 0273
Collèges communautaires 0275
Commerce 0688
Économie domestique 0278
Éducation permanente 0516
Éducation préscolaire 0518
Éducation sanitaire 0680
Enseignement agricole 0517
Enseignement bilingue et multiculturel 0282
Enseignement industriel 0521
Enseignement primaire. 0524
Enseignement professionnel 0747
Enseignement religieux 0527
Enseignement secondaire 0533
Enseignement spécial 0529
Enseignement supérieur 0745
Évaluation 0288
Finances 0277
Formation des enseignants 0530
Histoire de l'éducation 0520
Langues et littérature 0279
Lecture 0535
Mathématiques 0280
Musique 0522
Orientation et consultation 0519
Philosophie de l'éducation 0998
Physique 0523
Programmes d'études et enseignement 0727
Psychologie 0525
Sciences 0714
Sciences sociales 0534
Sociologie de l'éducation 0340
Technologie 0710

LANGUE, LITTÉRATURE ET LINGUISTIQUE

Langues
- Généralités 0679
- Anciennes 0289
- Linguistique 0290
- Modernes 0291

Littérature
- Généralités 0401
- Anciennes 0294
- Comparée 0295
- Mediévale 0297
- Moderne 0298
- Africaine 0316
- Américaine 0591
- Anglaise 0593
- Asiatique 0305
- Canadienne (Anglaise) 0352
- Canadienne (Française) 0355
- Germanique 0311
- Latino-américaine 0312
- Moyen-orientale 0315
- Romane 0313
- Slave et est-européenne 0314

PHILOSOPHIE, RELIGION ET THÉOLOGIE

Philosophie 0422
Religion
- Généralités 0318
- Clergé 0319
- Études bibliques 0321
- Histoire des religions 0320
- Philosophie de la religion 0322

Théologie 0469

SCIENCES SOCIALES

Anthropologie
- Archéologie 0324
- Culturelle 0326
- Physique 0327

Droit 0398
Économie
- Généralités 0501
- Commerce-Affaires 0505
- Économie agricole 0503
- Économie du travail 0510
- Finances 0508
- Histoire 0509
- Théorie 0511

Études américaines 0323
Études canadiennes 0385
Études féministes 0453
Folklore 0358
Géographie 0366
Gérontologie 0351
Gestion des affaires
- Généralités 0310
- Administration 0454
- Banques 0770
- Comptabilité 0272
- Marketing 0338

Histoire
- Histoire générale 0578
- Ancienne 0579
- Médiévale 0581
- Moderne 0582
- Histoire des noirs 0328
- Africaine 0331
- Canadienne 0334
- États-Unis 0337
- Européenne 0335
- Moyen-orientale 0333
- Latino-américaine 0336
- Asie, Australie et Océanie 0332

Histoire des sciences 0585
Loisirs 0814
Planification urbaine et régionale 0999
Science politique
- Généralités 0615
- Administration publique 0617
- Droit et relations internationales 0616

Sociologie
- Généralités 0626
- Aide et bien-àtre social 0630
- Criminologie et établissements pénitentiaires 0627
- Démographie 0938
- Études de l' individu et de la famille 0628
- Études des relations interethniques et des relations raciales 0631
- Structure et développement social 0700
- Théorie et méthodes 0344
- Travail et relations industrielles 0629

Transports 0709
Travail social 0452

SCIENCES ET INGÉNIERIE

SCIENCES BIOLOGIQUES

Agriculture
- Généralités 0473
- Agronomie. 0285
- Alimentation et technologie alimentaire 0359
- Culture 0479
- Élevage et alimentation 0475
- Exploitation des péturages 0777
- Pathologie animale 0476
- Pathologie végétale 0480
- Physiologie végétale 0817
- Sylviculture et faune 0478
- Technologie du bois 0746

Biologie
- Généralités 0306
- Anatomie 0287
- Biologie (Statistiques) 0308
- Biologie moléculaire 0307
- Botanique 0309
- Çellule 0379
- Écologie 0329
- Entomologie 0353
- Génétique 0369
- Limnologie 0793
- Microbiologie 0410
- Neurologie 0317
- Océanographie 0416
- Physiologie 0433
- Radiation 0821
- Science vétérinaire 0778
- Zoologie 0472

Biophysique
- Généralités 0786
- Medicale 0760

SCIENCES DE LA TERRE

Biogéochimie 0425
Géochimie 0996
Géodésie 0370
Géographie physique 0368
Géologie 0372
Géophysique 0373
Hydrologie 0388
Minéralogie 0411
Océanographie physique 0415
Paléobotanique 0345
Paléoécologie 0426
Paléontologie 0418
Paléozoologie 0985
Palynologie 0427

SCIENCES DE LA SANTÉ ET DE L'ENVIRONNEMENT

Économie domestique 0386
Sciences de l'environnement 0768
Sciences de la santé
- Généralités 0566
- Administration des hipitaux 0769
- Alimentation et nutrition 0570
- Audiologie 0300
- Chimiothérapie 0992
- Dentisterie 0567
- Développement humain 0758
- Enseignement 0350
- Immunologie 0982
- Loisirs 0575
- Médecine du travail et thérapie 0354
- Médecine et chirurgie 0564
- Obstétrique et gynécologie 0380
- Ophtalmologie 0381
- Orthophonie 0460
- Pathologie 0571
- Pharmacie 0572
- Pharmacologie 0419
- Physiothérapie 0382
- Radiologie 0574
- Santé mentale 0347
- Santé publique 0573
- Soins infirmiers 0569
- Toxicologie 0383

SCIENCES PHYSIQUES

Sciences Pures

Chimie
- Genéralités 0485
- Biochimie 487
- Chimie agricole 0749
- Chimie analytique 0486
- Chimie minérale 0488
- Chimie nucléaire 0738
- Chimie organique 0490
- Chimie pharmaceutique 0491
- Physique 0494
- PolymÇres 0495
- Radiation 0754

Mathématiques 0405
Physique
- Généralités 0605
- Acoustique 0986
- Astronomie et astrophysique 0606
- Electronique et électricité 0607
- Fluides et plasma 0759
- Météorologie 0608
- Optique 0752
- Particules (Physique nucléaire) 0798
- Physique atomique 0748
- Physique de l'état solide 0611
- Physique moléculaire 0609
- Physique nucléaire 0610
- Radiation 0756

Statistiques 0463

Sciences Appliqués Et Technologie

Informatique 0984
Ingénierie
- Généralités 0537
- Agricole 0539
- Automobile 0540
- Biomédicale 0541
- Chaleur et ther modynamique 0348
- Conditionnement (Emballage) 0549
- Génie aérospatial 0538
- Génie chimique 0542
- Génie civil 0543
- Génie électronique et électrique 0544
- Génie industriel 0546
- Génie mécanique 0548
- Génie nucléaire 0552
- Ingénierie des systömes 0790
- Mécanique navale 0547
- Métallurgie 0743
- Science des matériaux 0794
- Technique du pétrole 0765
- Technique minière 0551
- Techniques sanitaires et municipales 0554
- Technologie hydraulique 0545

Mécanique appliquée 0346
Géotechnologie 0428
Matières plastiques (Technologie) 0795
Recherche opérationnelle 0796
Textiles et tissus (Technologie) 0794

PSYCHOLOGIE

Généralités 0621
Personnalité 0625
Psychobiologie 0349
Psychologie clinique 0622
Psychologie du comportement 0384
Psychologie du développement 0620
Psychologie expérimentale 0623
Psychologie industrielle 0624
Psychologie physiologique 0989
Psychologie sociale 0451
Psychométrie 0632

ELECTRO-THERMAL SIMULATION OF MOSA AND DERIVATION OF THERMAL EQUIVALENT TEST SECTIONS

BY

LIYING HUANG

A Thesis submitted to the Faculty of Graduate Studies of the University of Manitoba in partial fulfillment of the requirements for the degree of

MASTER OF SCIENCE

ACKNOWLEDGEMENTS

I would like to express my profound gratitude to my supervisor, Dr. M.R. Raghuveer, for his invaluable guidance, encouragement, enthusiasm, comments and discussions in every phase of this study. Dr. Raghuveer did not only guide me but also taught me skills and discipline that every scientist should have. His rigorous scientific approach and strict demands on his students helped me to have successfully completed this study.

Funding from Manitoba Hydro and partial funding from NSERC, Canada is gratefully acknowledged.

I appreciate Mr. W.McDermid of Manitoba Hydro for his valuable input during the course of this work.

I would like to thank Mr. John Kendall for his help in setting up the experiments.

I would also like to thank Mr. Claudio Magnanini, Engineer of Hitachi Line S.A. in Rio De Janeiro, Brazil for providing us with the MOSA used in the tests. Grateful thanks are also due to Mr. Rogerio T. Verdolin and Mr. Fernando A. Chagas of the Electrical Energy Research Center, CEPEL, Rio de Janeiro, Brazil for facilitating provision of the MOSA.

In addition I wish to acknowledge my husband, Xinda Li, for his understanding and assistance.

Finally, this thesis is dedicated to my parents for their encouragement and support during this period of study.

ABSTRACT

In gapless metal oxide surge arresters (MOSA) leakage current flows through the valve elements continuously and generates a certain amount of heat. The temperature of the valve elements is determined by the thermal performance of the arrester in its environment. The steady state thermal behavior of MOSA is important because it affects its ageing and also its capacity to dissipate energies associated with overvoltages and surges. Since it is impractical to measure the variation of temperature along an actual arrester column, it is important to develop a simulation technique to enable studies of thermal capacity under different system and environmental conditions. This thesis describes a modelling technique to simulate the thermal behavior of MOSA based on finite difference method. Application of the suggested model yields the axial and radial variation of arrester temperature. The accuracy of the modelling technique is demonstrated experimentally. Electric model for simulating V–I characteristics and power generation in valve elements at leakage current region is also described.

A procedure to arrive at a thermal equivalent test section (TETS) is presented. The thermal equivalence between the test section and the actual MOSA is demonstrated by conducting tests on an actual MOSA and the test section.

The proposed model can be used to determine the thermal capability and stability of MOSA under different operating conditions i.e. different applied voltages and different magnitudes and durations of temporary overvoltages (TOV). It can also be applied to evaluate the thermal behavior of MOSA under different kinds of overvoltages provided the power generated in the valve elements is available.

SYMBOLS, DEFINITION, UNITS AND TYPICAL VALUES OF PARAMETERS

English Symbols

Symbol	Definition	Unit	Typical value
A	Surface area, cross–sectional area	m^2	
a_s	Solar azimuth		
c_p	Specific heat of valve element (J=w s)	J/kg ^{0}C	500
c_{pa}	Specific heat of air	J/kg ^{0}C	1006
c_{p1}	Specific heat of arrester housing	J/kg ^{0}C	1080
	Specific heat of nylon 6 (nylatron)	J/kg ^{0}C	1673
	Specific heat of plexiglass	J/kg ^{0}C	1422
	Specific heat of glass wool	J/kg ^{0}C	700
c_{p2}	Specific heat of electrode (aluminum)	J/kg ^{0}C	896
	Brass		385
	Electrode in [5]		461
D	Diameter of arrester	m	
d	Thickness of arrester housing sheds	m	
E	Electric field	V/m	
F_{1-2}	Radiation shape factor from element to arrester housing		
F_{i-ii}	Radiation shape factor from small element cylinder i to small housing cylinder ii		
G_r	Grashof number ($= \rho^2 \beta g \Delta T l^3 / \mu^2$)		
f	Ratio of sky radiation to direct solar radiation		
g	Gravitational acceleration	m/s^2	9.8
h	Convective heat transfer coefficient	$W/m^2 \, ^0C$	
h_{in}	Enclosed convection heat transfer coefficient between element and arrester housing	$W/m^2 \, ^0C$	

h_1	Convective heat transfer coefficient between vertical cylinder surface and ambient	$W/m^2\,{}^0C$	
h_{top}	Convective heat transfer coefficient between horizontal surface and ambient	$W/m^2\,{}^0C$	
h_s	Solar hour angle	degrees	
I_0	Solar constant	W/m^2	1353
I_b	Direct solar radiation energy flux	W/m^2	
I_r	Current	A	
i'	Angle between the sun's rays and the normal to the surface	degree	
i	Index in axial direction		
I	Index of shed		
j	Index in radial direction		
k	Thermal conductivity of valve element	$W/m\,{}^0C$	23
k_1	Thermal conductivity of arrester housing	$W/m\,{}^0C$	1.03
	Thermal conductivity of nylon 6 (nylatron)	$W/m\,{}^0C$	0.25
	Thermal conductivity of plexiglass	$W/m\,{}^0C$	0.15
	Thermal conductivity of glass wool	$W/m\,{}^0C$	0.038
	Thermal conductivity of polystyrene	$W/m\,{}^0C$	0.06
k_2	Thermal conductivity of metal electrode (aluminum)	$W/m\,{}^0C$	204
k_{air}	Thermal conductivity of air	$W/m\,{}^0C$	0.026
l	Length of MOSA	m	
l_e	Length of valve element	m	
l_p	Length of arrester housing	m	
l_1	Length of bottom electrode	m	
l_1'	Length of inside metal electrode at bottom	m	
l_2	Length of top electrode	m	
l_2'	Length of inside metal electrode at top	m	
l_f	Length of extended shed surface	m	
l_s	Length of supporter	m	

L	Latitude (50 degrees in Winnipeg)	degree
M	Number of element segments in radial direction: $=r_e/\Delta r$	
m_1	$=M+1$	
m_2	Number of shed segments in radial direction: $=l_f/\Delta r_1$	
$m_1 \times n_1$	The number of nets of valve element	
N	Number of element segments in axial direction: $=l_e/\Delta z$	
n_1	$=N+1$	
$N_u, N_{uav}, N_{uc}, N_{uf}$:	Nusselt number ($=hl/k$)	
n_f	Number of arrester housing sheds	
nn	Number of arrester housing segments in radial direction	
nn_1	$=nn+1$	
n_p	Number of arrester housing segments in axial direction	
nn_2	$=n_p+1$	
n_s	Number of segments of arrester supporter in axial direction	
Pr	Prandtl number ($= \mu c_p/k = v/\alpha$)	
Q_{cond}	Heat conduction	W
Q_{conv}	Heat convection	W
Q_{rad}	Heat radiation	W
Q”	Heat transfer rate per unit area (Heat flux)	W/m^2
q	Power input to valve elements per unit volume	W/m^3
q_i	Power input to valve element per unit volume at node ($i,j=1,2...m_1$)	W/m^3
q_{sun}	Heat input per unit area due to radiation of sun	W/m^2
q_{sky}	Heat input per unit area due to radiation of sky	W/m^2
q_{rad}	Heat input per unit area due to solar/sky radiation ($= q_{sun} + q_{sky}$)	W/m^2
R_a	Rayleigh number ($=G_r Pr = \beta g \Delta T L^3 / v \alpha$)	
R_e	Reynolds number	
r,z	Cylindrical coordinates	m
r_e	Radius of valve element	m
r_{el1}	Radius of inside electrode	m

r_{el2}	Radius of outside electrode	m	
r_j	Radius at node (i,j)	m	
r_{p1}	Inside radius of arrester housing	m	
r_{p2}	Outside radius of arrester housing	m	
r_{p3}	Radius of arrester housing shed	m	
$T=T(r,z,t)$: Temperature of valve element		^0C	
T_{amb}	Ambient temperature	^0C	
$T_{ij}=T_{ij}^n$: Element temperature at node (i,j) at n^{th} time step		^0C	
$TT=TT(r,z,t)$: Temperature of arrester housing		^0C	
$TT_{ij}=TT_{ij}^n$: Housing temperature at node (i,j) at n^{th} time step		^0C	
$TTT_1=TTT_1(t)=TTT_1(r,z,t)$: Temperature of top electrode		^0C	
$TTT_2=TTT_2(t)=TTT_2(r,z,t)$: Temperature of bottom electrode		^0C	
TF_{Ij}	Temperature of I^{th} shed of housing at node j at n^{th} time step	^0C	
$TS=TS(z,t)$: Temperature of support structure (porcelain)		^0C	
$TS_i=TS_i^n$: Temperature of support structure at n^{th} time step		^0C	
t	Time	s or hour	
v	Kinematic viscosity of air (μ/ρ_{air})	m^2/s	15.7×10^{-6}
V	Applied voltage	V	
V_{el}	Volume of top electrode	m^3	
V_∞	Velocity of air	m/s	
V_1	Volume	m^3	
z(I)	z coordinate of I^{th} shed	m	

Greek Symbols

α	Thermal diffusivity of valve element($=k/\rho c_p$)	m^2/s	
α_1	Thermal diffusivity of arrester housing	m^2/s	
α_{air}	Thermal diffusivity of air	m^2/s	22.1×10^{-6}
α_e	Thermal diffusivity of electrode	m^2/s	

α_s	Solar altitude angle	rad	
α_{sun}	Absorptivity of the arrester surface for solar radiation		
	arrester housing surface: α_{sun}=		0.95
β	Coefficient of cubical expansion (= $1/(T_{amb}+273)$)	1/ K	
δ_s	Declination angle	degrees	
$\Delta r, \Delta z$	Small increment of valve element in radial and axial directions		m
Δr_1, Δz_1	Small increment of arrester housing in radial and axial directions	m	
ΔT	Temperature difference between MOSA surface and air	^0C	
Δt	Time step	s	
ε	Radiation emissivity of valve element surface		0.9
ε_{el}	Radiation emissivity of electrode surface (aluminum)		0.95
ε_p	Radiation emissivity of arrester housing surface		0.95
μ	Absolute viscosity	kg/m s	1.85
ρ	Density of valve element	kg/m^3	5500
ρ_{air}	Density of air	kg/m^3	1.18
ρ_1	Density of arrester housing	kg/m^3	2400
ρ_1	Density of nylon 6	kg/m^3	1148
	Density of plexiglass	kg/m^3	1184
	Density of glass wool	kg/m^3	24
	Density of polystyren	kg/m^3	32
ρ_2	Density of electrode (aluminum)	kg/m^3	2736
	Brass		8522
	Electrode in [5]		7800
ρc_p	Volumetric heat capacity	$J/m^3\,^0C$	
σ	Stefan–Boltzmann constant	$W/m^2 K^4$	5.67×10^{-8}
$\bar{\tau}_{atm}$	Atmospheric transmittance		

LIST OF FIGURES

LIST OF TABLES

TABLE OF CONTENTS

Chapter 1

INTRODUCTION

Since their introduction for use in the electronics industry by the Matsushita Electric Industry Co. of Osaka, Japan, in 1968, gapless metal oxide surge arresters (MOSA) have developed rapidly and are now used as protective devices in power systems. Their popularity is due to their excellent performance and the many advantages they offer over the conventional gapped silicon carbide arresters.

1.1 V–I Characteristics of MOSA

The exploitation of the highly nonlinear voltage–current characteristics of valve elements has resulted in the elimination of series gaps in the arrester. Typical V–I characteristics [1] of a valve element are shown in Fig. 1.1, which has been divided into two distinct regions: a low current region and a high current region. In the low current region (leakage current region) for applied ac or dc voltages, the resistive component of the current depends on the granular layer and thus is influenced by the manufacturer's selection of materials and productions. Hence, there is considerable variation of the V–I characteristics in this region for elements from different production lots and, in particular, for different manufacturers. At higher temperature the electron energy increases. Consequently the electrons can cross the barriers more easily. Therefore, the resistive current component exhibits a high temperature dependence as expressed by Eq. 1.1.

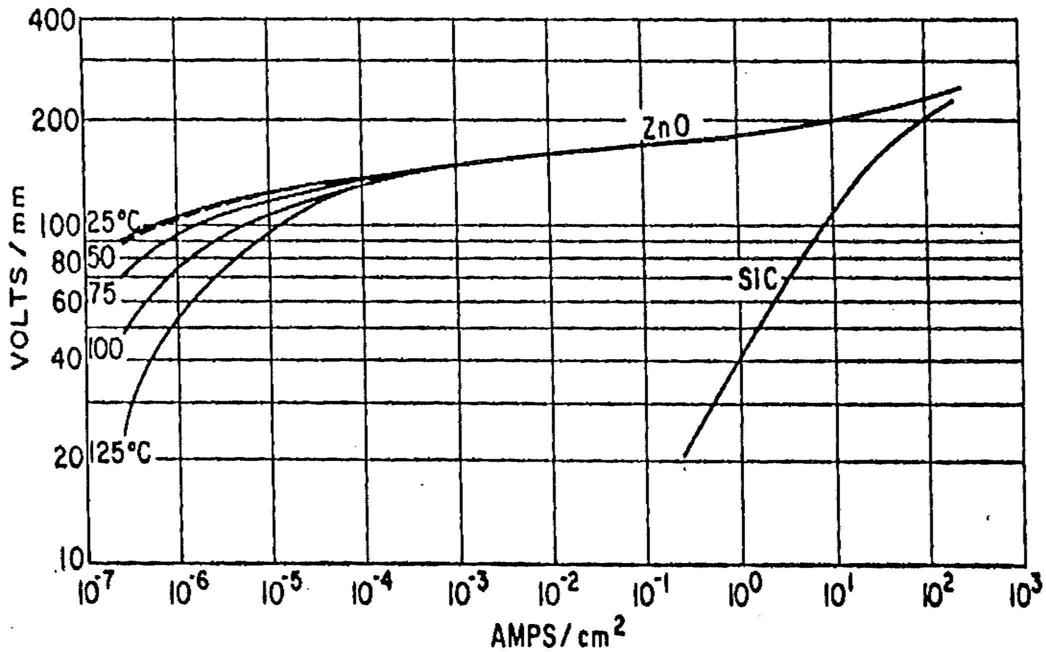

Figure 1.1 V–I characteristics of a typical valve element

$$I = I_0(E)e^{-\frac{W_c}{KT}} \tag{1.1}$$

where, W_c is the activation energy for conduction, which is equal to 0.6–0.8 eV. K is Boltzmann's constant which has the value of 0.86×10^{-4} eV/ ^{0}K, and T is the valve element temperature in ^{0}K.

In the high current region, the V–I characteristics, which are no longer ohmic and temperature dependent, are described by the relation:

$$I = CV^{\alpha}; \qquad \alpha = \alpha(V) \tag{1.2}$$

where $\alpha(V)$ is a measure of the element nonlinearity (≥30).

1.2 Thermal Stability of MOSA

Thermal stability is one of the dominant problems in the application of MOSA. Since MOSA has no series gaps, the resistive leakage current flows through the valve elements continuously, and generates a certain amount of heat. The generated heat is transferred to the environment by means of conduction, convection and radiation. If the heat generation exceeds the heat loss from the valve elements, the excess energy stored in the elements leads to an increase in its temperature. Conversely, if the heat loss exceeds the heat generation, the temperature of the elements decreases. Typical heat loss and heat generation curves of a valve element[2,3] are shown in Fig. 1.2. To attain thermal stability, the heat generation must be balanced with the heat loss from the valve element. Under normal operating conditions, the temperature of valve element is maintained at an operating temperature at the first intersection point of the heat loss–input curves, i.e. point A in Fig. 1.2. If the applied voltage or initial element temperature exceeds a certain level, the heat loss and gain curves may not intersect as shown in Fig. 1.3. Consequently, there will be no thermal equilibrium and the temperature of the valve elements will increase boundlessly to infinity. Thermal runaway and arrester failure result.

On the other hand, when a MOSA absorbs energies associated with various transient overvoltages, the valve element's temperature rises abruptly. If the temperature rise is less than a certain critical temperature, i.e. point B in Fig. 1.2, the second intersection point of heat loss–input curves, the heat loss exceeds the heat generation and thermal equilibrium will be restored, but if the temperature rise exceeds the critical temperature, the amount of heat generation becomes greater than the heat loss and the MOSA can not return to the former thermally stable condition from the temporary high temperature state, resulting in thermal run away.

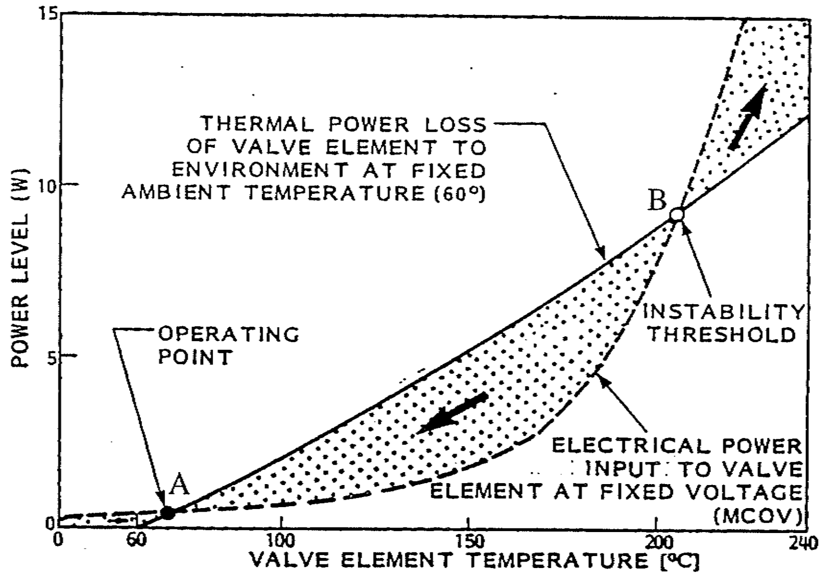

Figure 1.2 Heat loss–input characteristics

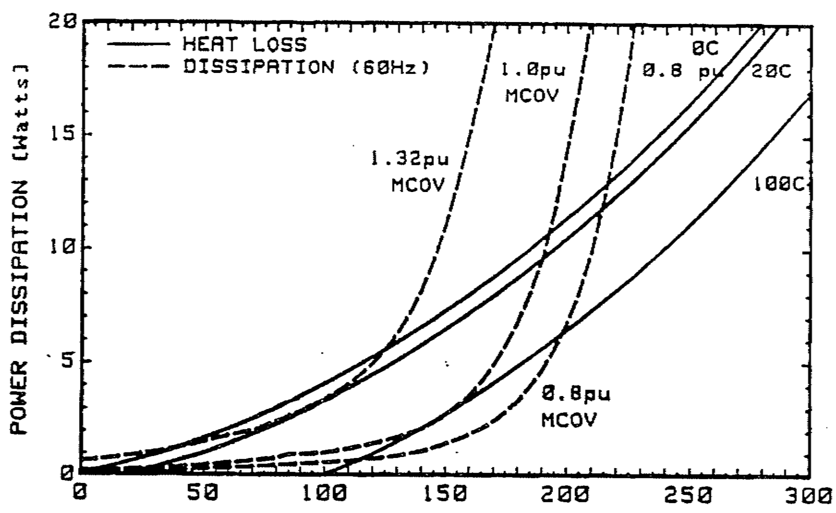

Temperature (^0C)

Figure 1.3 Effect of ambient temperature and operating voltage on thermal stability of a MOSA

One of the important problems in the application of MOSA is therefore particularly related to thermal stability and capability of MOSA, which depends on the arrester construction, ambient conditions, material characteristics and applied voltages.

1.3 Thermal Models of MOSA

As described above, the steady state thermal behaviour of MOSA is important because it affects its ageing and also its capacity to dissipate energies associated with overvoltages and surges. However, it is very difficult and indeed impractical to conduct thermal stability tests directly on a MOSA unit. Only a few measurements on actual high voltage arresters have been reported[4–7]. Therefore, in order to find steady state thermal condition and energy absorption capability, an appropriate method is to build an electro–thermal model of MOSA. The thermal characteristics of a MOSA can be evaluated by conducting tests on a thermal equivalent test section (TETS) whose parameters are adjusted to match the thermal properties of the MOSA which it represents. Several test sections have been described in literature [4,5,8]. Recently, mathematical models have been developed to simulate thermal properties of MOSA [2,3,10,11].

1.3.1 Thermally Equivalent Test Sections (TETS)

Two test sections as shown in Fig. 1.4 were first constructed[4] in 1981. In the test section of Fig. 1.4 (a), the periphery of the valve element is covered with a certain heat insulating material. In another test section, Fig. 1.4 (b), cooling metal fins are provided at both ends of the valve element in order to increase heat dissipation capability. The test was carried out with applied ac voltage from 2.9kV to 3.8kV which is equal to the voltage applied to the single element in an actual system. Equivalency between a MOSA and the two test sections was not established. As presented in [4], the heat dissipation rate of a typical MOSA is between that of these two test sections and closer to the one shown in Fig. 1.4 (a).

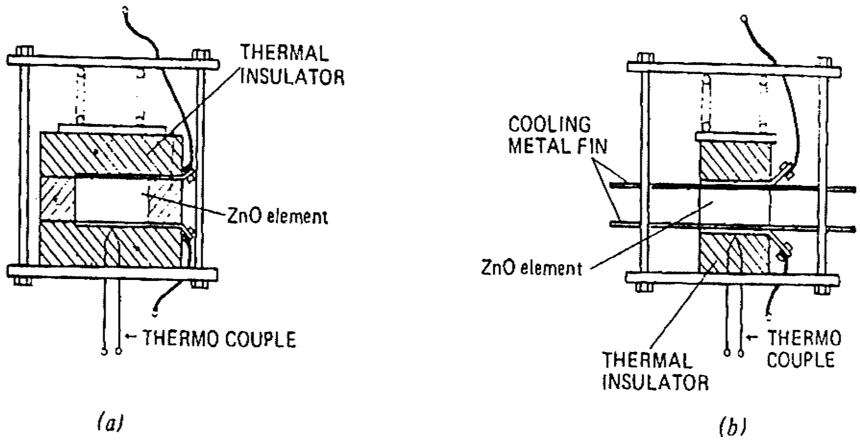

Figure 1.4 Construction of test specimen

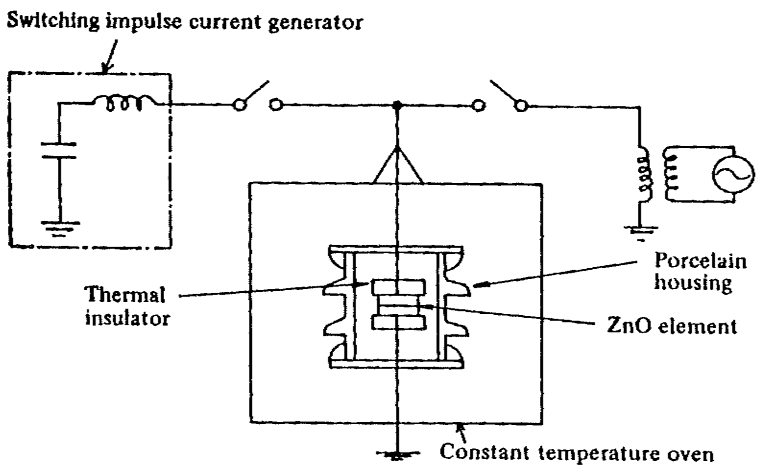

Figure 1.5 Construction of small model unit

Fig. 1.5 shows another small model unit used to examine thermal capability and stability of a MOSA[8]. In this test section two valve elements were sandwiched between epoxy resin insulators to suppress thermal dissipation in the axial direction of the column. This assembly was contained in a porcelain housing. The test results were obtained by changing the ac voltage applied to the elements to check on the occurrence of thermal runaway. The experiment results in [8] show that the heat dissipation capability of an 84kV porcelain type MOSA is about one half of that of the test section. Again the authors of [8], as in [4], have not established thermal equivalence between the test section and an actual arrester.

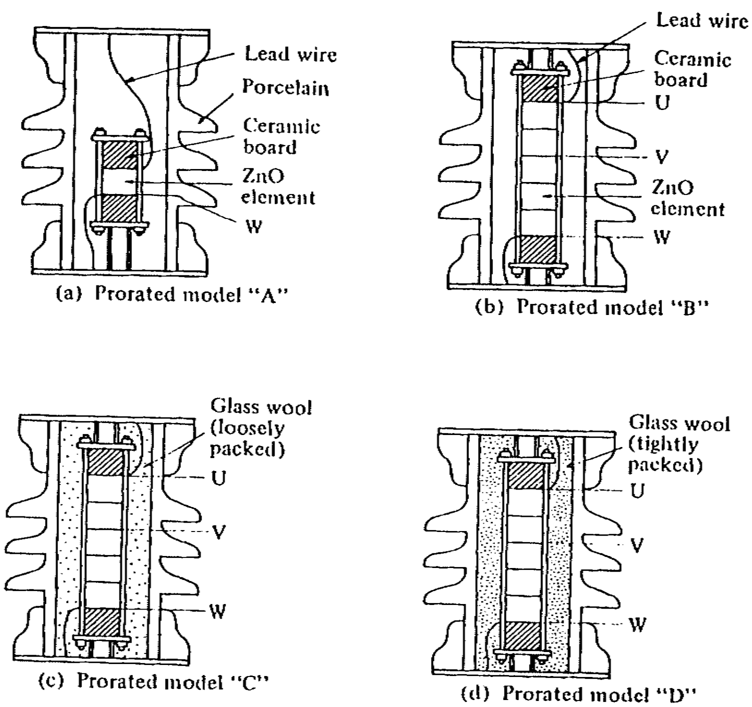

Figure 1.6 Structure of four types of test sections

Nishiwaki et al [5] demonstrated thermal runaway phenomenon experimentally on an 84kV porcelain–type MOSA and established the temperature when such thermal runaway occurred. Then four test sections were fabricated as shown in Fig. 1.6. These test sections of MOSA were designed for obtaining a test section which possesses thermal runaway temperature limits and heat dissipation time constants approximately identical to those of the 84kV porcelain–type MOSA. For test sections c and d in Fig. 1.6, the valve elements were still sealed in porcelain housing but their surroundings were packed with glass wool. In this case the test section d was found to be thermally equivalent to the 84kV MOSA.

None of the above authors have discussed the design procedures used to construct the test sections. It can be seen that the main problem lies in the establishment of thermal equivalence between a test section and an actual surge arrester. This has been done, with partial success, by conducting tests on both actual and test sections. The design of the test section was then presumably altered until thermal equivalence was established. This is a cumbersome and impractical procedure. A better method is to use a mathematical technique in designing the test section.

1.3.2 Mathematical Models

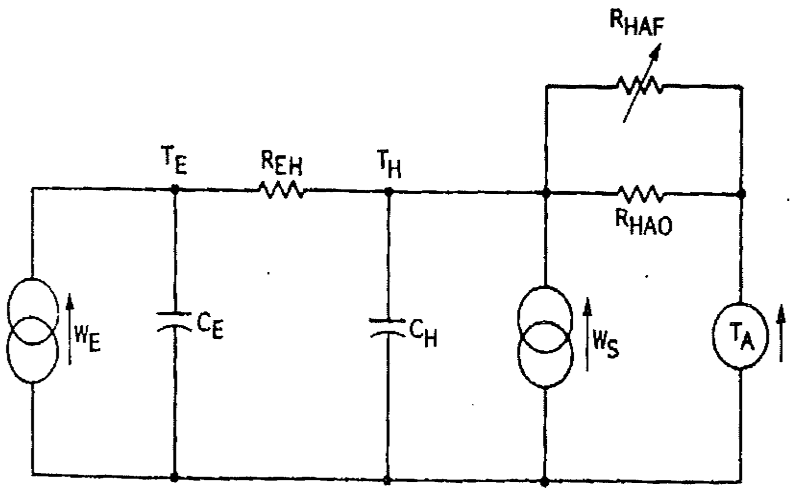

C_E, C_H: thermal capacities of the valve element and adjacent housing respectively
R_{EH}: thermal resistance from element to housing

R_{HAO} thermal resistance from housing to ambient, radiation and natural convection components

R_{HAF} thermal resistance from housing to ambient, forced convection component only

T_E, T_H: valve element and housing temperature respectively

T_A: ambient temperature

W_E: electrical power input to valve element
W_s: heat input due to solar radiation

Figure 1.7 Equivalent electrical circuit

The thermal properties of MOSA were first represented as a simple electric analog model as shown in Fig. 1.7, [2], by Lat in 1983, where the valve elements, air space and porcelain housing are reduced to simple electrical equivalents based on representing heat flow as current and temperature as voltage. This model consists of two capacitors to represent the thermal capacities of the valve elements and the porcelain housing and a few resistors to represent heat transfer between the elements and the housing, and between the housing and the ambient surroundings by conduction, convection and radiation.

Later, Lat used the same thermal model and validated it for a distribution type arrester [3].

As Lat himself points out, his model neglects axial heat flow among valve elements and the model parameters are derived on the basis of radial heat loss only. This assumption results in the theoretically predicted temperature being higher than the measured value.

Similar to Lat's model, an electric equivalent circuit was derived in 1987, [10], to calculate the performance of MOSA. Axial heat flow within the arrester column is accounted for in this model by cascading several identical analog circuit segments to form a ladder network. The analog circuits are connected by resistances of the valve elements which determine the axial conductive heat flow. In this model, power generation in the valve elements is treated as a constant current source, and the use of the model is restricted to a configuration of stacked valve elements without housing. Two years later, the same technique was used to calculate thermal properties of MOSA with a porcelain housing [11].

In [6], a model similar to the one developed by Lat is used to predict the temperature–time profile of valve elements in near thermal runaway conditions.

Taking into account the temperature variation of the volt–ampere characteristics, the authors in [7] implemented a thermal model of MOSA to simulate the arrester thermal performance under polluted conditions. The simulation uses an equivalent electrical network to represent the thermal performance and an over simplified model of surface pollution.

In all the electric analog models, reviewed above, it is necessary to find the precise values of the parameters (i.e. values of the capacitors and resistances). The model parameters were determined analytically from the physical dimensions of a particular arrester unit or derived by experimental measurements on an actual unit. Usually only empirically derived equations for calculating parameters can be found in literature. Experimental methods to determine the parameters of an electro–thermal model similar to the one of Lat is described in [12].

From the above it can be noted that all the mathematical models use similar equivalent electrical circuits to represent the thermal properties of MOSA. All the above models are based on the following simplifications and assumptions:

(1) Lumped components of thermal resistance and heat capacity are used although these properties are in reality distributed parameters.

(2) Some thermal parameters are linearized. Actually, the heat transfer modes of radiation and convection are highly nonlinear.

(3) Axial heat loss from metal electrodes is neglected.

(4) The models do not recognize the change of heat transfer mode in different parts of the arrester, i.e. coefficient of convective heat transfer depends on the configuration and position of the heated surface.

(5) The models do not allow temperature change in the radial direction of valve elements. The axial variation of temperature can be calculated, but the accuracy depends on the number of analog ladder circuits used to represent the variation in this direction.

Recently a finite difference based thermal analysis has been reported in [13], but the method is applied only to an arrester test section. Once again absence of axial heat transfer is assumed. Therefore the author considered only radial heat transfer and simplified heat transfer modes. However, temperature measurements in an actual arrester [7,8] indicate that a temperature variation does exist along an arrester column and axial heat transfer takes place. More heat is dissipated in the axial direction of a short arrester. Therefore, such an assumption introduces inaccuracies and limits the use of the model.

Because of a lot of limitations in all above models, a more elaborate model is needed to enable simulated studies of thermal capacity of MOSA under different systems and environmental conditions.

1.4 Proposed Thermal Equivalent Models

In this thesis an accurate modelling technique is suggested to simulate the thermal behaviour of MOSA based finite difference method. Another contribution is a procedure suggested for arriving at a thermal equivalent test section based on the known configuration and data about an actual arrester.

1.4.1 Mathematical Model

In this study the thermal properties of MOSA are first identified. Partial differential equations (PDE) and their boundary conditions of MOSA are then derived and solved numerically using finite difference method (FDM). This derivation overcomes the drawbacks of the previous models. Finally, a computer program is developed to simulate thermal behaviour of MOSA. The proposed model has many advantages over other models.

(1) Accurate heat transfer modes of conduction, convection and radiation are applied in this model. Fin theory is used to account for external heat transfer from the sheds of the arrester housing.

(2) The proposed model yields the temporal variation of valve element, electrode and housing temperature distribution in both the axial and radial directions.

(3) The model can be used to simulate thermal behaviors of MOSA under steady state and transient conditions.

(4) The model can be applied to find the time variation of temperature along the length of an energized stack of valve elements and to locate the hottest point in the arrester column.

(5) The suggested modelling technique can be applied to any configuration of MOSA.

The accuracy of the proposed model is demonstrated by comparison of simulated and experimental results; The experiments are conducted on an actual 84kV arrester.

1.4.2 Thermally Equivalent Test Section (TETS)

The developed mathematical model is used to analyze both the MOSA and the test section and to arrive at a design of TETS. Such an approach is preferred to an experimental one [4,8,5] as the later is cumbersome.

A thermal equivalent test section of a 84kV MOSA are derived. A procedure for arriving at a TETS is discussed. Thermal stability, capability and arrester ageing tests can now be conducted directly on the TETS.

Either the mathematical model or the TETS may be used to choose suitable arresters for a particular application and to achieve optimal design of MOSA with regard to protection levels, energy absorption capabilities and lifetime.

Chapter 2

HEAT TRANSFER MODES

Whenever two systems are not in thermal equilibrium due to a temperature difference between them, energy is transferred from the hotter system to colder system in an attempt

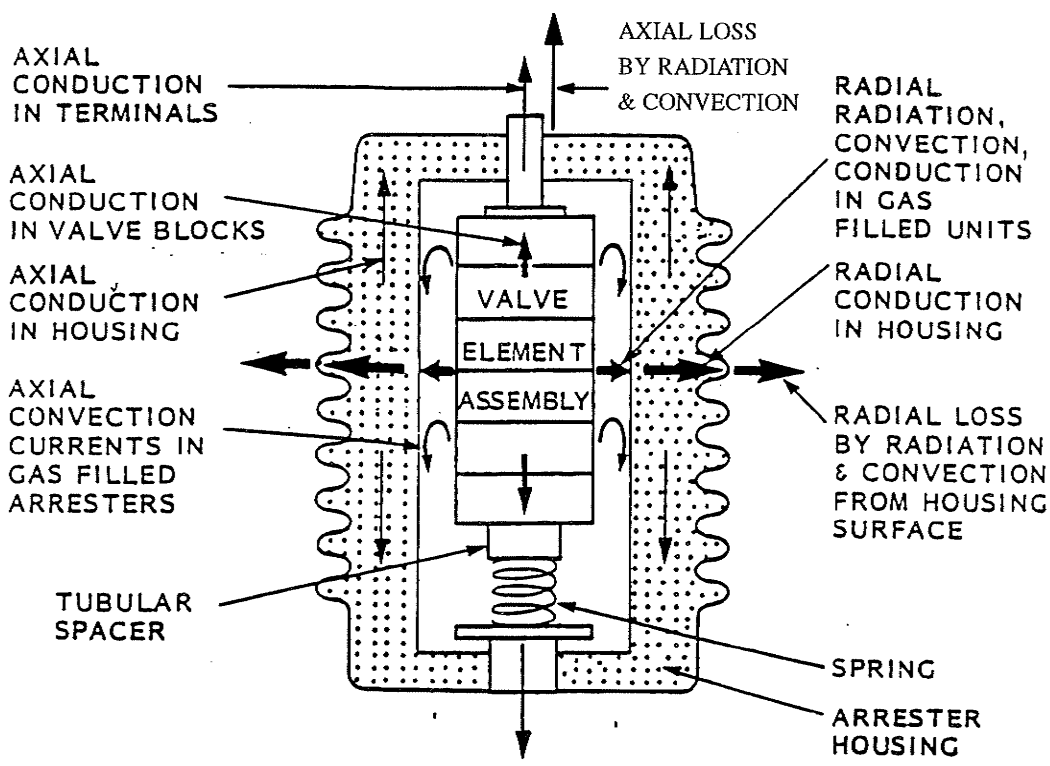

Figure. 2.1 Heat flow paths in a typical MOSA

to achieve equilibrium. There are three modes of heat transfer: conduction, convection and radiation. In the case of MOSA as shown in Fig. 2.1, all three modes occur simultaneously. Electric energy heats the valve elements, and is transferred by conduction, convection and radiation to the arrester housing and electrodes. The energy then is convected and radiated to the ambient. When heat generation equals to the heat loss, the system reaches thermal equilibrium. The thermal model of MOSA is derived in accordance with the following thermal mechanisms and laws of conduction, convection and radiation [27–46].

2.1 Conduction

Heat conduction is an energy transfer due to interaction between molecules at different temperatures. It occurs in solids, liquids and gases but is of more consequence in solids. The fundamental law of conduction is due to Fourier:

$$Q'' = -k\frac{\partial T}{\partial n} \qquad (2.1)$$

where Q" is the heat transfer rate per unit area normal to the n direction, k is the thermal conductivity and $\partial T/\partial n$ is the temperature gradient in the n direction.

Heat transfer rate per unit length by conduction from the exterior surface of an inner cylinder to the interior surface of an outer cylinder is

$$Q' = \frac{2\pi k}{\ln\frac{R}{r}}(T_2 - T_1) \quad \text{(W/m)} \qquad (2.2)$$

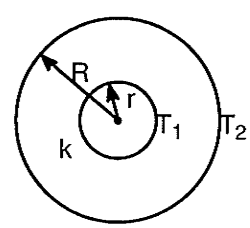

where T_1 and T_2 are the temperatures of the exterior surface of inner cylinder and the interior surface of outer cylinder respectively.

In the case of MOSA heat transfer due to conduction from the valve elements to housing may be neglected because it is very small compared to the convection and radiation terms.

2.2 Convection

Convective heat transfer occurs between a solid surface and its adjacent fluid due to the motion of the fluid. The convective heat transfer in MOSA happens between air and valve element, arrester housing and electrode interfaces. The fundamental law of convection is expressed by Eq. 2.3, generally known as Newton's law of cooling.

$$Q'' = h \cdot \Delta T \tag{2.3}$$

where ΔT is the temperature difference between solid surface and fluid.

The convection heat transfer coefficient, h, is a complex and variable quantity depending on the geometry of surface, fluid flow, fluid properties and different environmental conditions, which is mostly obtained by experiments. The following empirical expressions of convection coefficient are employed for application in Chapter 3.

2.2.1 Free Convection

Free convection occurs only in gravitational fields, which depends largely on the geometry of the surface and the physical properties of the fluid. The coefficient, h, is incorporated in the Nusselt number, N_u, which is related to the Rayleigh number, R_a, Grashof number, G_r, and Prandtl number, P_r.

(1) Horizontal heated upward–facing surface [27]

On a horizontal heated upward facing surface (top electrode of MOSA), the convective coefficient, h_{top}, is expressed by

$$h_{top} = N_{uav}\, k_{air} / L^* \tag{2.4}$$

where

$$N_{uav} = \begin{cases} 0.34(R_a)^{1/4} & (2.6\times10^4 < R_a < 10^7) \\ 0.15(R_a)^{1/3} & (10^7 < R_a < 3\times10^{10}) \end{cases} \qquad (2.5)$$

and

$$R_a = G_r \cdot P_r = \frac{\varrho_{air}^2 \cdot c_{pa} \cdot \beta \cdot g \cdot \Delta T \cdot L^3}{\mu k_{air}} = \frac{\beta g \Delta T L^{*3}}{\nu \alpha_{air}} \qquad (2.6)$$

$L^* = D/4$

(2) Vertical cylindrical surface [28]

The convective coefficient on an external vertical cylindrical surface (exterior surface of MOSA) is given by

$$h_1 = N_{uc}\, k_{air} / l \qquad (2.7)$$

where,

$$N_{uc} = \frac{0.9\zeta N_{up}}{\ln(1 + 0.9\zeta)} \qquad \text{for } R_a \geq 10^5 \qquad (2.8)$$

$$N_{uc} = \frac{1.8 l/D}{\ln\left\{1 + \frac{1.8}{\frac{4}{3} C_l (R_a^*)^{1/4}}\right\}} \qquad \text{for } R_a < 10^5 \qquad (2.9)$$

$$R_a^* = \frac{\beta g \Delta T D^4}{\nu \alpha_{air} l}, \qquad C_l = 0.386 \qquad (2.10)$$

R_a is calculated from Eq. 2.6 with $L^* = l$, and the coefficients involved in Eq. 2.8 are obtained from

$$N_{up} = \frac{2.8}{\ln(1 + \frac{2.8}{N_u^T})} \qquad \zeta = \frac{2l/D}{N_{up}^T} \tag{2.11}$$

$$N_u^T \approx N_{up}^T = \frac{4}{3} C_l (R_a)^{1/4} \tag{2.12}$$

(3) Enclosed convection [29]

For heat transfer by convection in the enclosed volume between two coaxial cylinders (inside surfaces of MOSA), the convective coefficient is denoted by h_{in}.

$$h_{in} = N_{uf}\, k_{air} / l \tag{2.13}$$

$$N_{uf} = 0.55\ (R_a)^{1/4} \tag{2.14}$$

R_a is still calculated from Eq. 2.6 with $L^* = l$.

2.2.2 Forced Convection

Heat transfer by wind induced forced convection from an exterior surface of MOSA must be taken into consideration to accurately depict field conditions.

(1) Horizontal heated upward–facing surface[27]

$$h_{top} = 0.592 \frac{k_{air}}{D} (R_e)^{0.5} \qquad (R_e < 300{,}000) \tag{2.15}$$

$$h_{top} = 0.0362 \frac{k_{air}}{D} \left(R_e^{0.8} - (R_{ecrit})^{0.8} + 18.2 (R_{ecrit})^{0.5}\right) \tag{2.16}$$

$$(R_e > 300{,}000)$$

where, $$R_e = \frac{\varrho_{air} v_\infty D}{\mu}, \qquad R_{ecrit} = 300{,}000 \tag{2.17}$$

(2) Vertical cylindrical surface [30]

$$h_1 = \frac{k_{air}}{D} B(R_e)^{n'} \tag{2.18}$$

where, the dimensionless numbers n' and B can be found in Table 2.1.

Table 2.1 Constants n' and B in Eq. 2.18

R_e	n'	B
1–4	0.330	0.891
4–40	0.385	0.821
40–4000	0.466	0.615
4000–40,00	0.618	0.174
40,000–250,000	0.805	0.0239

2.3 Radiation

Thermal radiation is a process of heat transfer from one body to another due to electromagnetic waves. The calculation of thermal radiation is based on the Stefan–Boltzmann law.

2.3.1 Grey Bodies in Large Surroundings

The heat transfer rate, Q_{21}, from the large surroundings to a grey body is described by

$$Q_{21} = \varepsilon_1 \cdot \sigma \cdot A_1 \cdot (T_2{}^4 - T_1{}^4) \tag{2.19}$$

where, T_2 and T_1 are the temperature of surroundings and grey bodies. ε_1 is the emissivity of the grey body surface, and A_1 is the surface area of grey body.

2.3.2 Two Coaxial Cylinders:

Heat transfer rate, Q_{12} , from surface 1, exterior surface of inner cylinder, to surface 2, interior surface of outer cylinder, is

$$Q_{21} = \frac{\sigma \cdot (T_1^4 - T_2^4)}{R_a'} \tag{2.20}$$

$$R_a' = \frac{1-\varepsilon_1}{A_1\varepsilon_1} + \frac{1}{A_1F_{12}} + \frac{1-\varepsilon_2}{A_2\varepsilon_2} \tag{2.21}$$

where F_{12} is geometric radiation shape factor; A_1, A_2 are the surface areas of surface 1 and surface 2 respectively; ε_1 and ε_2 are the emissivities of surface 1 and surface 2 respectively.

2.3.3 Computation of Radiation Shape Factors [31]

Knowledge of the radiation shape factor, F_{12}, is required to calculate radiation heat transfer from the valve element to the arrester housing and electrodes. Because the elements and the housing are divided into small cylinders in the numerical calculations of Chapter 3, the radiant energy of one small cylinder is transferred to other neighboring cylinders. It has been found by calculation that more than 98% of the radiant energy from one small cylindrical surface on the valve element is transferred to the other 3 closest adjacent interior cylindrical surfaces of the arrester housing. This is due to the small air gap between the valve element and housing. The radiation shape factors, F_{i-ii}, involved in the calculation of Chapter 3 are evaluated as follows.

(1) Two concentric cylinders of equal length, one contained within the other

For two concentric cylinders as shown in Fig. 2.2, the radiation shape factor, F_{b-a}, from the curved interior surface of the outer cylinder, b, to the curved exterior surface of inner cylinder, a, is

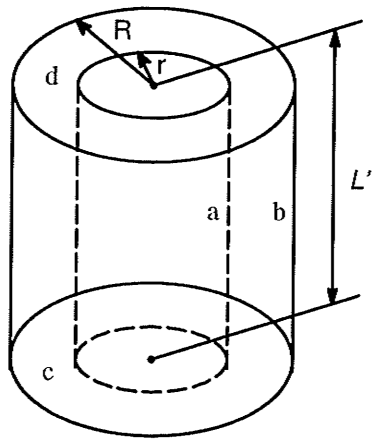

Figure 2.2 Two concentric cylinders

$$F_{b\to a} = \frac{r}{R}\left\{1 - \frac{1}{\pi}\left[\cos^{-1}\frac{L'^2 - R^2 + r^2}{L'^2 + R^2 - r^2}\right.\right.$$

$$-\frac{1}{2rL'}\left(\sqrt{(L'^2 + R^2 + r^2)^2 - 2rR^2}\cos^{-1}\frac{r(L'^2 - R^2 + r^2)}{R(L'^2 + R^2 - r^2)}\right.$$

$$\left.\left.\left. + (L'^2 - R^2 + r^2)\sin^{-1}\frac{r}{R} - \frac{\pi}{2}(L'^2 + R^2 - r^2)\right)\right]\right\} \qquad (2.22)$$

Radiation shape factor, $F_{a\text{-}b}$, is therefore calculated by

$$F_{a\to b} = \frac{F_{b\to a}\cdot A_b}{A_a} \quad \text{due to} \quad F_{1\to 2}\cdot A_1 = F_{2\to 1}\cdot A_2 \qquad (2.23)$$

where, $A_b = 2\,\pi\,R\,L'$, $A_a = 2\,\pi\,r\,L'$, R is the radius of outer cylinder, r is the radius of inner cylinder, and L' is the length of cylinder.

Radiation shape factor, $F_{a\text{-}c}$ and $F_{a\text{-}d}$, between curved interior surface of outer cylinder, a, and bottom and top annulus contained between a and b is:

$$F_{a \to c} = F_{a \to d} = \frac{1}{2}(1 - F_{a \to b}) \tag{2.24}$$

Above shape factors may be used in the temperature calculation of test sections.

(2) Two concentric cylinders of unequal length, one contained within the other:

Fig. 2.3 shows the configuration of 6 segments of the two cylinders.

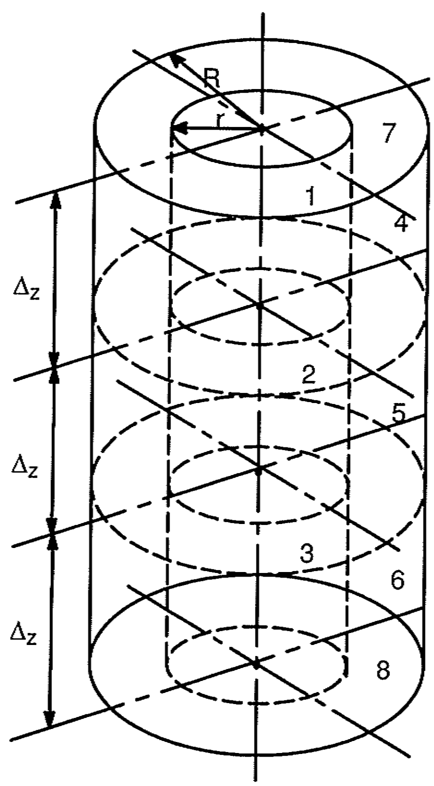

Figure. 2.3 Configuration of 6 segments of two cylinders

Radiation shape factor, F_{2-5}, from exterior surface of middle inner cylinder 2 to interior surface of middle outer cylinder 5 is:

$$F_{2\to5} = \frac{F_{5\to2} \cdot A_5}{A_2} = F_{1\to4} = F_{3\to6} \qquad (225)$$

$$F_{5\to2} = \frac{r}{R}\left\{1 - \frac{1}{\pi}\left[\cos^{-1}\frac{\Delta z^2 - R^2 + r^2}{\Delta z^2 + R^2 - r^2}\right.\right.$$

$$-\frac{1}{2r\Delta z}\left(\sqrt{(\Delta z^2 + R^2 + r^2)^2 - 2rR^2}\cos^{-1}\frac{r(\Delta z^2 - R^2 + r^2)}{R(\Delta z^2 + R^2 - r^2)}\right. \qquad (2.26)$$

$$\left.\left.\left. + (\Delta z^2 - R^2 + r^2)\sin^{-1}\frac{r}{R} - \frac{\pi}{2}(\Delta z^2 + R^2 - r^2)\right)\right]\right\} \quad = F_{4\to1} = F_{6\to3}$$

Radiation shape factor, $F_{1\text{–}7}$, from exterior surface of top inner cylinder 1 to top annulus 7 contained between 1 and interior surface of top outer cylinder 4 is

$$F_{1\to7} = F_{3\to8} = \frac{1}{2}(1 - F_{2\to5}) \qquad (2.27)$$

and

$$F_{7\to1} = \frac{F_{1\to7} \cdot A_1}{A_7} = F_{8\to3} \qquad (2.28)$$

Radiation shape factor, $F_{2\text{–}4}$ from surface 2 to surface 4 is

$$F_{2\to4} = F_{2\to6} = \frac{1}{2}(F_{2\to4+5+6} - F_{2\to5}) \qquad (2.29)$$

where, $A_1 = A_2 = A_3 = 2\,\pi\, r\, \Delta z$, $A_4 = A_5 = A_6 = 2\,\pi\, R\, \Delta z$, and $A_7 = A_8 = \pi\,(R^2 - r^2)$.

2.4 Energy Input Due to Solar/Sky Radiation [30, 32]

Radiation from the sun and sky may provide a significant power input to the arrester surface in the field:

$$q_{rad} = q_{sun} + q_{sky} \qquad (W/m^2) \tag{2.30}$$

2.4.1 Energy Input Due to the Sun

Energy input due to the sun is given by

$$q_{sun} = \alpha_{sun} I_b \cos i' \tag{2.31}$$

(1) Calculation of I_b

The radiation flux density, I_b, can be described by

$$I_b = I_0 \bar{\tau}_{atm} \tag{2.32}$$

The atmospheric transmittance, $\bar{\tau}_{atm}$, is given by

$$\bar{\tau}_{atm} = a_0 + a_1 e^{-k' cosec(\alpha_s)} \tag{2.33}$$

where the constants, a_0, a_1 and k' are a function of altitude as shown in Table 2.2, and α_s is calculated by Eq. 2.34.

$$\sin(\alpha_s) = \sin(L)\sin(\delta_s) + \cos(L)\cos(\delta_s)\cos(h_s) \tag{2.34}$$

Table 2.2 23km haze model

Altitude above sea level(km)	0	0.5	1.0	1.5	2.0	2.5
a_0	0.1283	0.1742	0.2195	0.2582	0.2915	0.320
a_1	0.7559	0.7214	0.6848	0.6532	0.6265	0.602
k'	0.3872	0.3426	0.3139	0.2910	0.2745	0.268

Altitude above sea level in Winnipeg is 200–500 m, and a_0, a_1 and k' can be obtained by interpolation from Table 2.2.

In Eq. 2.34, the declination angle, δ_s, is given by Eq. 2.35, and solar hour angle, h_s, can be found from Fig. 2.4, i.e., $h_s = 45^0$ at 3 o'clock.

$$\delta_s = 23.45 \sin\left(360\frac{284+N'}{365}\right) \tag{2.35}$$

where N' is the data or the day of the year. For example, N'=1 on Jan. 1; N'=32 on Feb. 1; N' = 210 for the month of August.

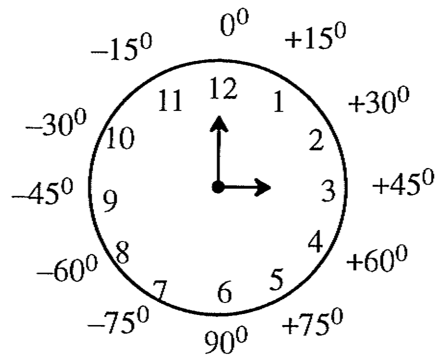

Figure. 2.4 Calculation of solar hour angle

(2) Calculation of i'

The angle between the sun's rays and the normal to the surface, i', may be different at various parts of arrester surface.

On the horizontal surface of the top electrode, i' can be calculated by Eqs. 2.36–2.37.

$$\cos i' = \sin a_s \tag{2.36}$$

$$a_s = \frac{\cos\delta_s \sin h_s}{\cos\alpha_s} \tag{2.37}$$

On a vertical surface facing to east or west, i' is calculated by

$$\cos i' = \cos(a_s - a_w)\cos\alpha_s \tag{2.38}$$

where, $a_w = 90^0$ for the eastward facing surface, and $a_w = -90^0$ for the westward facing surface.

On a vertical surface facing south or north, i' is calculated by

$$\cos i = \cos(L) \sin(\delta_s) + \sin(L) \cos(\delta_s) \cos(h_s) \quad (3.39)$$

A mean value of i' is calculated for application in the mathematical model of Chapter 3 because the model assumes no circumferential variation of arrester temperature.

2.4.2 Energy Received From the Sky

The energy absorbed by the arrester surface during the daytime is evaluated by

$$q_{sky} = \alpha_{sun} f I_b \quad (3.40)$$

where the ratio of sky radiation to direct solar radiation, f, may be calculated by interpolation from Table 2.3.

Table 2.3 f changes with i'

i'	0^0	10^0	20^0	30^0	40^0	50^0	60^0	70^0	80^0	90^0
f	0.16	0.17	0.18	0.19	0.22	0.26	0.32	0.44	0.71	1.33

Knowledge of heat transfer modes described in this chapter is important for the derivation of thermal model of MOSA in the following chapter.

Chapter 3

MATHEMATICAL MODEL

In this chapter, mathematical models to simulate thermal behaviour of complete arrester as well as test sections are presented. At first the partial differential equations governing thermal behaviour of MOSA and the associated boundary conditions are derived. Then they are solved by using the finite difference technique. Electrical model to represent power density input to valve elements is also described. Finally, flow chart of the developed computer program to calculate temperature distribution under both steady state and transient conditions of MOSA is presented.

It is assumed that there is no circumferential variation of temperature in the MOSA, and therefore the temperature depends only on the radial, r, and axial, z, coordinates as shown in Fig. 3.1. Fig. 3.2 shows the cross section of MOSA to be simulated. The figure shows some modelling detail such as sheds and coordinates of boundary surfaces. The initial temperature distribution of MOSA is assumed to be equal to ambient. Based on the fundamental principles of heat transfer described in Chapter 2 and energy conservation, mathematical model of MOSA is derived as follows.

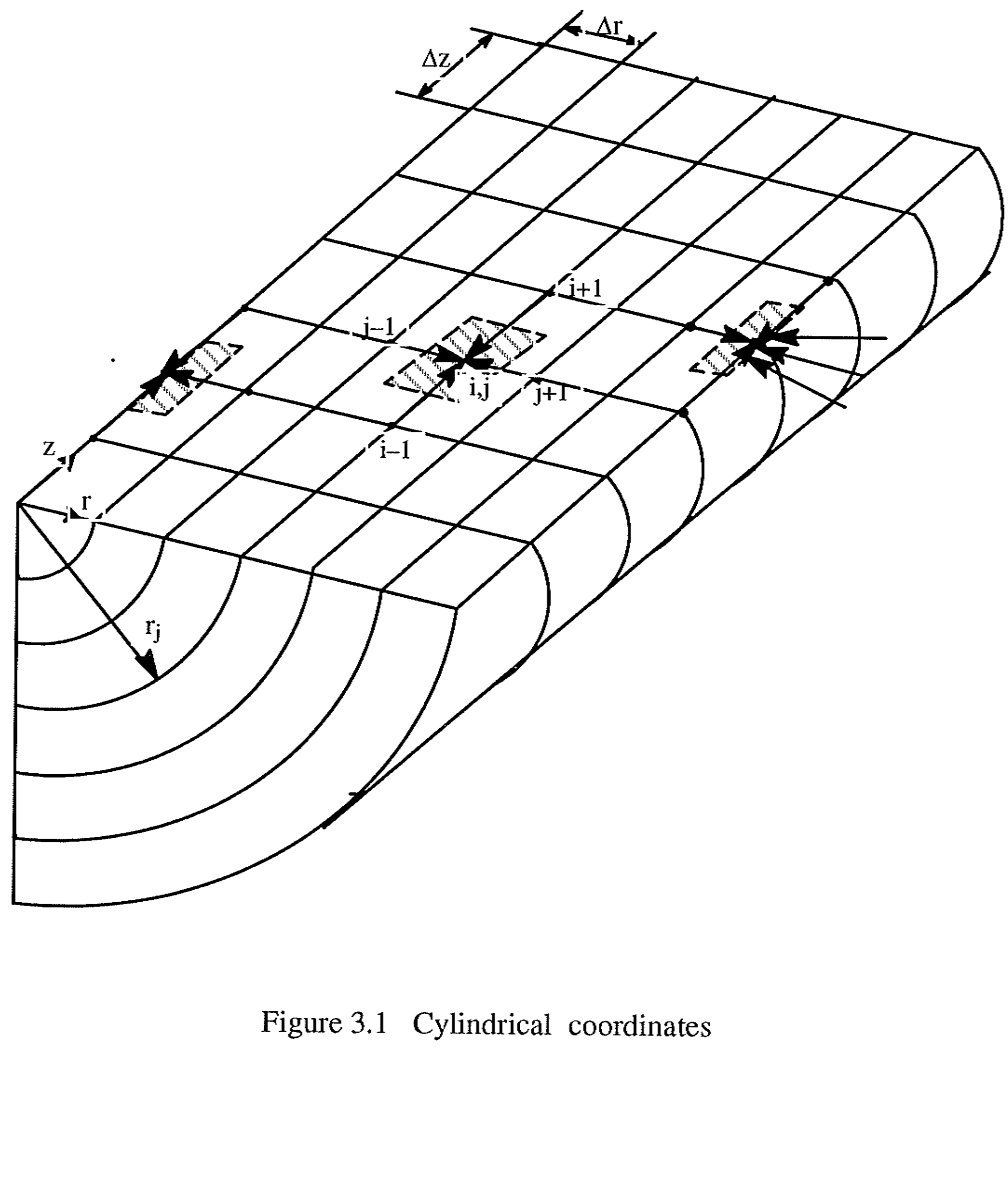

Figure 3.1 Cylindrical coordinates

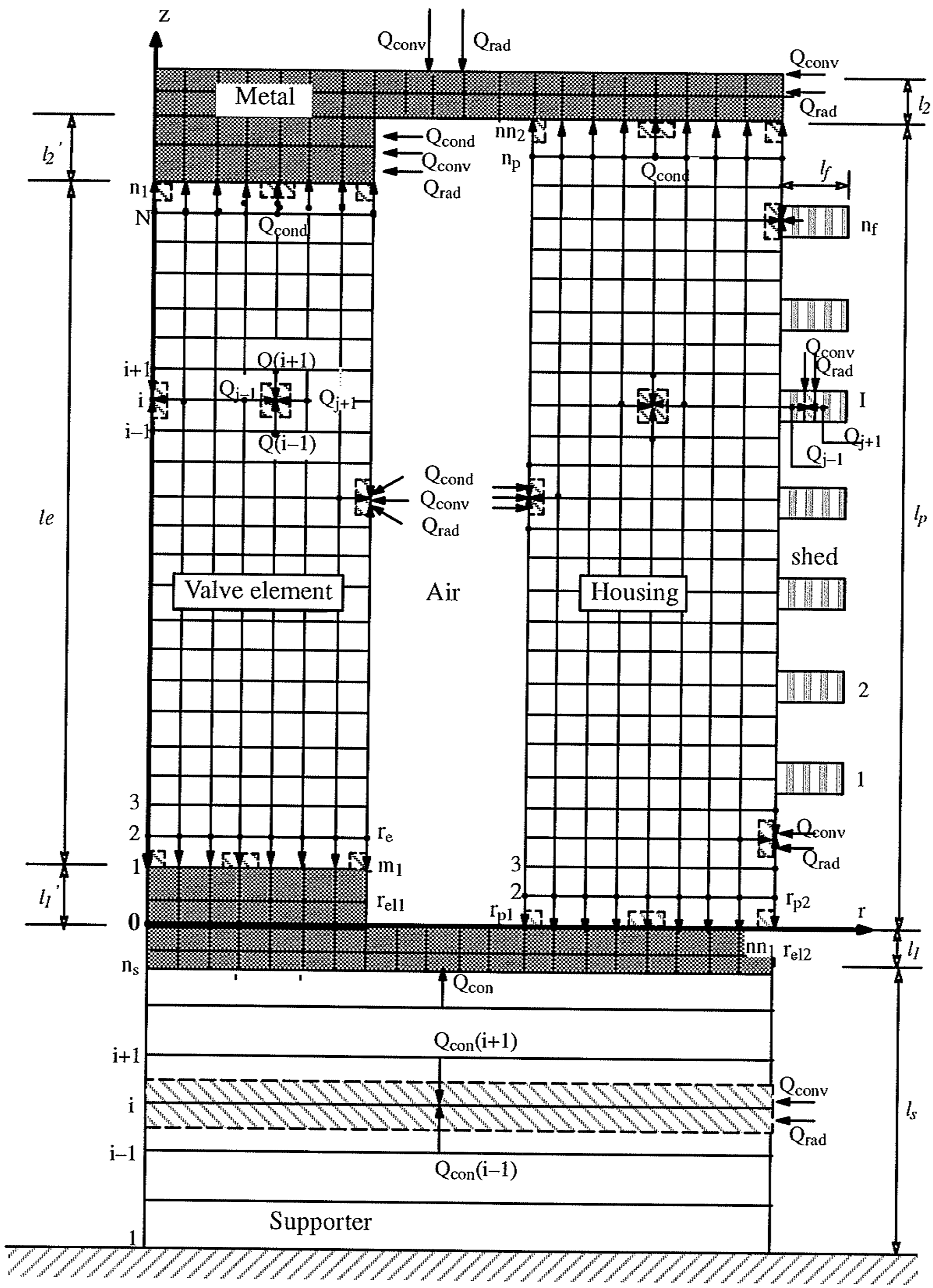

Figure 3.2 Cross section of MOSA to be simulated

3.1 Partial Differential Equations Governing Thermal Behaviour; Boundary Conditions [33–38]

Partial differential equations(PDE), along with associated boundary conditions of MOSA, are established in this section.

3.1.1 Metal Oxide Valve Elements

The governing heat equation for conduction in cylindrical coordinates is

$$\frac{\partial^2 T}{\partial r^2} + \frac{\partial T}{r\partial r} + \frac{\partial^2 T}{\partial z^2} + \frac{q}{k} = \frac{\partial T}{\alpha \partial t} \tag{3.1}$$

The valve element surface is exposed to enclosed convection, radiation and conduction heat transfer to the interior surface of arrester housing, and therefore the boundary conditions are derived as in Eq. 3.2.

$$\begin{aligned} -k2\pi r_e \left[\frac{\partial T}{\partial r}\right]_{r=r_e} &= h_{in}(2\pi r_e)\cdot\left([T]_{r=r_e} - [TT]_{r=r_{p1}}\right) + \frac{\sigma\left(\left[T^4\right]_{r_e} - \left[TT^4\right]_{r_{p1}}\right)}{R_a'} \\ &+ \frac{2\pi k_{air}\left([T]_{r_e} - [TT]_{r_{p1}}\right)}{\ln\frac{r_{p1}}{r_e}} \end{aligned} \tag{3.2}$$

where

$$R_a' = \frac{1-\varepsilon_e}{\varepsilon_e \cdot 2\pi r_e} + \frac{1}{F_{1\to 2}\cdot 2\pi r_{p1}} + \frac{1-\varepsilon_p}{\varepsilon_p \cdot 2\pi r_{p1}\Delta z_1} \tag{3.3}$$

Conduction from valve element surface to housing across the air layer is very small and can be neglected.

Along the line of symmetry,

$$\left[\frac{\partial T}{\partial r}\right]_{r=0} = 0 \tag{3.4}$$

At the contacted surface with the electrodes,

$$[T]_{z=l_1'} = TT_1 \qquad [T]_{z=l_e+l_1'} = TT_2 \qquad (3.5)$$

Calculation of the enclosed convective heat transfer coefficient, h_{in}, and the geometric radiation shape factor, F_{1-2}, of two concentric cylinders is described in Chapter 2.

3.1.2 Arrester Housing

In the arrester housing the PDE is

$$\frac{\partial^2 TT}{\partial r^2} + \frac{\partial TT}{r\partial r} + \frac{\partial^2 TT}{\partial z^2} = \frac{\partial TT}{\alpha_1 \partial t} \qquad (3.6)$$

The interior surface of the housing is also exposed to conduction, enclosed convection and radiation heat transfer and the boundary conditions can be derived as in Eq. 3.7. The exterior surface of the housing is subject to free or forced convection and radiation in its surroundings, and its boundary condition is derived as in Eq. 3.8. Radiation energy, q_{rad}, input to the exterior surface of housing from the sun and the sky may be taken into account in the field.

$$-k_1 \cdot 2\pi r_{p1}\left[\frac{\partial TT}{\partial r}\right]_{r=r_{p1}} = \frac{2\pi k_{air}\left([TT]_{r_{p1}} - [TT]_{r_e}\right)}{\ln\frac{r_{p1}}{r_e}} + h_{in}(2\pi r_{p1})\cdot\left([TT]_{r=r_{p1}} - [T]_{r=r_e}\right) + \frac{\sigma\left([TT^4]_{r_{p1}} - [T^4]_{r_e}\right)}{R_a'} \qquad (3.7)$$

$$-k_1\left[\frac{\partial TT}{\partial r}\right]_{r=r_{p2}} = h_1\cdot\left([TT]_{r=r_{p1}} - T_{amb}\right) + \delta\varepsilon_p\left([TT^4]_{r_{p2}} - T_{amb}^4\right) + q_{rad} \qquad (3.8)$$

Calculation of convective heat transfer coefficient, h_1, and solar/sky radiation energy input, q_{rad}, to the housing surface have been discussed in Chapter 2.

At the contacted surface with the electrodes,

$$[TT]_{z=0} = TTT_1 \qquad [T]_{z=l_p} = TTT_2 \tag{3.9}$$

3.1.3 Electrodes

Electrodes are subject to free or forced convection, radiation to surroundings and heat conduction from valve elements and housing. The electrodes are also subject to enclosed convection as well as radiation and conduction on the interior surfaces. Electrodes may be modelled as short or long.

Case 1: short electrodes

Eqs. 3.10–3.12 are derived by assuming that the metal electrode temperature is independent of coordinate because of its excellent thermal conductivity.

Top electrode:

$$-hA_1\cdot(TTT_2-T_{amb}) \quad -\varepsilon_{el}\sigma A_1(TTT_2^4-T_{amb}^4)-kA_2\left[\frac{\partial T}{\partial z}\right]_{z=l_1'+l_e} -kA_2'\left[\frac{\partial TT}{\partial z}\right]_{z=l_p}$$

$$-h_{in}A_4\cdot\left(TTT_2-[TT]_{r=r_{p1}}\right) \quad -\frac{\sigma\left(TTT_2^4-\left[TT^4\right]_{r=r_{p1}}\right)}{R_a'} \quad -\frac{2\pi k_{air}l_2'\left(TTT_2-[TT]_{r=r_{p1}}\right)}{\ln\frac{r_{p1}}{r_{el1}}}$$

$$+\,q_{rad}\,(A_1+A_3) \quad = \varrho_2 c_{p2} V_{el}\frac{\partial TTT_2}{\partial t} \tag{3.10}$$

$$R_a' = \frac{1-\varepsilon_{el}}{\varepsilon_{el}\cdot A_4}+\frac{1}{F_{1\rightarrow 2}\cdot A_4}+\frac{1-\varepsilon_p}{\varepsilon_p\cdot A_5}$$

Bottom electrode:

$$-h_1A_1\cdot(TTT_1-T_{amb})\ -\varepsilon_{el}\sigma A_1(TTT_1^4-T_{amb}^4)-kA_2\left[\frac{\partial T}{\partial z}\right]_{z=l_1'}\ -kA_2'\left[\frac{\partial TT}{\partial z}\right]_{z=0}$$

$$-k_1A_3\left[\frac{\partial TS_1}{\partial z}\right]_{z=-l_1}-h_{in}A_4\cdot\left(TTT_1-[TT]_{r=r_{p1}}\right)\ -\frac{\sigma\left(TTT_1^4-\left[TT^4\right]_{r=r_{p1}}\right)}{R_a'}$$

$$-\frac{2\pi k_{air}l_1'\left(TTT_1-[TT]_{r=r_{p1}}\right)}{\ln\frac{r_{p1}}{r_{el1}}}+q_{rad}A_1\ =\varrho_2c_{p2}V_{el}\frac{\partial TTT_1}{\partial t} \qquad (3.11)$$

$$\left[\frac{\partial TTT_1}{\partial t}\right]_{t\to\infty}=\left[\frac{\partial TTT_2}{\partial t}\right]_{t\to\infty}=0 \qquad (3.12)$$

where, A_1 = Contact area between metal electrode and ambient.

A_2 = Contact area between electrode and valve element.

A'_2 = Contact area between electrode and housing.

A_3 = Contact area between electrode and porcelain supporter of MOSA.

A_4 = Electrode interior surface area.

A_5 = Interior surface area of housing related to heat transfer to electrode interior surface.

Case 2: long electrodes

Heat conduction in a longer metal electrode should be considered in the calculation of temperature distribution of MOSA. In this case, the governing heat equation for conduction are expressed as in Eqs. 3.13–3.14, and the associated boundary conditions of electrodes are established as in Eqs. 3.15–3.20.

$$\frac{\partial^2 TTT_2}{\partial r^2}+\frac{\partial TTT_2}{r\partial r}+\frac{\partial^2 TTT_2}{\partial z^2}=\frac{\partial TTT_2}{\alpha_2 \partial t} \qquad (3.13)$$

$$\frac{\partial^2 TTT_1}{\partial r^2}+\frac{\partial TTT_1}{r\partial r}+\frac{\partial^2 TTT_1}{\partial z^2}=\frac{\partial TTT_1}{\alpha_2 \partial t} \qquad (3.14)$$

At the outside vertical surface,

$$-k_2\left[\frac{\partial TTT_2}{\partial r}\right]_{r=r_{el2}} = h_1\cdot\left([TTT_2]_{r=r_{el2}} - T_{amb}\right)$$
$$+\sigma\varepsilon_{p2}\left(\left[TTT_2^4\right]_{r_{el2}} - T_{amb}^4\right) + q_{rad} \qquad (3.15)$$

$$-k_2\left[\frac{\partial TTT_1}{\partial r}\right]_{r=r_{el2}} = h_1\cdot\left([TTT_1]_{r=r_{el2}} - T_{amb}\right)$$
$$+\sigma\varepsilon_{p2}\left(\left[TTT_1^4\right]_{r_{el2}} - T_{amb}^4\right) + q_{rad} \qquad (3.16)$$

At the outside horizontal surface,

$$-k_2\left[\frac{\partial TTT_2}{\partial z}\right]_{z=l_p+l_2} = h_{top}\cdot\left([TTT_2]_{z=l_p+l_2} - T_{amb}\right)$$
$$+\sigma\varepsilon_{p2}\left(\left[TTT_2^4\right]_{z=l_1+l_e+l_2} - T_{amb}^4\right) + q_{rad} \qquad (3.17)$$

At the contacted surface with the support structure,

$$[TTT_1]_{z=-l_1} = [T_1]_{z=-l_1} \qquad (3.20)$$

At the inside surfaces,

$$-k_2 2\pi r_{el1}\left[\frac{\partial TTT_2}{\partial r}\right]_{r=r_{el1}} = h_{in}(2\pi r_{el1})\cdot\left([TTT_2]_{r=r_{el1}}-[TT]_{r=r_{p1}}\right)$$

$$+\frac{2\pi k_{air}\left([TTT_2]_{r_{el1}}-[TT]_{r_{p1}}\right)}{\ln\frac{r_{p1}}{r_{el1}}}+\frac{\sigma\left(\left[TTT_2^4\right]_{r_{el1}}-\left[TT^4\right]_{r_{p1}}\right)}{R_a'} \qquad (3.18)$$

$$-k_2 2\pi r_{el1}\left[\frac{\partial TTT_1}{\partial r}\right]_{r=r_{el1}} = h_{in}(2\pi r_{el1})\cdot\left([TTT_1]_{r=r_{el1}}-[TT]_{r=r_{p1}}\right)$$

$$+\frac{2\pi k_{air}\left([TTT_1]_{r_{el1}}-[TT]_{r_{p1}}\right)}{\ln\frac{r_{p1}}{r_{el1}}}+\frac{\sigma\left(\left[TTT_1^4\right]_{r_{el1}}-\left[TT^4\right]_{r_{p1}}\right)}{R_a'} \qquad (3.18)$$

$$R_a'=\frac{1-\varepsilon_{el}}{\varepsilon_{el}\cdot 2\pi r_{el1}}+\frac{1}{F_{1\to 2}\cdot 2\pi r_{p1}}+\frac{1-\varepsilon_p}{\varepsilon_p\cdot 2\pi r_{p1}\Delta z_1}$$

3.2 Finite Difference Equations [39–42]

To solve numerically, using the method of finite differences, the partial differential equations are approximated with finite difference expressions at each node, and are transformed to a set of algebraic equations which can easily be solved digitally.

3.2.1. Valve Element and Arrester Housing Interior

(1) Valve element

In the valve element interior nodes (i=2,3, ...N; j=2, 3, ...M) (except r=0), heat conduction is the only mode of heat transfer.

By Taylor's series, finite difference approximations for partial derivatives are

$$\frac{\partial^2 T}{\partial r^2} \approx \frac{T^n_{i,j+1} - 2T^n_{i,j} + T^n_{i,j-1}}{\Delta r^2} \qquad \frac{\partial^2 T}{\partial z^2} \approx \frac{T^n_{i+1,j} - 2T^n_{i,j} + T^n_{i-1,j}}{\Delta z^2} \tag{3.21}$$

$$\frac{\partial T}{\partial r} \approx \frac{T^n_{i,j+1} - T^n_{i,j-1}}{2\Delta r} \qquad \frac{\partial T}{\partial t} \approx \frac{T^{n+1}_{i,j} - T^n_{i,j}}{\Delta t} \tag{3.22}$$

Substituting Eqs. 3.21–3.22 in Eq. 3.1, we obtain

$$\frac{T^{n+1}_{i,j} - T^n_{i,j}}{\Delta t} \cdot \varrho \cdot c_p = k\left[\frac{T^n_{i+1,j} - 2T^n_{i,j} + T^n_{i-1,j}}{\Delta z^2} + \frac{T^n_{i,j+1} - 2T^n_{i,j} + T^n_{i,j-1}}{\Delta r^2}\right]$$

$$+\frac{k}{r_j} \cdot \frac{(T^n_{i,j+1} - T^n_{i,j-1})}{2\Delta r} + q_i \tag{3.23}$$

where, n and n+1 denote the n^{th} and $(n+1)^{th}$ step of calculation.

(2) Arrester housing

Similarly, at interior nodes in the housing (i=2,3, ...n_p; j=2, 3, ...nn), the FDE is

$$\frac{TT^{n+1}_{i,j} - TT^n_{i,j}}{\Delta t} \cdot \varrho_1 \cdot c_{p1} = k_1\left[\frac{TT^n_{i+1,j} - 2TT^n_{i,j} + TT^n_{i-1,j}}{\Delta z^2} + \frac{TT^n_{i,j+1} - 2TT^n_{i,j} + TT^n_{i,j-1}}{\Delta r^2}\right]$$

$$+\frac{k}{r_j} \cdot \frac{(TT^n_{i,j+1} - TT^n_{i,j-1})}{2\Delta r} \tag{3.24}$$

3.2.2 Axis of Symmetry (r=0)

Along centrally located nodes at r=0, the finite difference representation of Eq. 3.1 is obtained as

$$\frac{T_{i,j}^{n+1}-T_{i,j}^{n}}{\Delta t}\cdot\varrho\cdot c_p = k\cdot\lim_{r\to 0}\left(\frac{\partial^2 T}{\partial r^2}+\frac{1}{r}\cdot\frac{\partial T}{\partial r}+\frac{\partial^2 T}{\partial z^2}\right)+q = k\left(2\frac{\partial^2 T}{\partial r^2}+\frac{\partial^2 T}{\partial z^2}\right)+q$$

$$= k\left[\frac{T_{i-1,j}^{n}-2T_{i,j}^{n}+T_{i+1,j}^{n}}{\Delta z^2}+\frac{4\left(T_{i,j+1}^{n}-T_{i,j}^{n}\right)}{\Delta r^2}\right]+q_i \qquad (3.25)$$

3.2.3 Valve Element Surface

The surface nodal equations are found by applying the principle of conservation of energy at the surface. The nodal equations must account for conduction to the cylindrical surface from within the valve element as well as heat loss due to convection and radiation.

At any node (i, j) heat flow into it due to conduction from the neighboring nodes is given by

$$Q_{cond} = k\cdot\frac{T_{i+1,j}-T_{i,j}}{\Delta z}\cdot A_1 + k\cdot\frac{T_{i-1,j}-T_{i,j}}{\Delta z}\cdot A_1 + k\cdot\frac{T_{i,j-1}-T_{i,j}}{\Delta r}\cdot A_2$$

$$+ k_{air}\cdot\frac{(TT_{i,1}-T_{i,j})\cdot 2\pi\Delta z}{\ln\frac{r_{p1}}{r_e}} \qquad (3.26)$$

where, $A_1 = \pi(r_j^2-(r_j-\frac{\Delta r}{2})^2)$ $\qquad A_2 = 2\pi(r_j-\frac{\Delta r}{2})\cdot\Delta z$

and heat loss due to convection and radiation is given by

$$Q_{conv} = h_{in} \cdot A_3 \cdot (TT_{i,1} - T_{i,j}) \tag{3.27}$$

$$Q_{rad} = \sigma \sum_{ii} \frac{(TT_{ii,1} + 273)^4 - (T_{i,j} + 273)^4}{R'_{a,ii}} \tag{3.28}$$

where,

$$A_3 = 2\pi r_e \Delta z\ , \qquad R'_{a,ii} = \frac{1-\varepsilon_e}{\varepsilon_e \cdot A_3} + \frac{1}{F_{i-ii} \cdot A_3} + \frac{1-\varepsilon_p}{\varepsilon_p \cdot 2\pi r_{p1} \Delta z_1}$$

F_{i-ii} is the radiation shape factor from a small valve element cylindrical surface i to the adjacent small arrester housing cylindrical surface, ii (ii=1 to 3), which can be calculated by Eqs. 2.25 –2.28.

Thus, the finite difference equation at node (i, j) is

$$\frac{T_{i,j}^{n+1} - T_{i,j}}{\Delta t} \cdot \varrho \cdot c_p \cdot V_l = Q_{cond} + Q_{conv} + Q_{rad} + q_i \cdot V_l \tag{3.29}$$

where, $V_l = A_1 \cdot \Delta z$

3.2.4 Interior Surface of Arrester Housing

Eqs. 3.29–3.33 are similar representations for the interior surface of arrester housing.

$$Q_{cond} = k_1 \cdot \frac{TT_{i+1,j} - TT_{i,j}}{\Delta z_1} \cdot A_1 + k_1 \cdot \frac{TT_{i-1,j} - TT_{i,j}}{\Delta z_1} \cdot A_1 + k_1 \cdot \frac{TT_{i,j+1} - TT_{i,j}}{\Delta r_1} \cdot A_2$$

$$+ k_{air} \cdot \frac{(T_{i,m_1} - TT_{i,j}) \cdot 2\pi \Delta z_1}{\ln \frac{r_{p1}}{r_e}} \tag{3.30}$$

$$Q_{conv} = h_{in} \cdot A_3 \cdot (T_{i,m_1} - TT_{i,j}) \tag{3.31}$$

$$Q_{rad} = \sigma \sum_{ii} \frac{(T_{ii,m_1} + 273)^4 - (TT_{i,j} + 273)^4}{R'_{a,ii}} \quad \text{and} \tag{3.32}$$

$$\frac{TT_{i,j}^{n+1} - TT_{i,j}}{\Delta t} \cdot \varrho_1 \cdot c_{p1} \cdot V_l = Q_{cond} + Q_{conv} + Q_{rad} \tag{3.33}$$

where, $A_1 = \pi\left[\left(r_j + \frac{\Delta r_1}{2}\right)^2 - r_j^2\right]$, $A_2 = 2\pi\left(r_j + \frac{\Delta r_1}{2}\right) \cdot \Delta z_1$,

$A_3 = 2\pi r_j \Delta z_1$, $V_l = A_1 \cdot \Delta z_1$

3.2.5 Exterior Surface of Housing

The exterior surface of arrester housing is modelled as a cylinder, and the finite difference expressions can be obtained.

At node (i,j), heat flow into it due to conduction from within the housing is expressed by

$$Q_{cond} = k_1 \cdot \frac{TT_{i+1,j} - TT_{i,j}}{\Delta z_1} \cdot A_1 + k_1 \cdot \frac{TT_{i-1,j} - TT_{i,j}}{\Delta z_1} \cdot A_1 + k_1 \cdot \frac{TT_{i,j-1} - TT_{i,j}}{\Delta r_1} \cdot A_2 \tag{3.34}$$

where, $A_1 = \pi[r_j^2 - (r_j - \frac{\Delta r_1}{2})^2]$ $A_2 = 2\pi(r_j - \frac{\Delta r_1}{2}) \cdot \Delta z_1$

Heat loss from it due to convection is expressed by

$$Q_{conv} = h_1 \cdot A_3 \cdot (T_{amb} - TT_{i,j}) \tag{3.35}$$

where, $A_3 = 2\pi r_j \Delta z_1$

Heat loss and input due to radiation is expressed by

$$Q_{rad} = \sigma \varepsilon_p \cdot A_3 \cdot \left[(T_{amb} + 273)^4 - (TT_{i,j} + 273)^4 \right] + A_3 \cdot q_{rad} \tag{3.36}$$

Thus, the finite difference equation is expressed as

$$\frac{TT_{i,j}^{n+1} - TT_{i,j}}{\Delta t} \cdot \varrho_1 \cdot c_{p1} \cdot V_l = Q_{cond} + Q_{conv} + Q_{rad} \tag{3.37}$$

where, $V_l = A_1 \cdot \Delta z_1$

3.2.6 Exterior Surface of Arrester Housing and Sheds

Numerical calculations have shown that the exterior surface of an arrester housing may not be simplified as a cylinder on account of heat transfer modes. There may be a significant temperature drop between the base and tip of shed at high temperature of MOSA and this affects heat transfer. Therefore, fin theory is applied to derive the following equations for accurately calculating heat transfer from the extended surface of arrester housing. The sheds are modelled as radial fins of rectangular profile as shown in Fig. 3.3.

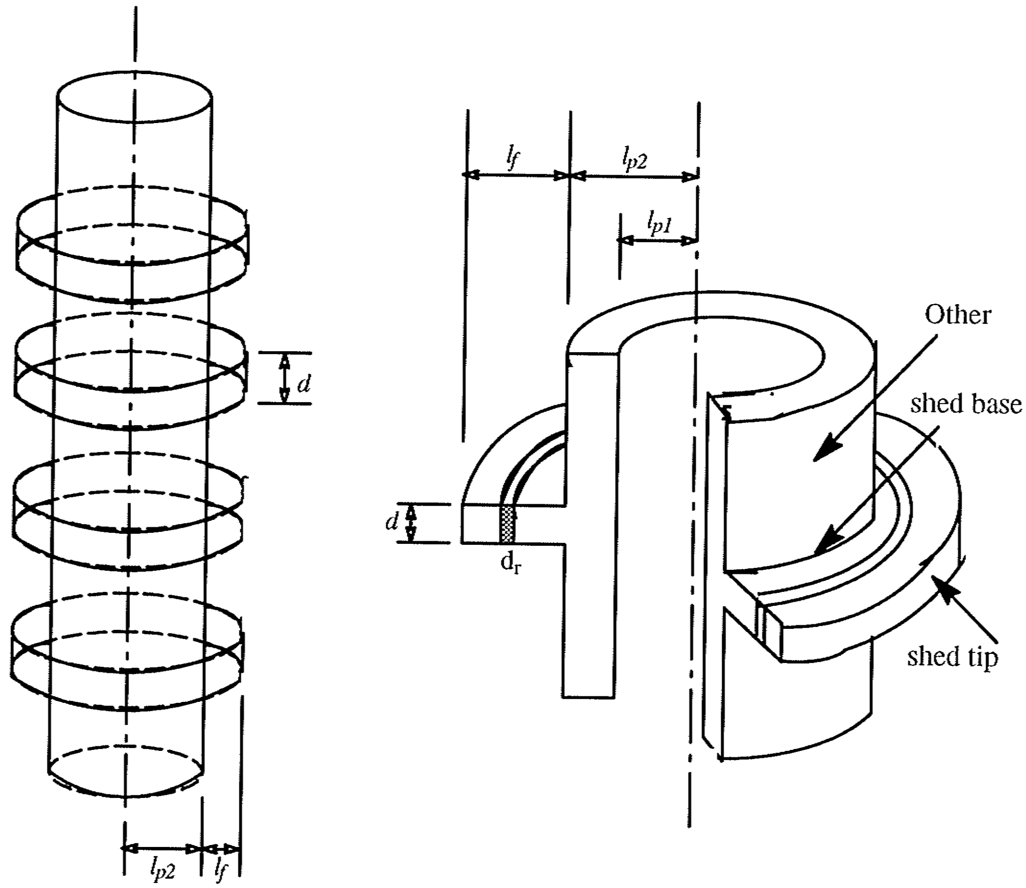

Figure 3.3 Shed representation

(1) shed interior

It is assumed that the shed temperature changes only in the radial direction because it is thin.

Heat conduction:

$$Q_{cond} = k_1 \cdot \frac{TF_{I,j-1} - TF_{I,j}}{\Delta r_1} \cdot A_1 + k_1 \cdot \frac{TF_{I,j+1} - TF_{I,j}}{\Delta r_1} \cdot A_2 \tag{3.38}$$

where, $A_1 = 2\pi\left(r_j - \frac{\Delta r_1}{2}\right) \cdot d \qquad A_2 = 2\pi\left(r_j + \frac{\Delta r_1}{2}\right) \cdot d$

Heat convection and radiation:

$$Q_{conv} = 2h \cdot A_3 \cdot \left(T_{amb} - TF_{I,j}\right) \tag{3.39}$$

$$Q_{rad} = 2\sigma\varepsilon_p \cdot A_3 \cdot \left[(T_{amb} + 273)^4 - (TF_{i,j} + 273)^4\right] + q_{rad} \cdot A_3 \tag{3.40}$$

where, $A_3 = 2\,\pi\, r_j\, \Delta r_1$,

The PDE is

$$\frac{TF_{I,j}^{n+1} - TF_{I,j}}{\Delta t} \cdot \varrho_1 \cdot c_{p1} \cdot V_l = Q_{cond} + Q_{conv} + Q_{rad} \tag{3.41}$$

where, $V_l = A_3 \cdot d$

(2) shed tip temperature (Vertical portion)

The PDE is

$$\frac{TF_{I,m_2+1}^{n+1} - TF_{I,m_2+1}}{\Delta t} \cdot \varrho_1 \cdot c_{p1} \cdot V_l = Q_{cond} + Q_{conv} + Q_{rad} \tag{3.42}$$

where

$$Q_{cond} = k_1 \cdot \frac{TF_{I,m_2} - TF_{I,m_2+1}}{\Delta r_1} \cdot A_1 \tag{3.43}$$

$$Q_{conv} = h_1 A_2 \cdot (T_{amb} - TF_{i,m_2+1}) + 2h \cdot A_3 \cdot (T_{amb} - TF_{I,m_2+1}) \tag{3.44}$$

$$Q_{rad} = \sigma\varepsilon_p \cdot [(T_{amb} + 273)^4 - (TF_{I,m_2+1} + 273)^4] \cdot (A_2 + 2A_3) + q_{rad} \cdot (A_2 + A_3)$$

(3.45)

and $A_1 = 2\pi(r_{p3} - \frac{\Delta r_1}{2}) \cdot d$ $\quad A_2 = 2\pi(r_{p3} \cdot d$

$A_3 = \pi\left[r_{p3}^2 - (r_{p3} - \frac{\Delta r_1}{2})^2 \right]$ $\quad V_I = A_2 \cdot \Delta z_1$

(3) shed base: z=z(I)

At the shed base conduction is the only heat transfer mode.

$$Q_{cond} = k_1 \cdot \frac{TT_{i,nn} - TF_{I,1}}{\Delta r_1} \cdot A_1 + k_1 \cdot \frac{TF_{I,2} - TF_{I,1}}{\Delta r_1} \cdot A_3$$

$$+ k_1 \cdot \frac{TT_{i+1,nn_1} - TF_{I,1}}{\Delta z_1} \cdot A_2 + k_1 \cdot \frac{TT_{i-1,nn_1} - TF_{I,1}}{\Delta z_1} \cdot A_2 \qquad (3.46)$$

$$\frac{TF_{I,1}^{n+1} - TF_{I,1}}{\Delta t} \cdot \varrho_1 \cdot c_{p1} \cdot V_I = Q_{cond} \qquad (3.47)$$

where, $A_1 = 2\pi(r_{p2} - \frac{\Delta r_1}{2}) \cdot \Delta z_1$ $\quad A_2 = \pi\left[r_{p2}^2 - (r_{p2} - \frac{\Delta r_1}{2})^2 \right]$

$A_3 = 2\pi(r_{p2} + \frac{\Delta r_1}{2}) \cdot \Delta z_1$ $\quad V_I = A_2 \cdot \Delta z_1$

(4) Other cylindrical external surface to which sheds are attached: $z \neq z(I)$

$$Q_{cond} = k_1 \cdot \frac{TT_{i,nn} - TT_{i,nn_1}}{\Delta r_1} \cdot A_1 + k_1 \cdot \frac{TT_{i+1,nn_1} - TT_{i,nn_1}}{\Delta z_1} \cdot A_2 + k_1 \cdot \frac{TT_{i-1,nn_1} - TT_{i,nn_1}}{\Delta z_1} \cdot A_2 \tag{3.48}$$

$$Q_{conv} = h_1 \cdot A_4 \cdot (T_{amb} - TT_{i,nn_1}) \tag{3.49}$$

$$Q_{rad} = \sigma \varepsilon_p \cdot A_4 \cdot \left[(T_{amb} + 273)^4 - (TT_{i,nn_1} + 273)^4 \right] + q_{rad} \cdot A_4 \tag{3.50}$$

$$\frac{TT_{I,nn_1}^{n+1} - TT_{I,nn_1}}{\Delta t} \cdot \varrho_1 \cdot c_{p1} \cdot V_I = Q_{cond} + Q_{conv} + Q_{rad} \tag{3.51}$$

where, $A_4 = 2\pi \cdot r_{p2} \Delta z_1$ and the value of A_1, A_2, A_3 and V_I is the same as above.

3.2.7 Electrode Temperature

(1) Short electrode (case 1 of 3.1.3) :

Heat input and loss from the top electrode is due to conduction, convection and radiation in accordance with Eqs. 3.52–3.55.

Heat transfer to the top electrode due to conduction from valve element is:

$$Q_{cond1} = \sum_{j=2}^{m} k \cdot \frac{T_{n,j} - TTT_2}{\Delta z} \cdot A_1 + k \cdot \frac{T_{n,1} - TTT_2}{\Delta z} \cdot A_2 + k \cdot \frac{T_{n,m_1} - TTT_2}{\Delta z} \cdot A_3 \tag{3.52}$$

where, $A_1 = \pi \cdot 2 r_j \Delta r$ $A_2 = \pi \left(\frac{\Delta r}{2} \right)^2$ $A_3 = \pi \left[r_e^{\,2} - (r_e - \frac{\Delta r}{2})^2 \right]$

and heat conduction from housing is:

$$Q_{cond2} = \sum_{j=2}^{nn} k_1 \cdot \frac{TT_{n_p,j} - TTT_2}{\Delta z_1} \cdot A_4 + k_1 \cdot \frac{TT_{n_p,1} - TTT_2}{\Delta z_1} \cdot A_5 + k_1 \cdot \frac{TT_{n_p,nn_1} - TTT_2}{\Delta z_1} \cdot A_6 \tag{3.53}$$

where, $A_5 = \pi \left[(r_{p1} + \frac{\Delta r_1}{2})^2 - r_{p1}^{\,2} \right]$ $A_6 = \pi \left[r_{p2}^{\,2} - (r_{p2} - \frac{\Delta r_1}{2})^2 \right]$

$A_4 = \pi \cdot 2 \cdot rr_j \Delta r_1$

The electrode is subjected to free convection on the interior surface and free or forced convection on its exterior surface.

$$Q_{conv} = (T_{amb} - TTT_2) \cdot (h_{top} \cdot A_7 + h_1 \cdot A_8) + h_{in}(TT_{i,1} - TTT_2) \cdot A_8' \tag{3.54}$$

where, $A_7 = \pi (r_{el2})^2$ $A_8 = 2\pi \cdot r_{el2} l_2$

$A_8' = 2\pi \cdot r_{el1} l_2'$

Heat transfer due to radiation:

$$Q_{rad} = \sigma\varepsilon_{el}\cdot\left[(T_{amb}+273)^4-(TTT_2+273)^4\right]\cdot(A_7+A_8)$$

$$+\sigma\frac{(TT_{i,1}+273)^4-(TTT_2+273)^4}{R_a^{'}} + q_{rad}\,(A_7+A_8) \tag{3.55}$$

where,

$$R_a^{'} = \frac{1-\varepsilon_{el}}{\varepsilon_{el}\cdot A_8^{'}} + \frac{1}{F_{1-2}\cdot A_8^{'}} + \frac{1-\varepsilon_{p1}}{\varepsilon_{p1}\cdot 2\pi r_{p1} l_{el1}}$$

The finite difference representation for the top electrode is

$$\frac{TTT_2^{n+1}-TTT_2}{\Delta t}\cdot\varrho_2\cdot c_{p2}\cdot V_l = Q_{cond1}+Q_{cond2}+Q_{conv}+Q_{rad} \tag{3.56}$$

where $V_l = A_7\cdot l_2 + \pi(r_{el1})^2 l_2^{'}$

Similarly, Eqs. 3.57–3.62 represent conditions at the bottom electrode.

$$Q_{cond1} = \sum_{j=2}^{m} k\cdot\frac{T_{2,j}-TTT_1}{\Delta z}\cdot A_1 + k\cdot\frac{T_{2,1}-TTT_1}{\Delta z}\cdot A_2 + k\cdot\frac{T_{2,m_1}-TTT_1}{\Delta z}\cdot A_3 \tag{3.57}$$

$$Q_{cond2} = \sum_{j=2}^{nn} k_1\cdot\frac{TT_{n_p,j}-TTT_1}{\Delta z_1}\cdot A_4 + k_1\cdot\frac{TT_{2,1}-TTT_1}{\Delta z_1}\cdot A_5 + k_1\cdot\frac{TT_{2,nn_1}-TTT_1}{\Delta z_1}\cdot A_6 \tag{3.58}$$

$$Q_{cond3} = k_1\cdot\frac{TS_{n_s}-TTT_1}{\Delta z_2}\cdot\pi(r_{p2})^2 \tag{3.59}$$

$$Q_{conv} = h_1(T_{amb}-TTT_1)\cdot 2\pi r_{p2}\cdot l_1 + h_{in}(TT_{i,1}-TTT_1)\cdot A_8^{'} \tag{3.60}$$

$$Q_{rad} = \sigma\varepsilon_{el}\cdot\left[(T_{amb}+273)^4-(TTT_1+273)^4\right]\cdot(2\pi r_{p2}\cdot l_1)$$

$$+\sigma\frac{(TT_{i,1}+273)^4-(TTT_1+273)^4}{R_a^{'}}+q_{rad}\cdot(2\pi r_{p2}\cdot l_1) \quad (3.61)$$

$$\frac{TTT_1^{n+1}-TTT_1}{\Delta t}\cdot\varrho_2\cdot c_{p2}\cdot V_l = Q_{cond1}+Q_{cond2}+Q_{cond3}+Q_{conv}+Q_{rad} \quad (3.62)$$

(2) Long electrode (case 2 of section 3.1.3) :

Similar to the derivation of the above finite difference equations in section 3.2.1–3.2.5, electrode nodal temperature in both radial and axial directions can be calculated.

–Electrode interior:

$$\frac{TTT_2^{n+1}(i,j)-TTT_2(i,j)}{\Delta t}\cdot\varrho_2\cdot c_{p2}$$

$$= k_2\left[\frac{TTT_2(i+1,j)-2TTT_2(i,j)+TTT_1(i-1,j)}{\Delta z^2}+\frac{TTT_2(i,j+1)-2TTT_2(i,j)+TTT_2(i,j-1)}{\Delta r^2}\right]$$

$$+\frac{k_2}{r_j}\cdot\frac{TTT_2(i,j+1)-TTT_2(i,j-1)}{2\Delta r} \quad (3.63)$$

Interior temperature of bottom electrode, $TTT_1(i,j)$, has the same expression as Eq. 3.63.

–Electrode interior surface:

On the interior surface of electrodes, heat transfer to the node (i,j) by conduction, Q_{cond}, convection, Q_{conv}, and radiation, Q_{rad}, have the same form as the Eqs. 3.26–3.28. Therefore, the FDE is

$$\frac{TTT_2(i,j)^{n+1} - TTT_2(i,j)}{\Delta t} \cdot \varrho_2 \cdot c_{p2} \cdot V_l = Q_{cond} + Q_{conv} + Q_{rad} \tag{3.64}$$

where, $V_l = \pi(r_{el1}{}^2 - (r_{el1} - \frac{\Delta r}{2})^2) \cdot \Delta z$

Interior surface temperature of bottom electrode, TTT_1(i,j), has the same expression as Eq. 3.64.

–Electrode exterior surface:

The finite difference equations on the exterior vertical surface of electrodes have the same form as the Eqs. 3.34–3.37 which apply to the exterior surface of the arrester housing.

On the horizontal surface of the top electrode:

$$Q_{cond} = k_2 \cdot \frac{TTT_2(i+1,j) - TTT_2(i,j)}{\Delta r} \cdot A_1 + k_2 \cdot \frac{TTT_2(i-1,j) - TTT_2(i,j)}{\Delta r} \cdot A_2 + k_2 \cdot \frac{TTT_2(i,j-1) - TTT_2(i,j)}{\Delta z} \cdot A_3 \tag{3.65}$$

where, $A_1 = 2\pi(r_j + \frac{\Delta r}{2}) \cdot \Delta z$ $A_2 = 2\pi(r_j - \frac{\Delta r}{2}) \cdot \Delta z$

$A_3 = \pi[(r_j + \frac{\Delta r}{2})^2 - (r_j - \frac{\Delta r}{2})^2]$

$$Q_{conv} = h_{top} \cdot A_3 \cdot (T_{amb} - TTT_2(i,j)) \tag{3.66}$$

$$Q_{rad} = \sigma\varepsilon_{el}{\cdot}A_3{\cdot}\left[(T_{amb} + 273)^4 - (TTT_2(i,j) + 273)^4\right] + A_3{\cdot}q_{rad} \tag{3.67}$$

Thus, the FDE is expressed as

$$\frac{TTT_2(i,j)^{n+1} - TTT_2(i,j)}{\Delta t}{\cdot}\varrho_2{\cdot}c_{p2}{\cdot}V_l = Q_{cond} + Q_{conv} + Q_{rad} \tag{3.68}$$

where, $V_l = A_3{\cdot}\dfrac{\Delta z}{2}$

3.2.8 Support Structure (Porcelain)

For the support structure, only axial temperature variation is allowed because radial temperature variation of the support is not significant and has little influence to the arrester heat transfer. In this case, Eqs. 3.69–3.72 hold. Temperature at the support bottom does not change with time and is specified to be ambient.

$$Q_{cond} = k_1{\cdot}\frac{TS_{i+1} - TS_i}{\Delta z_2}{\cdot}A_1 + k_1{\cdot}\frac{TS_{i-1} - TS_i}{\Delta z_2}{\cdot}A_1 \tag{3.69}$$

$$Q_{conv} = h_1{\cdot}A_2{\cdot}(T_{amb} - TS_i) \tag{3.70}$$

$$Q_{rad} = \sigma\varepsilon_p{\cdot}A_2{\cdot}\left[(T_{amb} + 273)^4 - (TS_i + 273)^4\right] \tag{3.71}$$

$$\frac{TS_i^{n+1} - TS_i}{\Delta t}{\cdot}\varrho_1{\cdot}c_{p1}{\cdot}V_l = Q_{cond} + Q_{conv} + Q_{rad} \tag{3.72}$$

where, $A_1 = \pi(r_{p2})^2$ $A_2 = 2\pi{\cdot}r_{p2}\Delta z_2$ $V_l = A_1{\cdot}\Delta z_2$

$TS_1 = T_{amb}$

3.3 Choice of Time Step: Δt

To maintain stability and convergence of the numerical solution, the time step , Δt, has to be chosen suitably.

From Eq. 3.23 (section 3.2.1), we have

$$T_{i,j}^{n+1} =$$

$$\frac{k \cdot \Delta t}{\varrho \cdot c_p}\left[\frac{T_{i-1,j}+T_{i+1,j}}{\Delta z^2}+\frac{T_{i,j-1}+T_{i,j+1}}{\Delta r^2}+\frac{1}{r_j}\frac{T_{i,j+1}-T_{i,j-1}}{2\Delta r}+\left(\frac{\varrho \cdot c_p}{k \cdot \Delta t}-\frac{2}{\Delta z^2}-\frac{2}{\Delta r^2}\right)T_{i,j}\right]+\frac{\Delta t}{\varrho \cdot c_p}q$$

For $\frac{\varrho \cdot c_p}{k \cdot \Delta t}-\frac{2}{\Delta z^2}-\frac{2}{\Delta r^2}>0$, we obtain

$$\Delta t < \frac{\varrho c_p}{k\left(\frac{2}{\Delta z^2}+\frac{2}{\Delta r^2}\right)} \tag{3.73}$$

From Eq. 3.24 (section 3.2.1) , we have

$$T_{i,j}^{n+1} =$$

$$\frac{k_1 \cdot \Delta t}{\varrho_1 \cdot c_{p1}}\left[\frac{TT_{i-1,j}+TT_{i+1,j}}{\Delta z_1^2}+\frac{TT_{i,j-1}+TT_{i,j+1}}{\Delta r_1^2}+\frac{1}{r_j}\frac{TT_{i,j+1}-TT_{i,j-1}}{2\Delta r_1}+\left(\frac{\varrho_1 \cdot c_{p1}}{k_1 \cdot \Delta t}-\frac{2}{\Delta z_1^2}-\frac{2}{\Delta r_1^2}\right)TT_{i,j}\right]$$

$$\frac{\varrho_1 \cdot c_{p1}}{k_1 \cdot \Delta t}-\frac{2}{\Delta z_1^2}-\frac{2}{\Delta r_1^2}>0 \qquad \Delta t < \frac{\varrho_1 c_{p1}}{k_1\left(\frac{2}{\Delta z_1^2}+\frac{2}{\Delta r_1^2}\right)} \tag{3.74}$$

From Eq. 3.25 (section 3.2.2) ,

$$T_{i,j}^{n+1} = \frac{k\cdot\Delta t}{\varrho\cdot c_p}\left[\frac{T_{i-1,j}+T_{i+1,j}}{\Delta z^2}+\frac{4T_{i,j+1}}{\Delta R^2}+\left(\frac{\varrho\cdot c_p}{k\cdot\Delta t}-\frac{2}{\Delta z^2}-\frac{4}{\Delta r^2}\right)T_{i,j}\right]+\frac{\Delta t}{\varrho\cdot c_p}q$$

$$\frac{\varrho\cdot c_p}{k\cdot\Delta t}-\frac{2}{\Delta z^2}-\frac{4}{\Delta r^2}>0 \qquad \Delta t<\frac{\varrho c_p}{k\left(\frac{2}{\Delta z^2}+\frac{4}{\Delta r^2}\right)} \qquad (3.75)$$

Thus, stability restricts the size of time step for a given space value of Δz and Δr. The time step is chosen smaller than that described in Eqs. 3.73–3.75 to get a stable solution.

3.4 Mathematical Simulation of Test Section

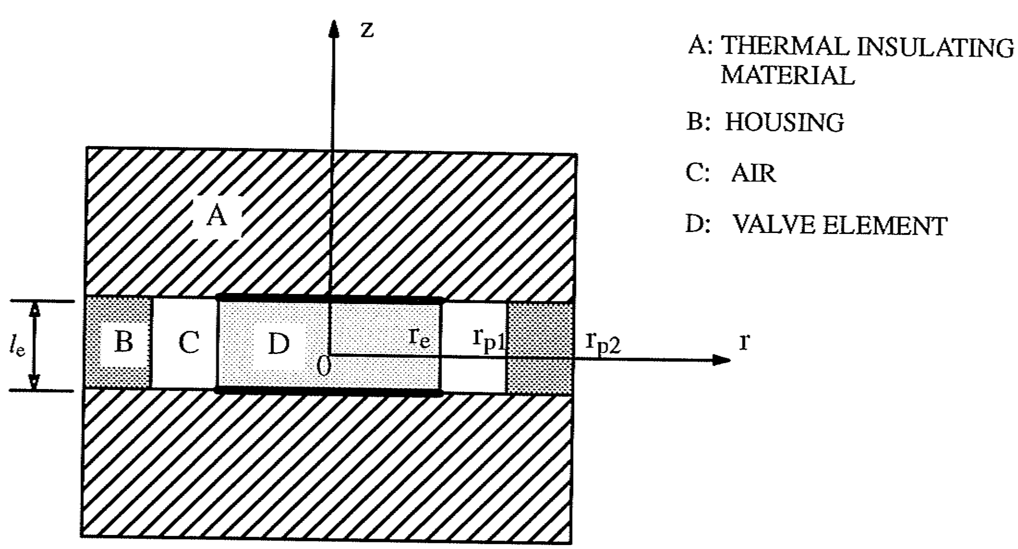

Figure 3.4 Configuration of a test section

Fig. 3.4 shows a single element test section. Because both ends of the valve element are thermally insulated by suitable insulating material to suppress axial heat follow, the axial heat transfer from the valve element may be negligible. In this model, only radial heat transfer is considered. Finite difference equations can be easily derived as follows based on the same principle described in the above sections.

3.4.1 Valve Element and Housing Interior

$$\frac{T_j^{n+1} - T_j^n}{\Delta t} \cdot \varrho \cdot c_p = k\left[\frac{T_{j+1}^n - 2T_j^n + T_{j-1}^n}{\Delta r^2}\right] + \frac{k}{r_j} \cdot \frac{(T_{j+1}^n - T_{j-1}^n)}{2\Delta r} + q \qquad (3.76)$$

$$\frac{TT_j^{n+1} - TT_j^n}{\Delta t} \cdot \varrho_1 \cdot c_{p1} = k_1\left[\frac{TT_{j+1}^n - 2TT_j^n + TT_{j-1}^n}{\Delta r^2}\right] + \frac{k_1}{r_j} \cdot \frac{(TT_{j+1}^n - TT_{j-1}^n)}{2\Delta r} \qquad (3.77)$$

3.4.2 Axis of Symmetry (r=0)

$$\frac{T_j^{n+1} - T_j^n}{\Delta t} \cdot \varrho \cdot c_p = k \cdot \lim_{r \to 0}\left(\frac{\partial^2 T}{\partial r^2} + \frac{1}{r} \cdot \frac{\partial T}{\partial r}\right) + q = k\left[\frac{4\left(T_{j+1}^n - T_j^n\right)}{\Delta r^2}\right] + q \qquad (3.78)$$

3.4.3 Valve Element Surface

$$Q_{cond} = k \cdot \frac{T_{j-1} - T_j}{\Delta r} \cdot A_1 + k_{air} \cdot \frac{(TT_1 - T_j) \cdot 2\pi l_e}{\ln \frac{r_{p1}}{r_e}} \qquad (3.79)$$

$$Q_{conv} = h_{in} \cdot A \cdot (TT_1 - T_j) \tag{3.80}$$

$$Q_{rad} = \frac{(TT_1 + 273)^4 - (T_j + 273)^4}{R_a'} \tag{3.81}$$

where, $A_1 = 2\pi(r_j - \frac{\Delta r}{2}) \cdot l_e$ $\qquad A = 2\pi r_e l_e$

$$R_a' = \frac{1-\varepsilon_e}{\varepsilon_e \cdot A_1} + \frac{1}{F_{1-2} \cdot A} + \frac{1-\varepsilon_p}{\varepsilon_p \cdot 2\pi r_{p1} l_e}$$

Radiation shape factor F_{1-2} can be calculated by Eqs. 2.22 –2.24.

$$\frac{T_j^{n+1} - T_j}{\Delta t} \cdot \varrho \cdot c_p \cdot V_l = Q_{cond} + Q_{conv} + Q_{rad} + q \cdot V_l \tag{3.82}$$

where, $V_l = \pi(r_j^2 - (r_j - \frac{\Delta r}{2})^2) \cdot l_e$

3.4.4 Interior Surface of the Housing

$$Q_{cond} = k_1 \cdot \frac{TT_{j+1} - TT_j}{\Delta r_1} \cdot A_1 + k_{air} \cdot \frac{(T_{m_1} - TT_j) \cdot 2\pi l_1}{\ln \frac{r_{p1}}{r_e}} \tag{3.83}$$

$$Q_{conv} = h_{in} \cdot A \cdot (T_{m_1} - TT_j) \tag{3.84}$$

$$Q_{rad} = \sigma \frac{(T_{m_1} + 273)^4 - (TT_j + 273)^4}{R_a'} \tag{3.85}$$

$$\frac{TT_{i,j}^{n+1} - TT_{i,j}}{\Delta t} \cdot \varrho_1 \cdot c_{p1} \cdot V_l = Q_{cond} + Q_{conv} + Q_{rad} \tag{3.86}$$

where, $A_1 = 2\pi\left(r_j + \frac{\Delta r_1}{2}\right) \cdot l_e$ $\qquad A = 2\pi r_j l_e$

$$V_l = \pi(r_j^2 - (r_j - \frac{\Delta r_1}{2})^2) \cdot l_e$$

3.4.5 Exterior Surface of the Housing

$$Q_{cond} = k_1 \cdot \frac{TT_{j-1} - TT_{i,j}}{\Delta r_1} \cdot A_1 \tag{3.87}$$

$$Q_{conv} = h_1 \cdot A \cdot (T_{amb} - TT_j) \tag{3.88}$$

$$Q_{rad} = \sigma \varepsilon_p \cdot A \cdot \left[(T_{amb} + 273)^4 - (TT_{i,j} + 273)^4\right] \tag{3.89}$$

$$\frac{TT_j^{n+1} - TT_j}{\Delta t} \cdot \varrho_1 \cdot c_{p1} \cdot V_l = Q_{cond} + Q_{conv} + Q_{rad} \tag{3.90}$$

where, $A_1 = 2\pi(r_j - \frac{\Delta r_1}{2}) \cdot l_e$ $\qquad A = 2\pi r_j l_e$

$$V_l = \pi[r_j^2 - (r_j - \frac{\Delta r_1}{2})^2] \cdot l_e$$

3.5 Electric Model

Power density, q_i, input into the valve elements at node (i,j=1,2,......m_1) at every time step is calculated as follows. Nonlinear voltage distribution along the valve element column due to temperature difference is taken into account in this electric model.

The resistive component of valve element leakage current has a strong temperature dependence; its value at a fixed ac or dc stress increases with temperature according to the following formula.

$$J_r = J_0(E)e^{-\frac{W_c}{K \cdot T}} \qquad (\mathrm{A/m^2}) \qquad (3.91)$$

Therefore, the power input, q, to the valve elements is a function of both applied field, E, and the temperature , T.

$$q = \eta \; E \; Jr = \eta \; E \; J_0(E)e^{-\frac{W_c}{KT}} \qquad (\mathrm{W/m^3}) \qquad (3.92)$$

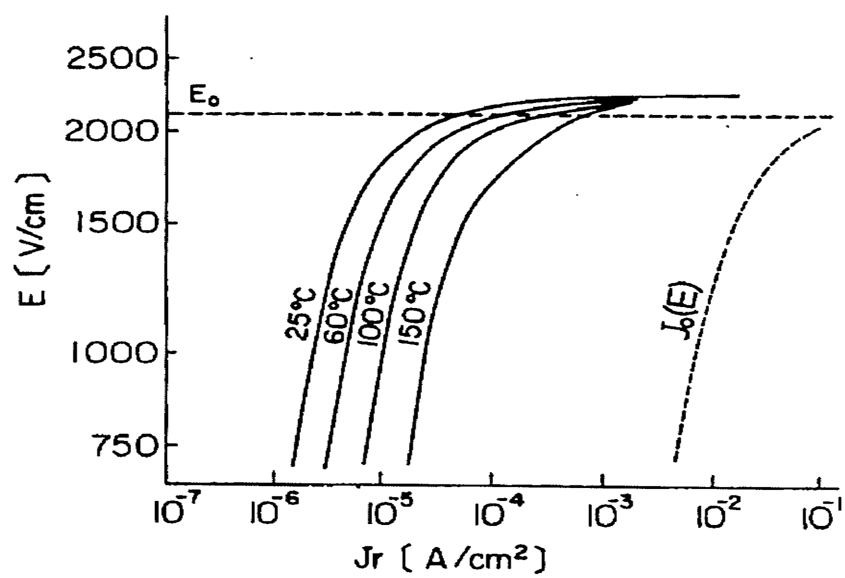

Figure 3.5 Relationship between J and E [4]

At t=0 (first time step), the power input to node (i,j) is calculated from Eq. 3.91 and Eq. 3.92 with $E=V/l_e$ * and $T=T_{i,j}=T_{amb}$. $J_0(E)$ is found from the known relation of $J_0(E)$ with E (Fig. 3.5) for the valve element under consideration.

On the next time step, the power input to the node (i,j) in a valve element is calculated as follows.

The mean temperature of all the valve elements in the arrester is found from

$$T_{mean} = \frac{1}{m_1 n_1} \sum_{i,j}^{n_1,m_1} T_{i,j} \tag{3.93}$$

where the summation is taken over all the nodes in all the valve elements comprising the arrester.

J_r is calculated from Eq. 3.91 using the mean valve element temperature from Eq. 3.93 and the mean value of $J_0(E)$ used in the previous step.

Next, the mean value of temperature, $T(i)_{mean}$, for a slice of the valve elements along the nodes in a radial direction is found for a fixed axial location, i.e. i=constant, j=1,2,......m_1 (see Fig. 3.6).

$$T(i)_{mean} = \frac{1}{m_1} \sum_{j=1}^{m_1} T_{i,j} \tag{3.94}$$

Using the above value of $T(i)_{mean}$, $J_0(E_i)$ at the present time step is found at node (i,j=1,2,...m_1) from Eq. 3.95.

---

* V is the applied voltage, and l_e is the length of valve element.

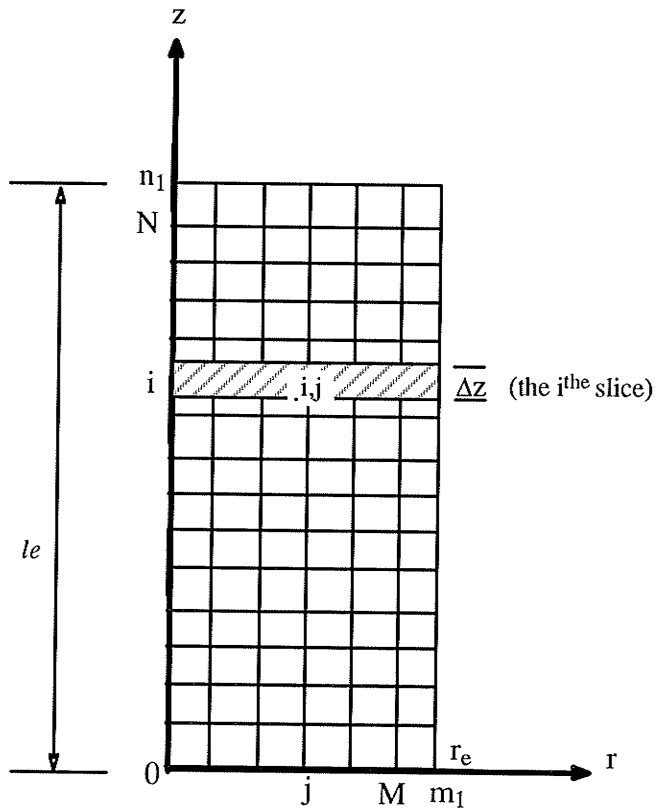

Figure 3.6 Cross section of valve elements

$$J_0(E_i) = \frac{J_r}{e^{-\frac{W_c}{K \cdot T(i)_{mean}}}} \qquad (3.95)$$

where E_i is the electric field at the i^{th} slice of the valve elements.

The value of E_i for every slice along the valve element column is found using the functional relationship between $J_0(E)$ and E. The value of E_i is valid only at the axial location considered in the valve element, and is varies in the axial direction due to axial temperature variation. The value of E_i does not vary in the radial direction.

Thus, the nonlinear voltage distribution along the arrester column due to temperature difference is taken into account and the voltage drop across a slice of a valve element is

$$V(i) = E(i)\,\Delta z \qquad \text{(Fig. 3.6)} \tag{3.96}$$

The resistance of this portion of the valve element is

$$R(i) = \frac{V(i)}{J_r \cdot \pi (r_e)^2} \tag{3.97}$$

and the power input to valve element at node ($i, j=1,2,\ldots m_1$) is given by

$$q_i = \eta\, E(i)\, Jr \tag{3.98}$$

The iteration proceeds as described above.

3.6 Flow Chart

Based on the mathematical model of MOSA discussed above, a computer program is developed to calculate the temperature distribution of MOSA under both transient and steady state conditions. The flow chart is shown in Fig. 5.7, and FORTRAN program (see appendix A) has been developed.

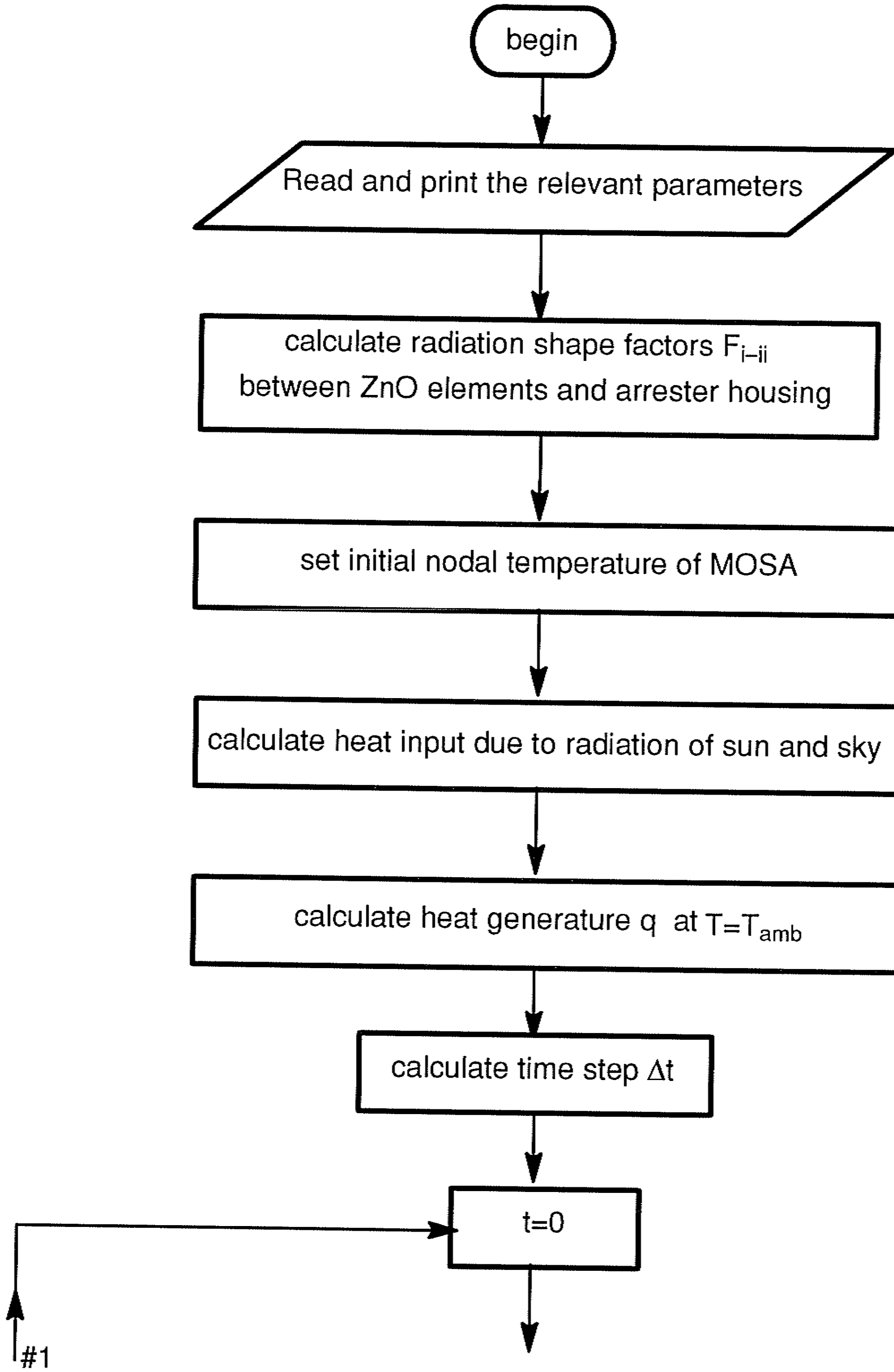
begin
Read and print the relevant parameters
calculate radiation shape factors F_{i-ii} between ZnO elements and arrester housing
set initial nodal temperature of MOSA
calculate heat input due to radiation of sun and sky
calculate heat generature q at $T=T_{amb}$
calculate time step Δt
t=0
#1

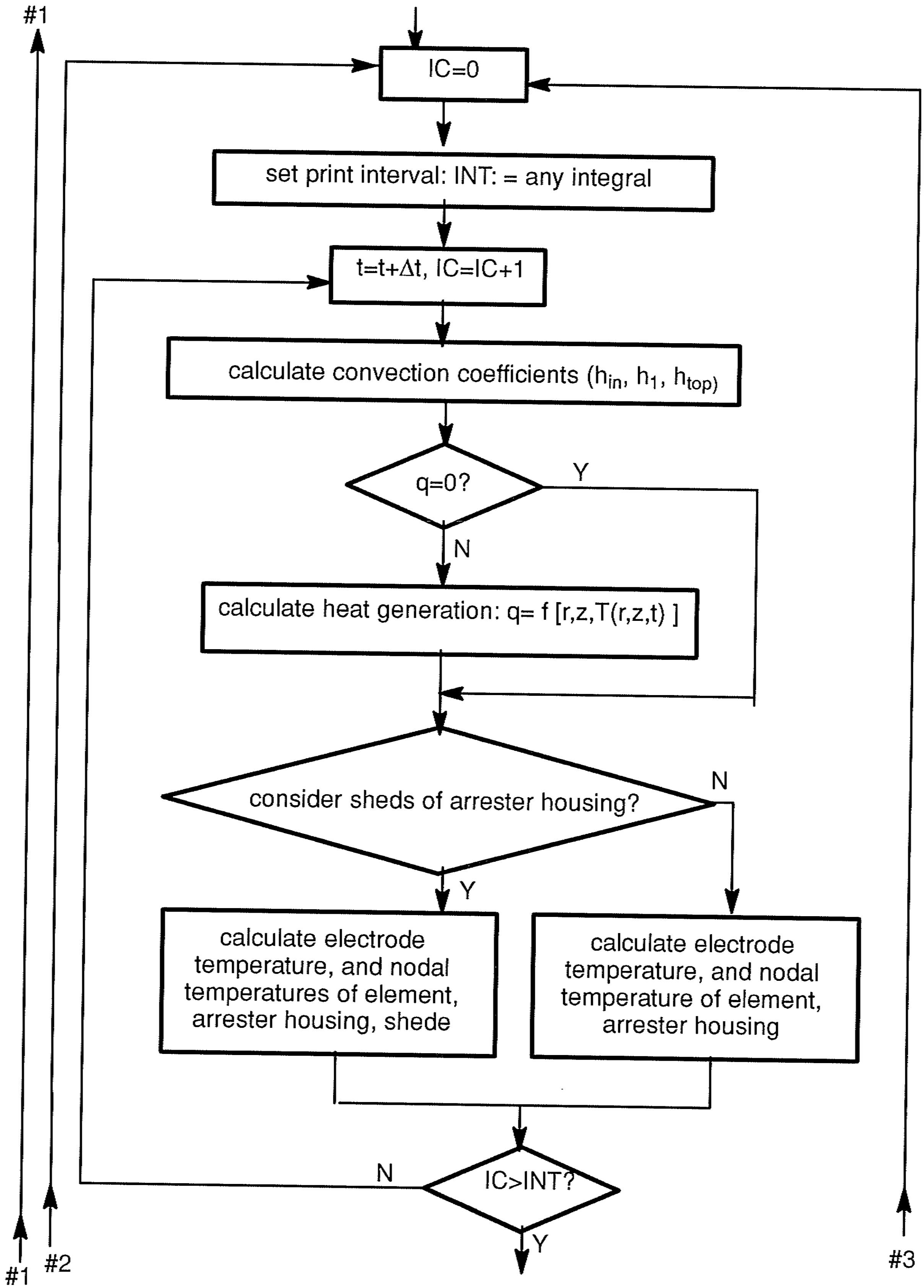
#1
IC=0
set print interval: INT: = any integral
t=t+Δt, IC=IC+1
calculate convection coefficients (h_in, h_1, h_top)
q=0?
Y
N
calculate heat generation: q= f [r,z,T(r,z,t)]
consider sheds of arrester housing?
N
Y
calculate electrode temperature, and nodal temperatures of element, arrester housing, shede
calculate electrode temperature, and nodal temperature of element, arrester housing
N
IC>INT?
Y
#1
#2
#3

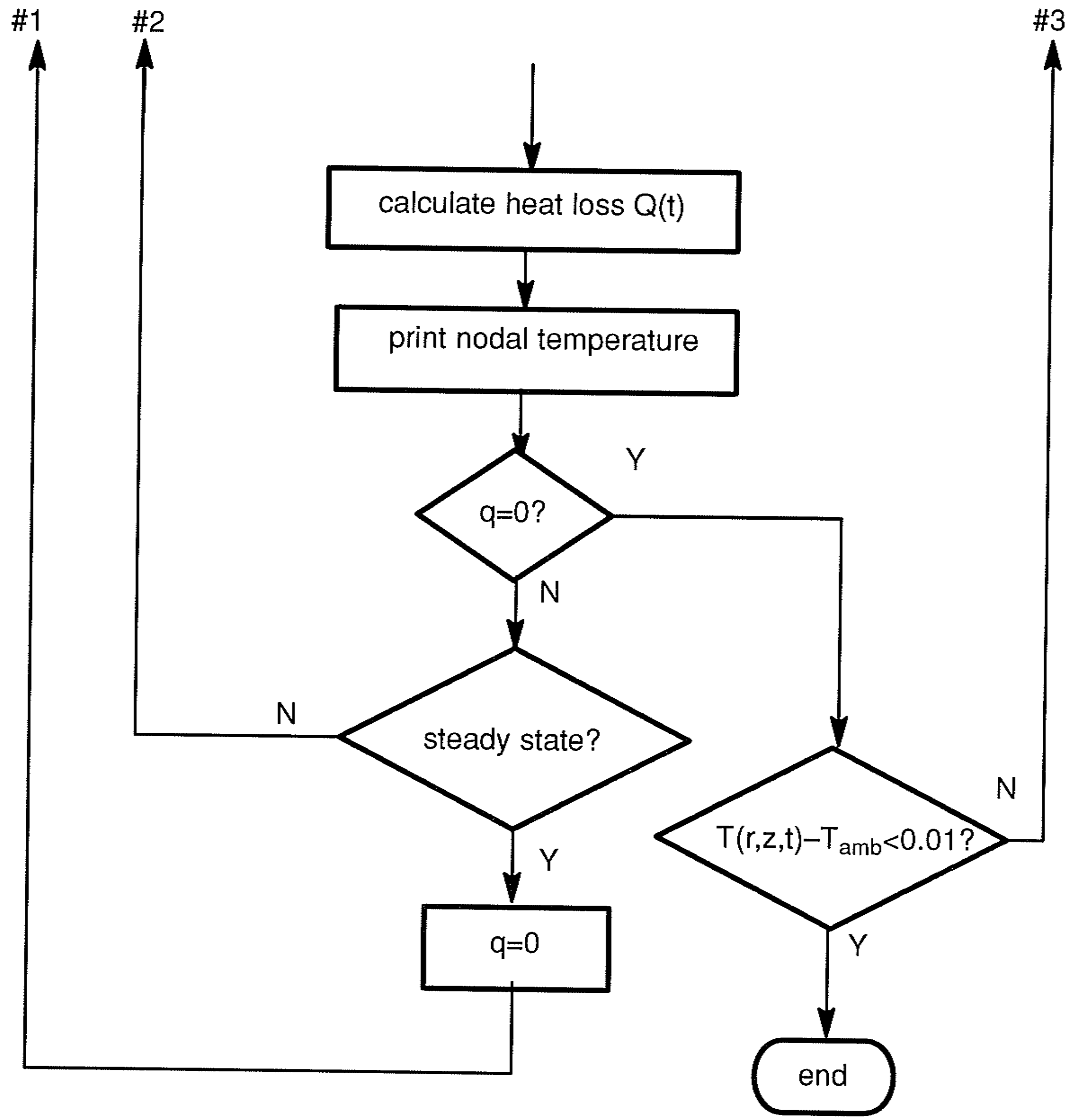

Figure 3.7 Flow chart of computer program for simulating the thermal properties of MOSA

Chapter 4

EXPERIMENTAL VERIFICATION OF MATHEMATICAL MODEL

The mathematical method proposed in Chapter 3 is applied to derive the temporal variation of temperature in an arrester column and the simulated data is compared with the experimental results which are available in literature[4]. The good agreement between the simulated and experimental results demonstrates the accuracy of the modelling technique. The accuracy of the model is also demonstrated by comparison of simulated data with experimental results obtained by conducting tests on an actual 84kV MOSA.

4.1 Comparison With Experimental Results in Literature [4]

Fig. 4.1 shows a sketch of the assembly of MOSA elements which is identical to the one used in [4] by Tominaga el al. The experimental results for this configuration are available in [4]. The voltage applied to the arrester column was 9.7kV as in [4]. The temporal variation of temperature was calculated at 3 points on the central axis of the arrester column and 1 point on each electrode. Fig. 4.2 shows the results. The experimental results, reproduced from [4], are shown in Fig. 4.3. Fig. 4.4 shows the axial temperature variation from $z = 0$ to $z = 4.8$ cm for $r = 0$, 0.9 and 1.5 cm at 4.45 hours after application of voltage. Corresponding experimental data from [4] is also shown in Fig. 4.4.

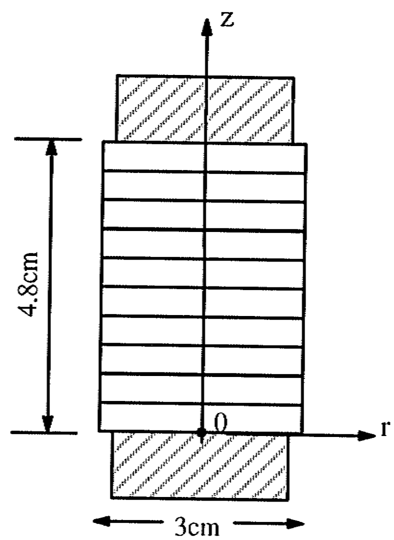

Figure 4.1 Stacked valve elements reproduced from [4]

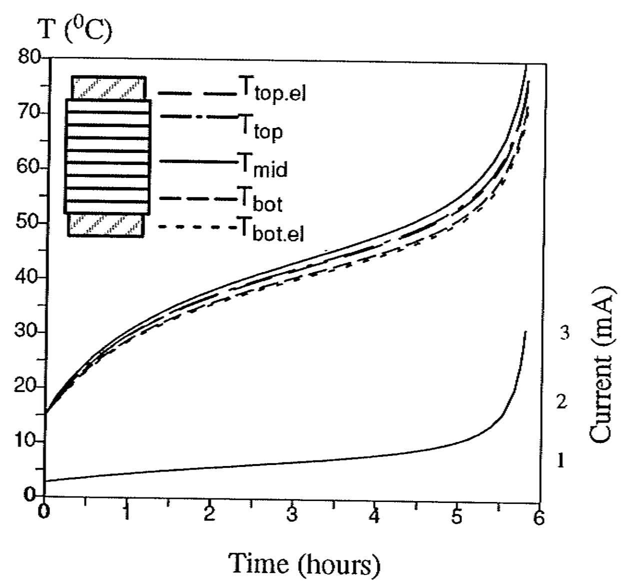

Figure 4.2 Temperature and resistive leakage current change with time (Simulated results)

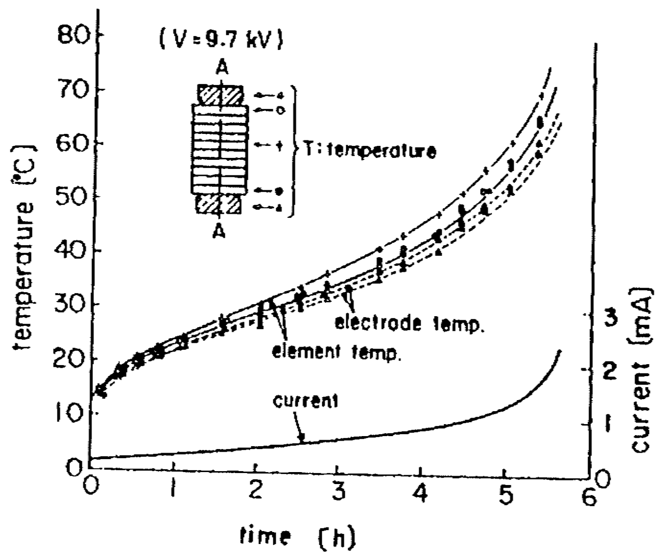

Figure 4.3 Temperature and leakage current change with time (Measured results)

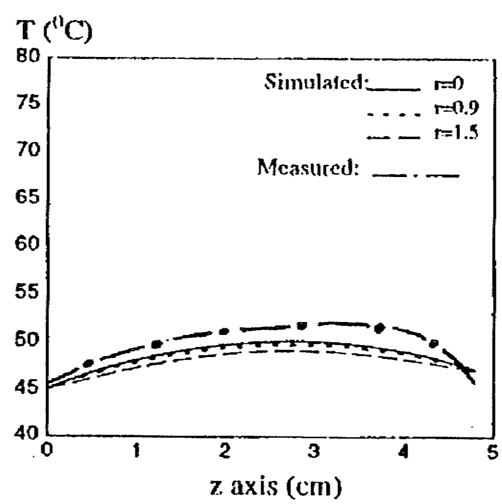

Figure 4.4 Temperature distribution of valve elements (4.4 hours after voltage application)

From above comparison (Figs. 4.2–4.4) it can be seen that the simulated and experimental results agree well.

From the simulation results (Fig. 4.4) , we can also note that the temperature variation in the radial direction in the elements is not significant, but the temperature variation along the valve element column is significant and can not be neglected.

4.2 Comparison With Experimental Results Conducted on a MOSA

Laboratory experiments were also conducted on a MOSA to verify the accuracy of the modelling technique proposed in Chapter 3. A good agreement is also obtained between experimental and simulated results.

4.2.1 Description of Surge Arrester Subjected to Test

Experiments were conducted to find the temporal variation of temperature distribution in a MOSA rated 84kV. The temperature along the valve element column was measured by thermocouples inserted through small holes in the porcelain housing. Along the valve element column, a total of three measuring spots were provided. Figs. 4.5–4.6 show the structure of the MOSA subjected to test and the positions of the three available measuring spots.

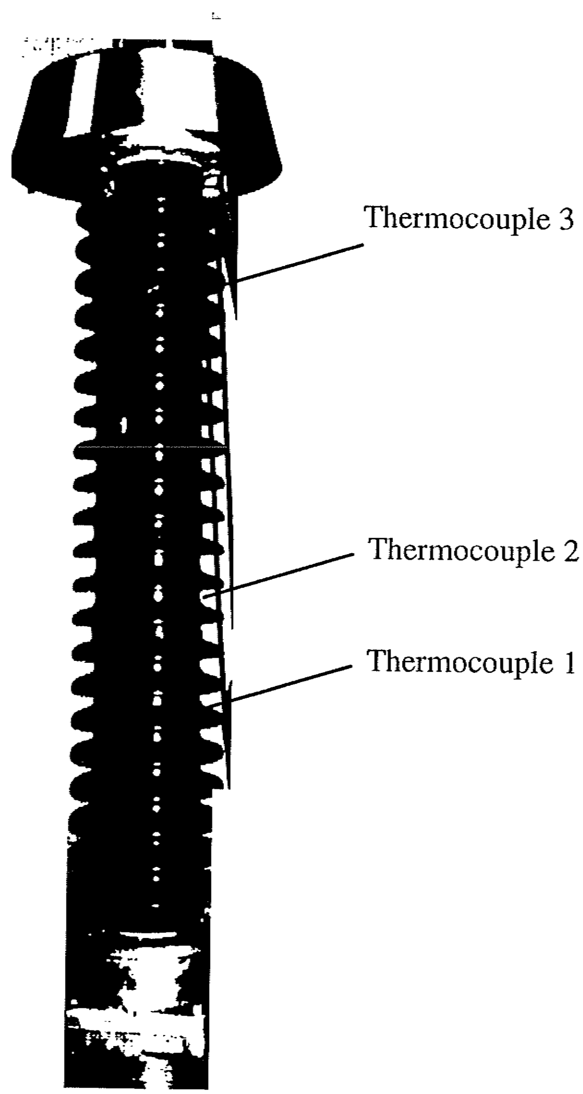

Figure. 4.5 84kV porcelain–type MOSA subjected to test

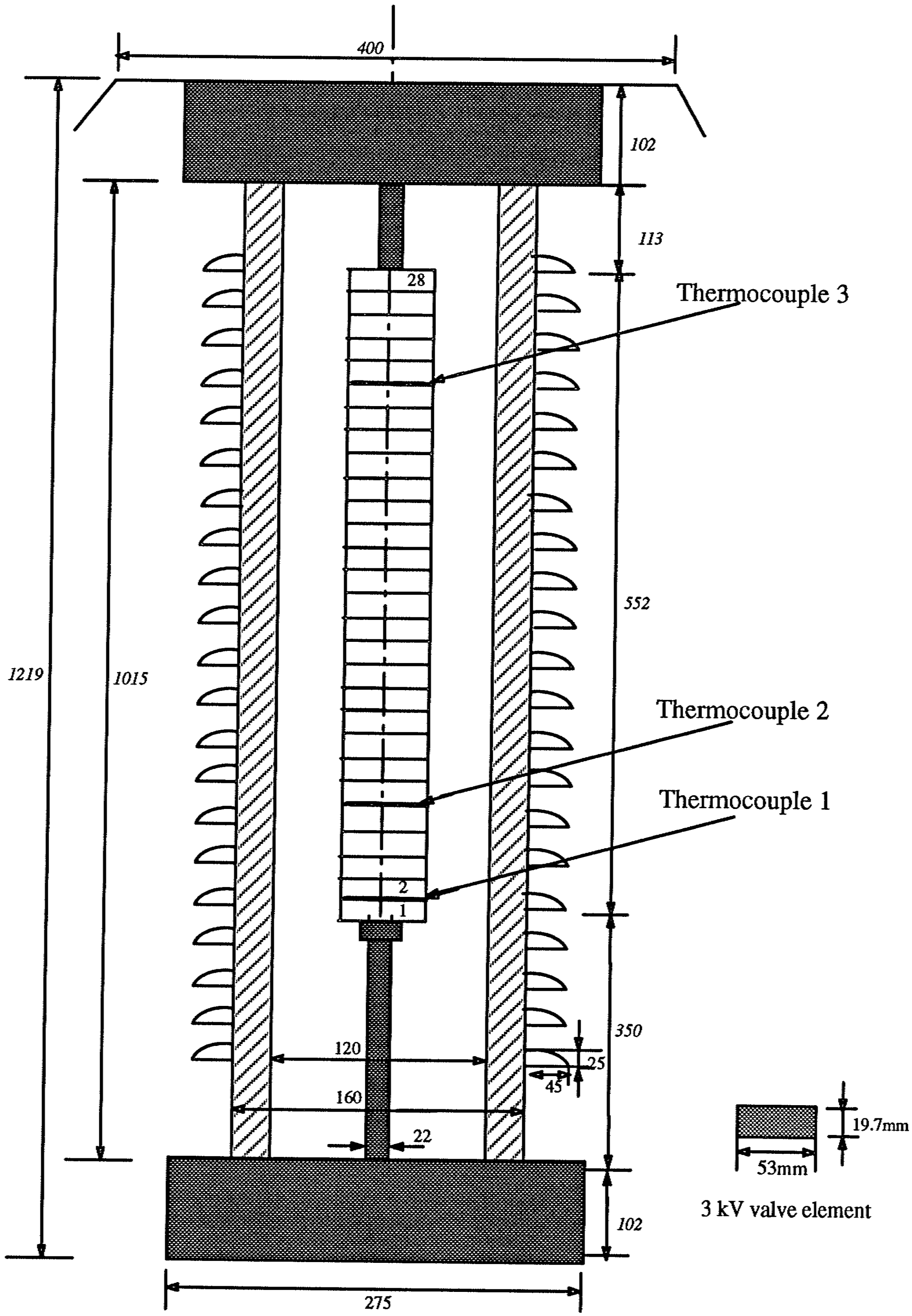

Figure 4.6 Configurations of MOSA shown in Fig. 4.5

4.2.2 Experimental Set Up

The test equipments set up for the measurement of valve element temperature and power generation due to resistive leakage current is shown in Figs. 4.7–4.8. A capacitive divider and a 100X (2.4pF, 10 MΩ) probe were used to measure the arrester voltage. The voltage ratio of the divider was calibrated by an electrostatic voltmeter. The total current flowing through the MOSA was measured with 1 ohm resistor inserted in series with arrester. Integration (Eq. 4.1) of the product of the voltage and current was carried out using the "data 6000 analyzer" (Fig. 4.9) for calculating the total power input to the valve elements. Fig. 4.9 shows the Data 6000 analyzer. Thermal controller (1mV/^{0}C) was used to find the valve element temperature measured by J type thermal couples.

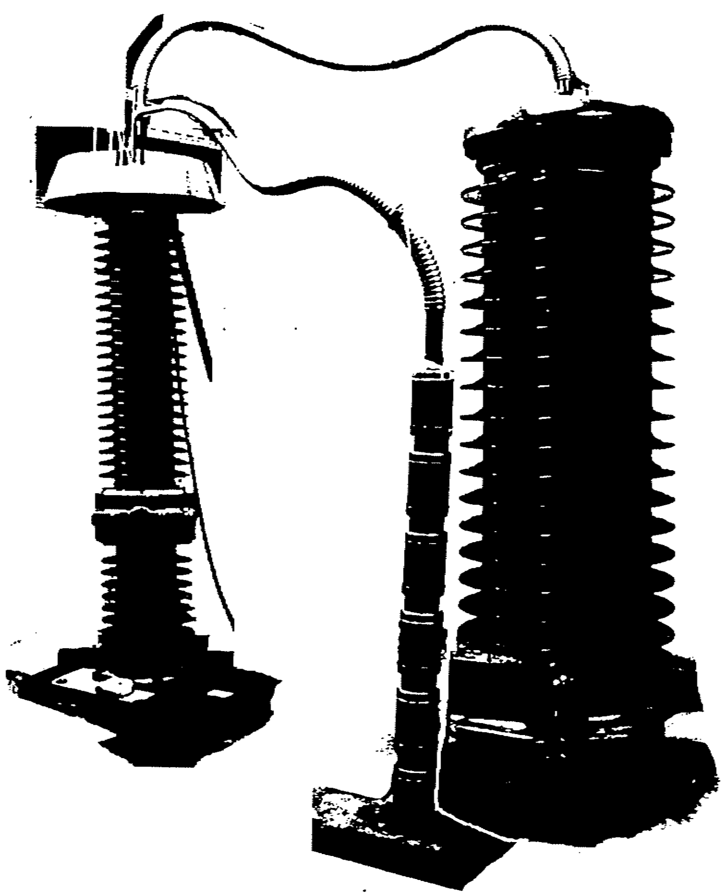

Figure. 4.7 Test set up

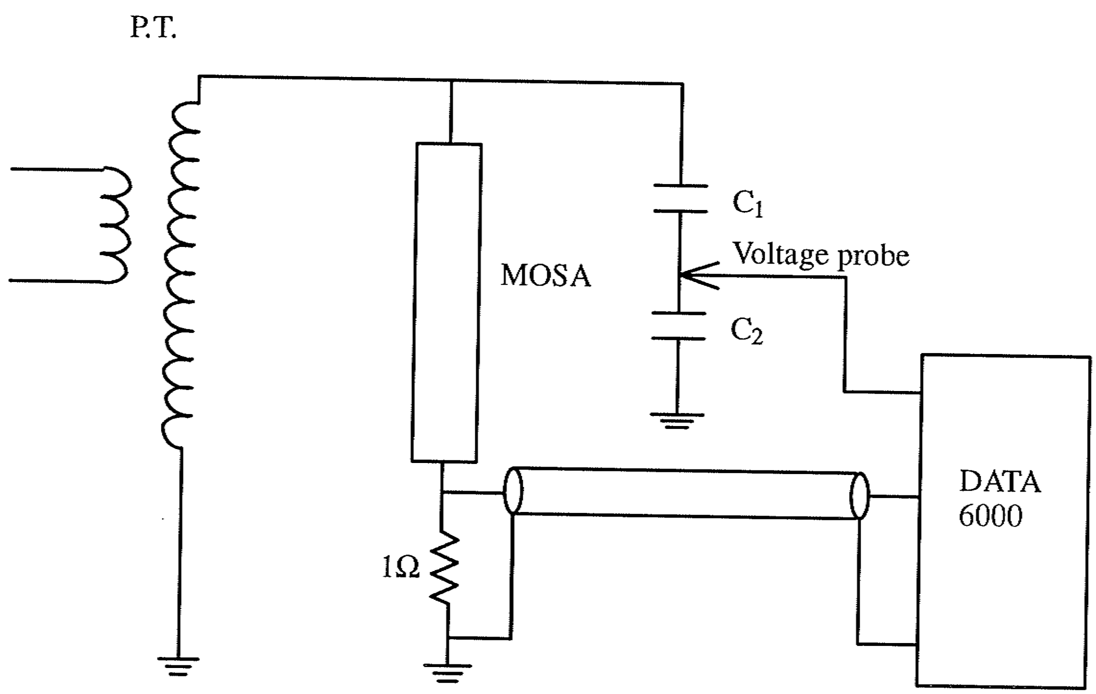

Figure. 4.8 Schematic diagram of the test circuit

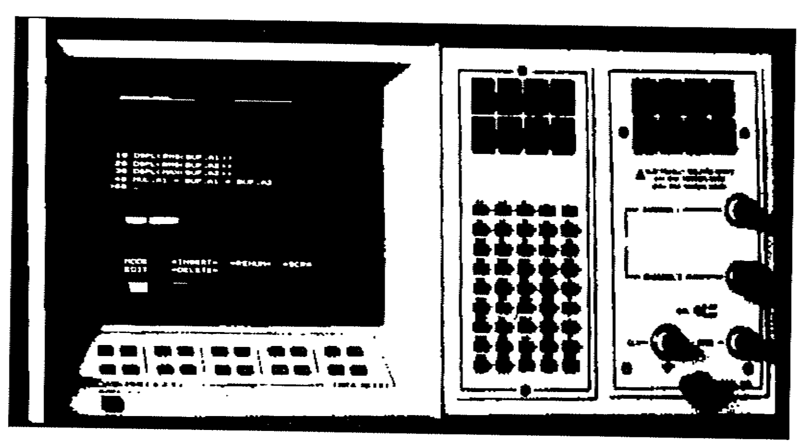

Figure. 4.9 Data 6000 analyzer

$$P = \frac{1}{T}\int_{0}^{T} v \cdot i dt \qquad \text{(W)} \qquad (4.1)$$

The tests were conducted at room temperature which ranged from 18^{0}C to 23^{0}C. A fixed voltage was applied to the MOSA from a 138 kV (4kVA) voltage transformer; the voltage application was interrupted at suitable intervals to measure the element temperature. Measurements of the temperature decay in valve elements were carried out with voltage off after attainment of steady state conditions.

Fig. 4.10 shows the total current flowing through the MOSA when 75kV (r.m.s.) voltage is applied.

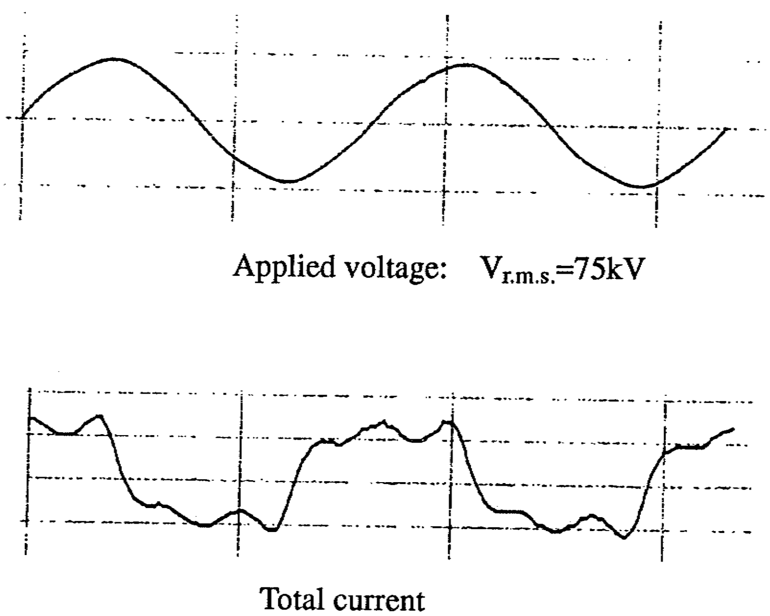

Total current:
I_{max}=1.25mA
$I_{r.m.s.}$=0.78mA

Resistive current:
I_R(r.m.s.)=0.1mA

Total power:
P=7.8W

Figure 4.10 Voltage and leakage current of MOSA

4.2.3 Comparison of Experimental and Simulated Results

In order to carry out the simulation the power generated in the valve elements, q_i, has to be known. This is a complex function of applied electric stress, valve element temperature and past history as discussed in section 3.5 of Chapter 3. The procedures for calculating power input to valve element at every time step described in section 3.5 can be followed if $J_0(E) - E$ curve is known. In the present work to simulate the MOSA shown in Fig. 4.1, the relationship between total power input to the valve elements, P(t), and time, t, was found experimentally with the aid of "data 6000 analyzer". Linearity was assumed and the valve element power input density was found from $P(t)/V_l$, $(=q_i)$, where V_l is the total volume of all the valve elements. In the simulation, the total number of nodes in the valve elements is 145 (29×5).

(1) 75kV Voltage Application

Alternating voltage of magnitude 75kV (r.m.s.) was applied to the MOSA and was disconnected after 12 hours when the steady state was obtained. During the test the ambient temperature ranged from 20^0C to 23^0C. The measured and simulated temporal variation of temperature distribution along the valve element column is shown in Fig. 4.11. The numbers 1, 2 and 3 in Fig. 4.11 refer to the thermocouple locations identified in Fig. 4.6. Fig. 4.12 shows the simulated axial temperature variation at 1, 3 and 9 hours after the voltage application.

Table 4.1 shows the relative difference between the simulated and experimental results. It can be seen that the mean error in the simulation at location 1, 2 and 3 were 3.6%, 1.5% and 2.3% respectively. The maximum error at same locations were 7.1%, 2.1% and 6.4% respectively. The simulated and experimental results agree well.

From the above results, it can be seen that the temperature of the valve elements reaches their steady state and thermal equilibrium is attained when the heat loss from the element is balanced with the heat input to it after 12 hours voltage application.

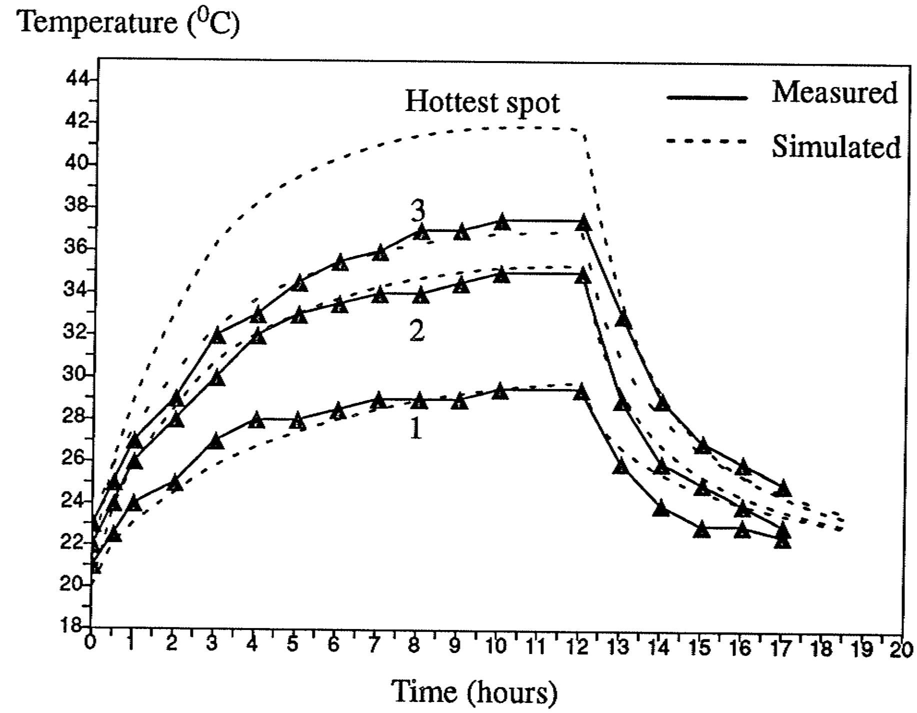

Figure 4.11 Temperature – time relationship at 4 locations in arrester energized at 75kV (T_{amb} = 20–23^{0}C)

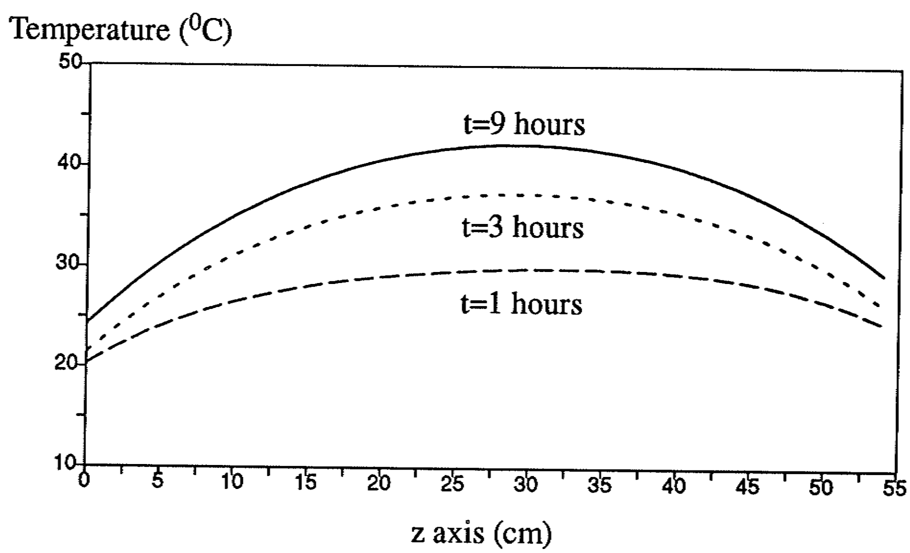

Figure 4.12 Axial temperature variation in valve element stack z=0 is stack bottom

Table 4.1 Relative difference between the simulated and measured results with arrester energized at 75kV

Time	curve 1 *			curve 2 *			curve 3 *		
	T (^{0}C)		Err	T (^{0}C)		Err	T (^{0}C)		Err
(Hours)	Simulated	Measured	(%)	Simulated	Measured		Simulated	Measured	(%)
1	23.035	24	4.0	25.822	26	0.7	27.564	27	2.1
2	24.497	25	2.0	28.558	28	2.0	30.169	29	4.0
3	25.803	27	4.4	30.765	30	2.6	32.364	32	1.1
4	26.686	28	4.5	32.073	32	0.2	33.688	33	2.1
5	27.401	28	2.1	33.006	33	0.0	34.640	34.5	0.4
6	28.002	28.5	1.8	33.727	33.5	0.7	35.373	35.5	0.4
7	28.507	29	1.7	34.292	34	0.9	35.945	36	0.2
8	28.914	29	0.3	34.704	34	2.1	36.357	37	1.7
9	29.246	29	0.9	35.009	34.5	1.5	36.655	37	0.9
10	29.499	29.5	0.0	35.203	35	0.6	36.837	37.5	1.8
12	29.805	29.5	1.0	35.318	35	0.9	36.910	37.5	1.6
13	26.733	26	2.8	29.381	29	1.3	30.897	33	6.4
14	25.467	24	6.1	26.817	26	3.1	28.171	29	2.9
15	24.633	23	7.1	25.351	25	1.4	26.523	27	1.8
16	24.020	23	4.4	24.410	24	1.7	25.407	26	2.3
17	23.536	22.5	4.6	23.746	23	3.2	24.587	25	1.7

* see Fig. 4.11

(2) Temporary Overvoltage Application

A temporary overvoltage (TOV) of magnitude 105kV (1.4×75kV) (r.m.s.) was applied to the MOSA for 90 seconds after attainment of steady state conditions at 75kV. After the 90 second period the voltage was returned to the former value of 75kV. In this test ambient temperature ranged from 18^{0}C to 21^{0}C. The measured and simulated temporal variation of temperature distribution along the valve element column is shown in Fig. 4.13. The numbers 1, 2 and 3 in Fig. 4.13 refer to the thermocouple locations identified in Fig. 4.6. Table 4.2 shows the relative difference between the simulated and experimental results. The maximum and mean errors in this case were 5.9% and 2.1% at location 1, 9.4% and 2.3% at location 2, and 4.9% and 1.5% at location 3 respectively. Once again the simulated results agree well with the experimental results.

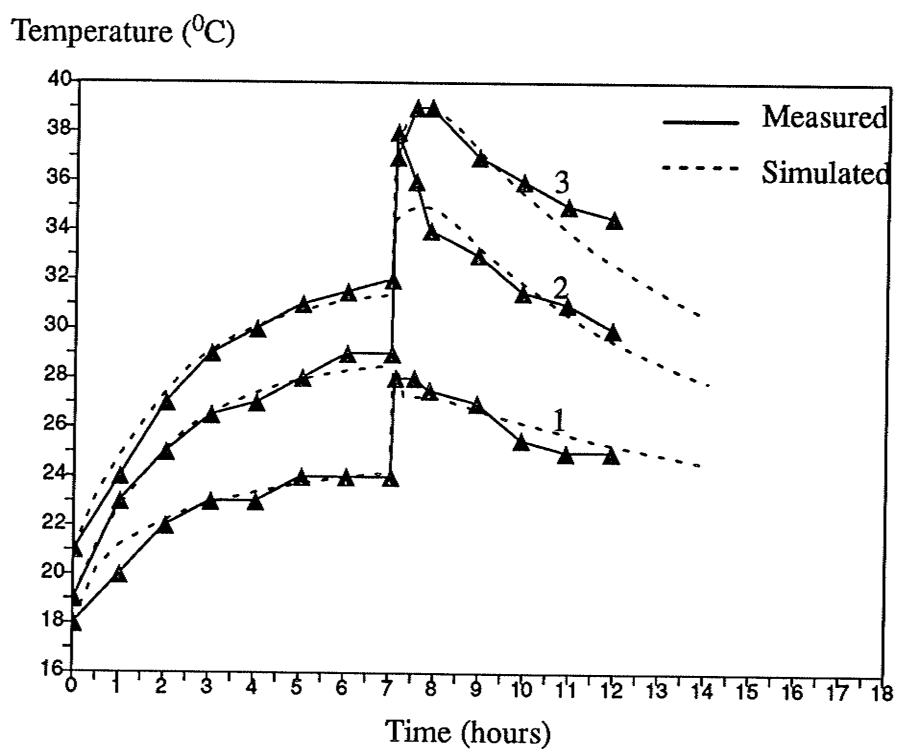

Figure 4.13 Temperature – time relationship at three locations under TOV application to arrester (T_{amb} =18–21^{0}C)

Table 4.2 Relative difference between the simulated and experimental results with arrester subjected to TOV

Time	curve 1 *			curve 2 *			curve 3 *		
	T (^{0}C)		Err	T (^{0}C)		Err	T (^{0}C)		Err
(Hours)	Simulated	Measured	(%)	Simulated	Measured		Simulated	Measured	
1	21.185	20	5.9	22.736	23	1.2	24.831	24	3.5
2	22.198	22	0.1	25.065	25	0.3	27.398	27	1.5
3	22.892	23	0.5	26.537	26.5	0.2	29.107	29	0.4
4	23.354	24	1.5	27.384	27	1.4	30.094	30	0.3
5	23.704	24	1.2	27.935	28	0.2	30.732	31	0.9
6	23.969	24	0.1	28.293	29	2.3	31.138	31.5	1.2
7	24.162	24	0.7	28.502	29	1.7	31.366	32	2.0
7.08	29.170	28	4.2	34.447	38	9.4	37.284	37	0.1
7.5	27.245	28	2.7	34.953	36	2.9	38.786	39	0.5
7.83	27.248	27.5	0.9	33.754	34	0.7	38.808	39	0.5
8.9	26.820	27	0.6	32.144	33	2.7	37.655	37	1.8
9.9	26.298	25.5	3.1	30.794	31.5	3.3	35.805	36	0.5
10.9	25.765	25	3.1	29.620	31	4.4	34.160	35	2.4
11.9	25.285	25	1.1	29.601	30	1.3	32.804	34.5	4.9

* see Fig. 4.13

After application of the TOV, the transient temperature rise was such that thermal runaway did not occur under application of the 75kV to the arrester.

(3) Measured and Simulated Results With Arrester Energized at 100kV

Heating and cooling curves of metal oxide valve elements stressed by 100kV (r.m.s.) are shown in Fig. 4.14. In this case, the applied voltage exceeds a critical level and thermal runaway will result. The measurement was terminated after 1 hour voltage application. Fig. 4.15 shows the temperature variation at z=37, 45, and 87cm on the external surface of the porcelain housing.

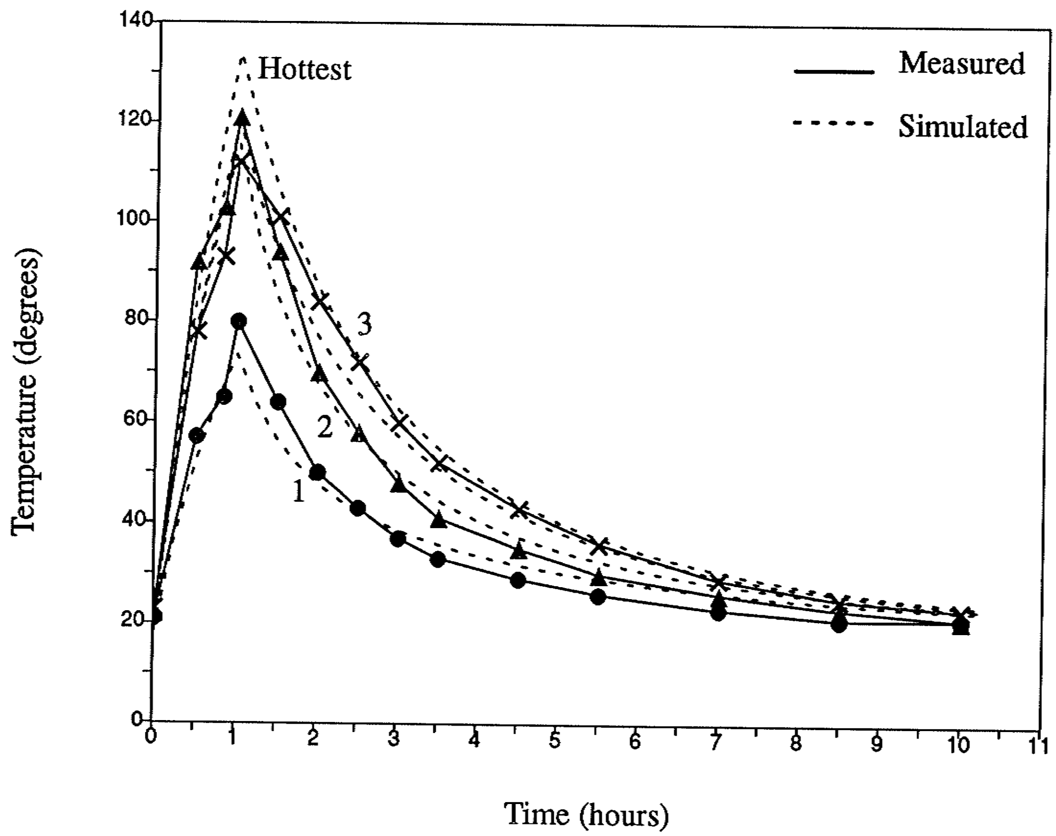

Figure 4.14 Temperature variation with time

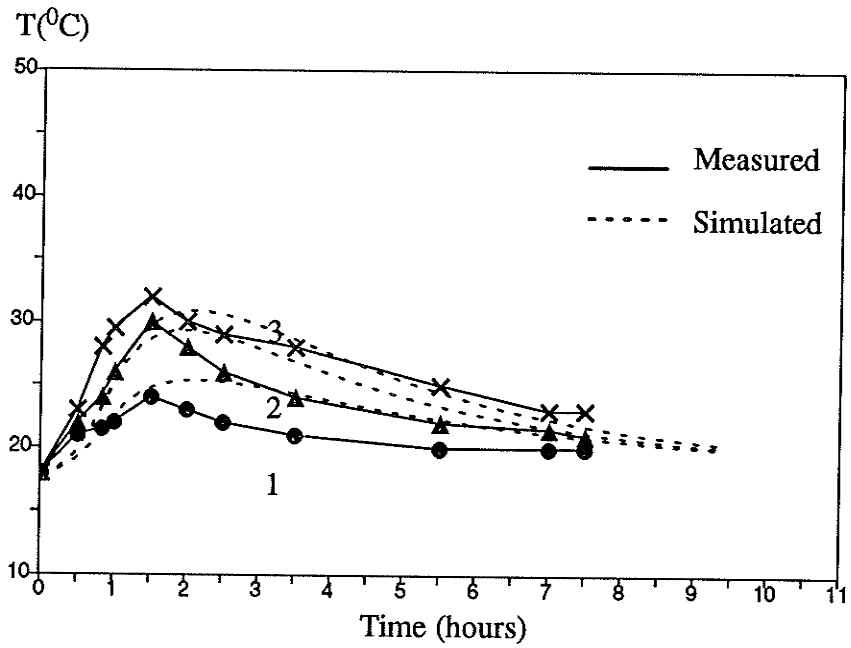

Figure 4.15 Temperature – time relationship on the external surface of porcelain housing

From the above comparison (Figs. 4.11–4.15), good agreement between the experimental and simulated results is apparent.

4.3 Sources of Errors

Errors exist in both simulation and experiment.

4.3.1 Errors Indicated in the Measurements of Valve Element Temperature

(1) The voltage was not continuously applied to the valve elements. The valve element temperature was measured after the applied ac voltage was temporarily disconnected.

(2) Temperature in valve elements could be only obtained at 3 points.

(3) Only the total power input, P(t), to the valve elements could be measured; the power input per unit volume is calculated by

$q(t)=P(t)/V_l$ (W/m^3)

(4) Other sources of possible errors due to environmental conditions existed, i.e. external air movement, the change of ambient temperature, etc.

4.3.2 Errors in the Simulation

(1) As described above, only total power input to valve elements can be measured. A uniform power input to the valve elements is assumed in the simulation to calculate the temperature distribution of the 84kV MOSA. In reality power generation in each element is different.

(2) The part of the arrester housing surface exposed to sun light receives more energy due to radiation, thus resulting in a non–uniform temperature distribution along circumference of the MOSA and destroying symmetry.

(3) Heat transfer coefficients, i.e. the temperature–dependent non linear behavior of the convective and radiative components, are found in literature, but they may subject to change for a particular application.

(4) Nonlinear voltage distribution along arrester column due to capacitance to ground is not considered.

(5) Finite difference method for solving the partial differential equations introduces some unavoidable errors.

Despite possible errors as discussed above, the data presented in Figs. 4.11–4.15 indicates that a maximum error between measured and simulated values is less then 10%, ranging from 0 to 9.4%. This demonstrates the relatively high degree of accuracy of the proposed modelling technique.

Chapter 5

THERMAL EQUIVALENT TEST SECTIONS

The thermal characteristics of a MOSA may be evaluated by using suitable test sections whose parameters are physically adjusted to match the thermal characteristics of the MOSA. In this chapter, thermal equivalent test sections (TETS) of an actual MOSA will be derived; a procedure to obtain a TETS of a MOSA will be presented.

It is difficult to design a TETS using an experimental approach [4,5,8] because such a method relies on trial and error. In the present study, the developed mathematical model was used to find the thermal properties of both the MOSA and the test sections. The heat dissipation capability (cooling curve) of the test section is made to be identical to that of the MOSA by adjusting the test section parameters such as thickness of the housing and air gap width between the valve element and the housing. Once the cooling curves of the test section and the MOSA reach equivalence, heating curves will be identical to that of the MOSA if a suitable voltage is applied.

5.1 Structure of Test Sections

Three single element test sections are shown in Figs. 5.1–5.3. A structure of a three element test section is shown in Fig. 5.4. Both ends of the element are covered with a suitable heat insulating material (polystyrene) to suppress axial thermal leakage. The element is contained in a plexiglass or nylatron (nylon 6) housing. In Fig. 5.2, the surroundings of the element are packed with glass wool. These simple test sections are used to model the actual 84kV MOSA shown in Fig. 4.5.

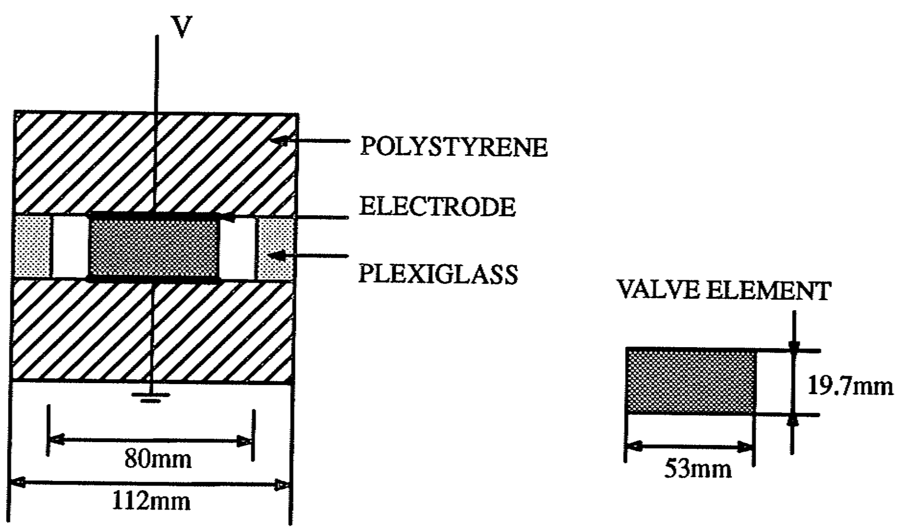

Figure. 5.1 Single element test section #1

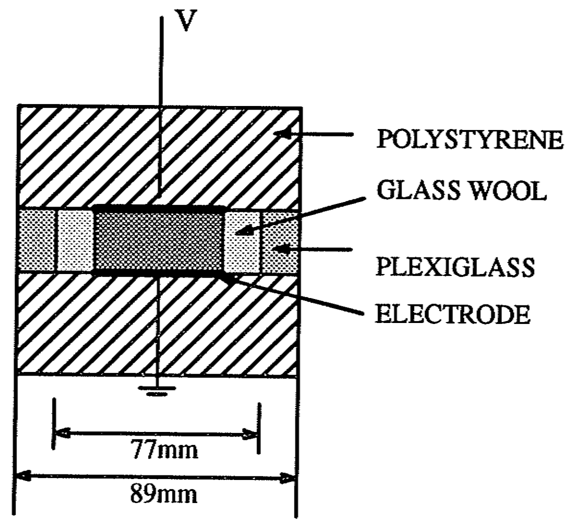

Figure 5.2 Single element test section #2

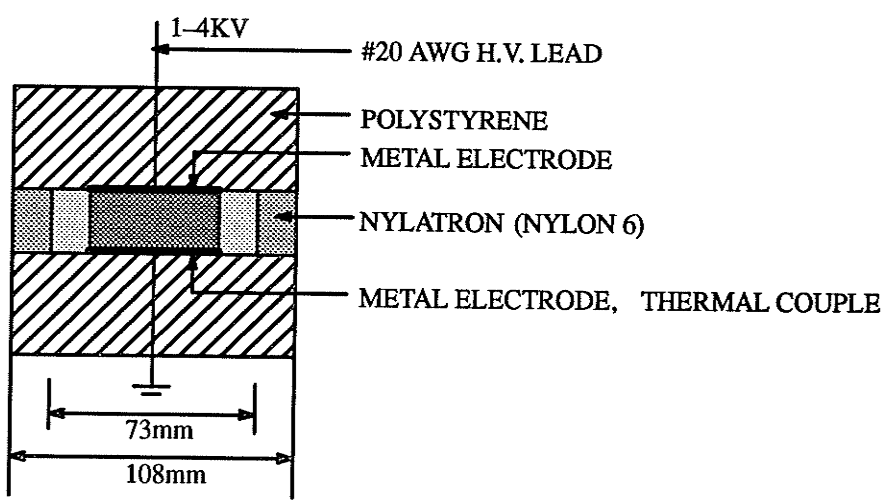

Figure. 5.3 Single element test section #3

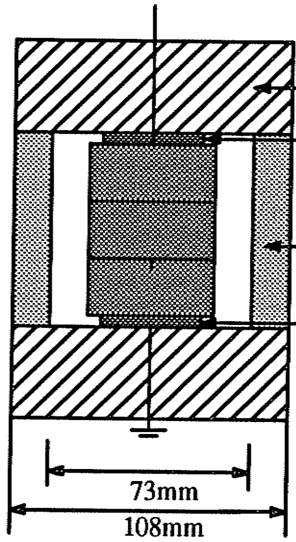

Figure 5.4 Three element test section

5.2 Simulated Results

Temporal variation of temperature distribution of the MOSA shown in Fig. 4.5 was obtained by simulation in Chapter 4. From the simulation results, the steady state maximum temperature and the steady state mean temperature in the arrester column, for 75kV applied voltage, are T_m (43^{0}C) and T_a (37^{0}C) respectively (see solid curves in Fig. 5.5–5.8).

In the simulation of a test section, a suitable voltage was applied to it until the temperature reached T_m in approximately the same time as it took in the case of the actual arrester. The cooling curve was then obtained. The thickness of the housing and air gap width between the valve element and the housing were changed so that the cooling curve of the test section matched that of the MOSA at the location of the occurrence of the maximum temperature. The dimensions of the TETS in Fig. 5.1 were arrived at in this manner. A similar procedure was followed to derive the parameters of the TETS with the valve element heated to the steady state mean temperature, T_a, of the MOSA column. It was found that no change in parameters was necessary in order to obtain a match of the cooling curve. The TETS parameters were the same in both cases. Fig. 5.5 shows the simulated results.

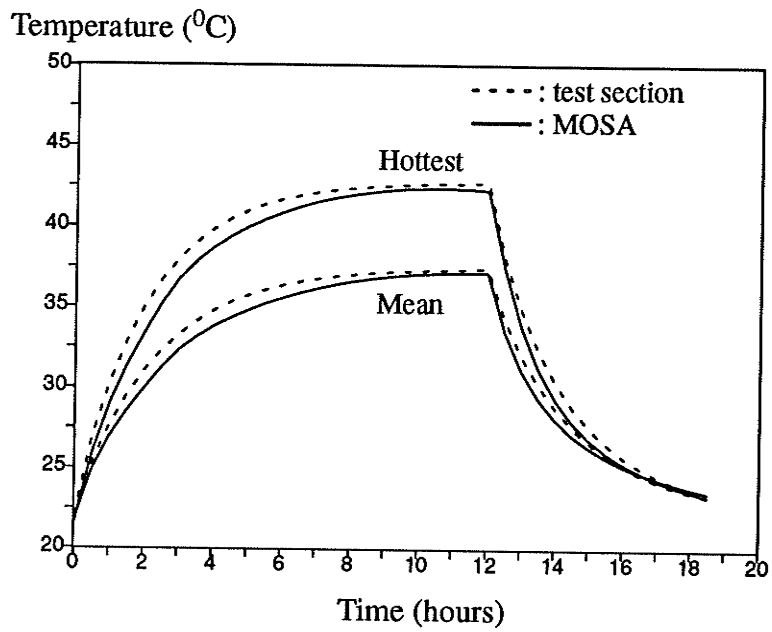

Figure 5.5 Heating and cooling curves of valve element in Fig. 5.1 (Simulated)

In Fig. 5.5 the dotted curves show the heating and cooling curves of the TETS, and the solid curves show the heating and cooling curves of the MOSA. The upper solid curve (labelled hottest) is the heating and cooling curve of the MOSA valve element, whose temperature (at 75kV applied voltage to MOSA) is the maximum, i.e. 43^{0}C. The upper dotted curve (labelled hottest) is the heating and cooling curve of the TETS which was subjected to a suitable voltage so that it reached the same maximum temperature (43^{0}C) in exactly the same time. The lower solid curve (labelled mean) is the mean heating and cooling curve of the MOSA valve elements (at 75kV applied voltage to MOSA). The lower dotted curve (labelled mean) is the heating and cooling curve of the TETS which was subjected to a suitable voltage so that it reached the steady state mean temperature (37^{0}C) in exactly the same time. It can be seen that this TETS have the same heat dissipation rate as that of the MOSA. The relative difference of the simulated results between the MOSA and the TETS is less then 4.8% as shown in Table 5.1.

Table 5.1 Comparison of cooling curves shown in Fig. 5.5

Time (Hours)	Mean temperature (simulated) (^{0}C)		Err (%)	Hottest spot temperature (simulated) (^{0}C)		Err (%)
	Single element model	Complete arrester		Single element model	Complete arrester	
13	31.997	31.081	3.0	35.366	33.809	4.6
15	26.638	26.320	1.2	28.109	26.815	4.8
16	25.204	25.196	0.3	26.195	25.325	3.4
18	23.565	23.802	1.0	24.027	23.636	1.7

The simulation results of Fig. 5.5 could not be verified experimentally because the plexiglass tube of outside diameter, 112mm, and inside diameter, 80mm, was not commercially available. A plexiglass tube of outside diameter, 89mm, and inside, diameter, 77mm, was available in the high voltage laboratory, and therefore a test section shown in Fig. 5.2 was fabricated. Fig. 5.6 shows the simulated results. In this case, the heating and cooling curves of the test section do not match those of the MOSA. Finally, "nylon 6" tube of outside diameter 108mm and inside diameter 73mm was found to be commercially available. These diameters are very close to the design values of the plexiglass tube (Fig. 5.1) and the thermal properties of the "nylon 6" are also close to those of the plexiglass. Consequently the test section shown in Fig. 5.3 was fabricated and the simulated results are shown in Fig. 5.7. It can be seen that this test section has the same heat dissipation rate as that of the MOSA and the heating and cooling curves match those of the MOSA. The relative difference of the simulated results between the MOSA and the TETS is less then 4.7% as shown in Table 5.2. Thus, this TETS can be used to examine the thermal properties of the MOSA. A three element TETS with same "nylon 6" tube is shown in Fig. 5.4 and the simulated results are shown in Fig. 5.8. The simulated results show that the heating and cooling curve of the three element TETS is also match that of the MOSA.

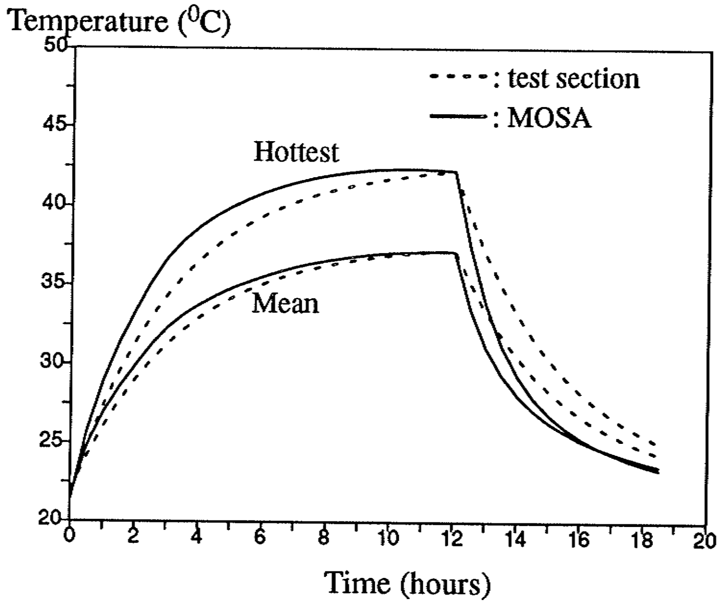

Figure 5.6 Heating and cooling curves of valve element in Fig. 5.2 (Simulated)

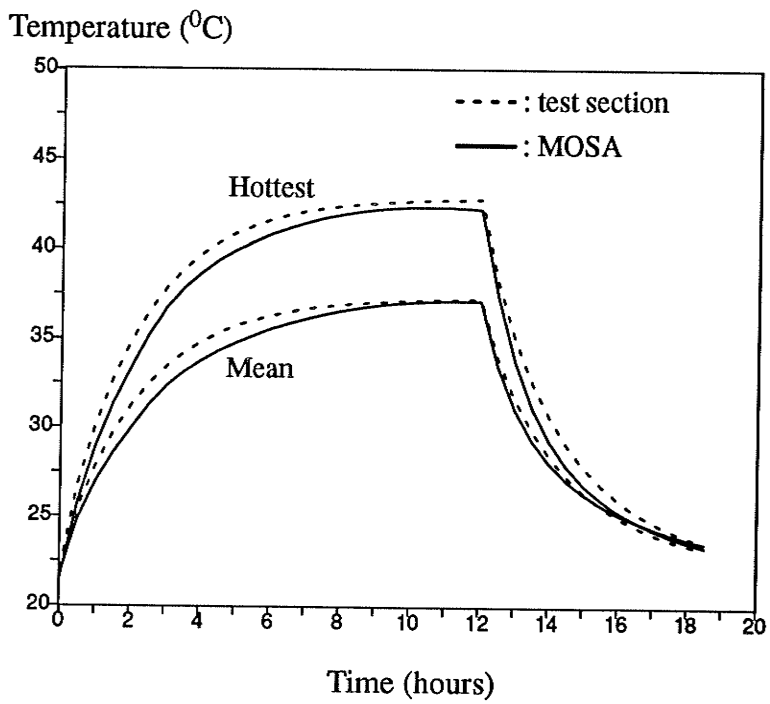

Figure 5.7 Heating and cooling curves of valve element in Fig. 5.3 (Simulated)

Table 5.2 Comparison of cooling curves shown in Fig. 5.7

Time (Hours)	Mean temperature (simulated) (^{0}C)		Err (%)	Hottest sport temperature (simulated) (^{0}C)		Err (%)
	Single element model	Complete arrester		Single element model	Complete arrester	
13	31.660	31.080	1.9	35.048	33.809	3.7
14	28.469	28.063	1.5	30.655	29.287	4.7
15	26.397	26.320	0.3	27.833	26.815	3.8
16	25.022	25.196	0.3	25.978	25.325	2.6
17	24.096	24.403	1.3	24.740	24.339	1.6
18	23.466	23.802	1.4	23.594	23.636	0.2

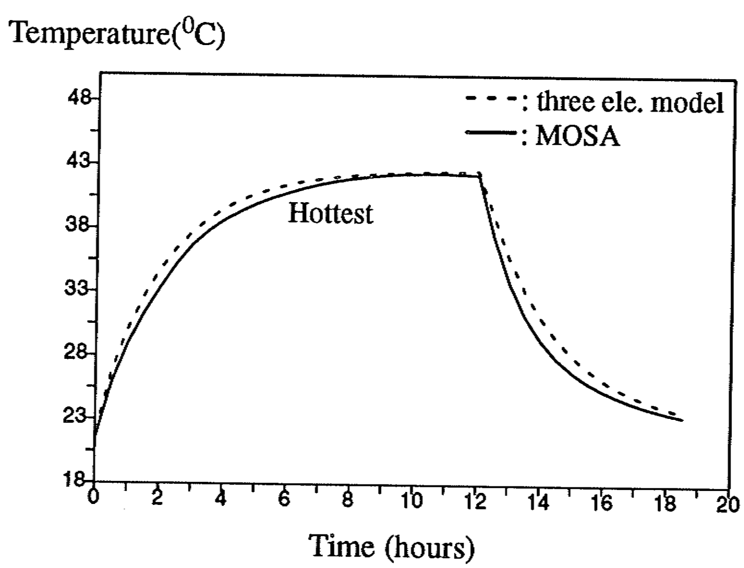

Figure 5.8 Heating and cooling curves of valve element in Fig. 5.4

5.3 Experimental Verification

The TETS shown in Fig. 5.3 was fabricated for test. The experimental set up is shown in Fig. 5.9. The leakage current of the valve element is shown in Fig. 5.10. The applied voltage was adjusted so that the maximum temperature, T_m (= steady state maximum temperature of the MOSA) was reached and steady state conditions established. The power was then shutdown and the cooling curve was obtained as shown in Fig. 5.11.

It can be seen that there is a good agreement between the simulated and experimental results. The relative difference between the simulated and measured value is less then 7.8% as shown in Table 5.3. This shows that the developed modelling technique may be conveniently used to find a TETS which accurately simulates the MOSA.

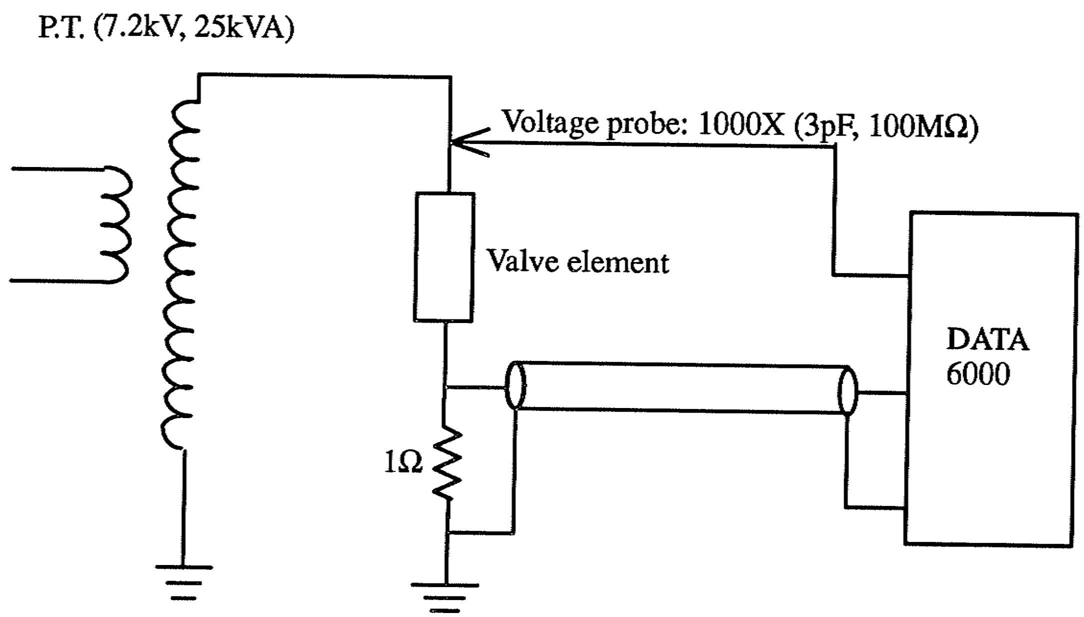

Figure 5.9 Schematic diagram of the test circuit

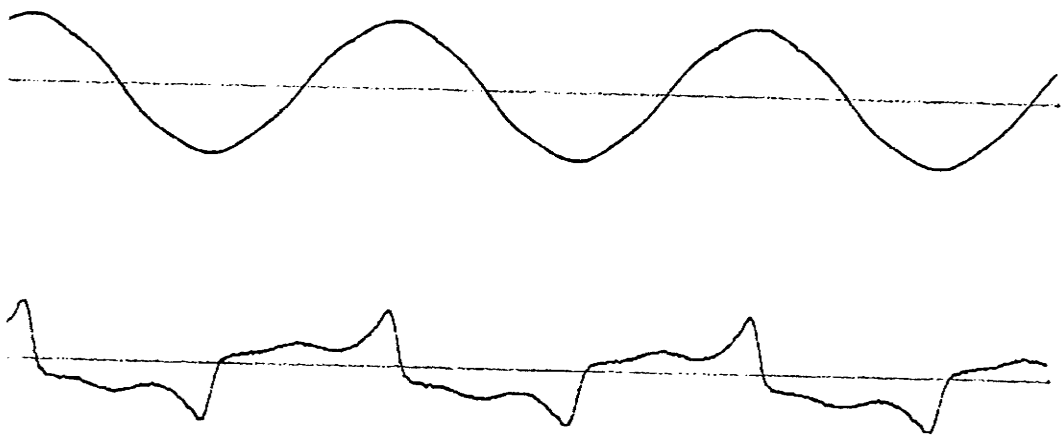

Figure 5.10 Typical oscillograph of applied voltage and total current of a valve element

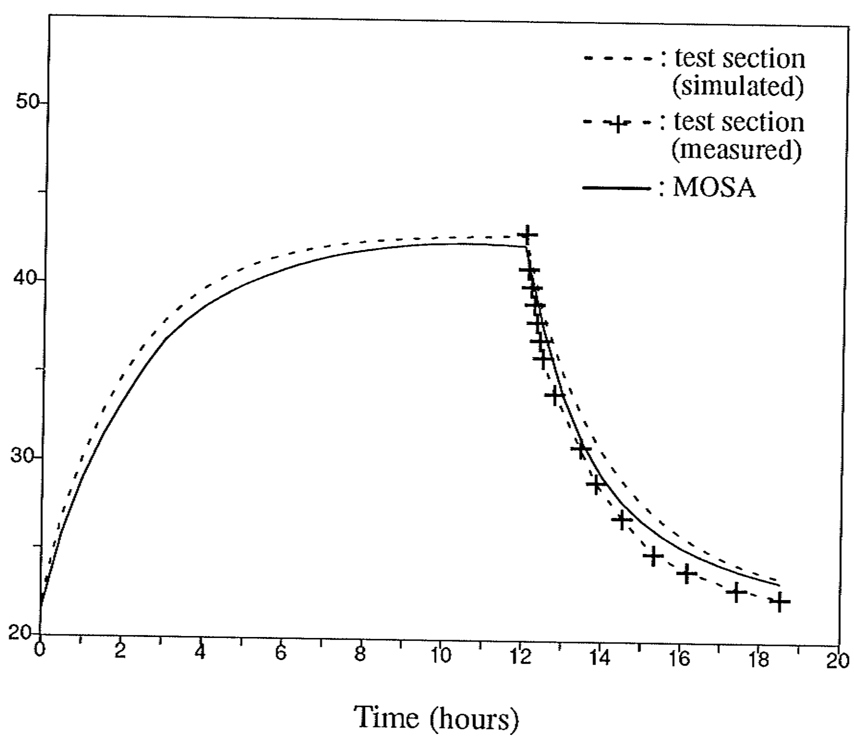

Figure. 5.11 Valve element temperature variation with time

Table 5.3 Comparison of cooling curves shown in Fig. 5.11

Time (Hours)	Single element model		Err (%)
	Simulated	Measured	
12.5	38.228	36.5	4.7
13	35.048	33	6.2
14	30.655	28.5	3.8
14.5	29.094	27	7.8
16	25.978	24.5	6.0
18.5	23.905	22.5	6.2

5.4 Outline of Procedure to Obtain Thermal Equivalent Test Section

From above a procedure to obtain a TETS can be outlined as follows.

Step 1. Measure the leakage current and power input to the valve elements of MOSA; Obtain the power dissipation – time relationship and therefore the $q_i - t$ relationship.

Step 2. Model the thermal behavior of MOSA as described in Chapter 3.

Step 3. Obtain by simulation the heating and cooling curves of the MOSA at the location of the hottest valve element.

Step 4. Obtain by simulation the cooling curves of TETS. Adjust the test section parameters such as the air gap width and thickness of the housing so that the cooling curve matches that of the MOSA.

5.5 Comparison of Test Section Designs

It is possible to design a TETS which employs insulation material such as glass wool between element and housing (Fig. 5.2). However, it is found that it is difficult to obtain thermal equivalence for a test section which employs glasswool. Moreover the thermal characteristics of glass wool change with the density i.e. tightness of packing. In addition the model does not have an air gap between the element and the housing as in the case of the MOSA. However, TETS with air gap between the element and the housing (shown in Fig. 5.1 and 5.3) are easier to fabricate than the model employing glass wool. The TETS with air gap is also involved the similar heat transfer modes i.e. convection in air gap as that of the MOSA. Thus, the suggested test section with air gap is more representative of an actual arrester. In addition the housing material of the suggested TETS can be any available insulating tube with the designed dimensions, which makes the TETS much easier to be obtained. Table 5.4 compares several designs of test sections. It can be see that it is convenient and easy to design a TETS using the proposed simulation technique.

Table 5.4 Comparison of test section designs

	IEC standard [50]	Canada standard [51]	Reference [4]	Reference [8]	Reference [5]	proposed TETS
number of elements	≥1	≥1	1	2	5	1–3
housing material	same as arrester housing	same as arrester housing	thermal Insulator	porcelain	porcelain	any insulating material
I.D. of housing	arrester housing I.D. ±5%	arrester housing I.D.	no housing	—	—	designed
housing length	long enough to enclose element	≥ 1 shed length; ≤ 110% ele. length	—	longer then the length of ele. + electrodes	longer then the length of ele. + electrodes	just long enough to enclosed element + electrodes
test section ends	thermal insulating material	thermal insulating material	thermal Insulator	air	ceramic board	any good thermal insulator
material between ele. and housing	—	—	thermal Insulator or air	air	air or glass wool	air
adjustment of thermal property	axial thickness of end insulation material	axial thickness of end insulation material	—	—	glass wool packing	housing thickness and radial length of air gap
thermal equivalence			not estab-lished	not established	difficult to obtain	equivalence demonstrated

Chapter 6

SUMMARY AND CONCLUSIONS

6.1 Conclusions

In this thesis, existing models of MOSA are briefly reviewed and the assumptions inherent in them are outlined in Chapter 1. The thermal properties of MOSA are identified and the heat transfer modes are discussed in Chapter 2. Based on the heat transfer modes and the principle of energy conservation, an improved mathematical model which overcomes the drawbacks of the previous models is described in Chapter 3. Chapter 4 verifies the accuracy of the suggested model by comparison of the predicted thermal behavior with existing experimental data in the literature[4] and with the experimental results obtained by conducting tests on an actual 84kV MOSA; the thermal performance of the 84kV MOSA under the influence of a temporary overvoltage is also evaluated. In Chapter 5 TETS of 84kV MOSA is derived using the mathematical model; A procedure to design a TETS is discussed; the thermal equivalence between the TETS derived by simulation and the 84kV MOSA which it represents is verified by conducting tests on the MOSA and the single element test section, which demonstrate the accuracy of the modelling technique.

The following conclusions can be drawn from the study in the thesis:

(1) A better and more accurate representation of heat transfer modes of conduction, convection and radiation has been applied in the derivation of mathematical model. Fin theory is used to account for external heat transfer from the sheds of the arrester housing, and heat transfer from electrodes is also taken into account.

(2) The proposed model yields the temporal variation of MOSA temperature distribution in both the axial and radial directions; the model can be used to simulate thermal behavior of MOSA under steady state and transient conditions.

(3) The suggested modelling technique can be applied to any configuration of arrester and different operating conditions i.e. different applied voltages and different magnitudes and durations of TOV. It can also be applied to evaluate the thermal behavior of MOSA under different kinds of overvoltages provided the power generated in the valve elements is available.

(4) A new and practical method to derive a TETS is recommended based on the modelling technique; It has proven that the derived TETS following the suggested procedure can be thermally identical to that of the MOSA which it represents.

(5) The good agreement between the simulated and experimental results demonstrates the accuracy of the modeling technique.

(6) The proposed model can be used to determine the thermal capability, stability and aging of MOSA.

6.2 Recommendations for Future Work

This thesis offers the following suggestions for future work:

(1) Simple methods are required to obtain an accurate value of the power input to the valve element under various conditions (i.e 60Hz, TOV, lightning and switching surges)

in order to obtain an accurate results of the temperature distribution in MOSA subjected a various of voltages.

(2) Nonlinear voltage distribution along the arrester column due to capacitance to ground and surface pollution should be considered.

(3) Simulation of MOSA may be carried out taking into account nonsymmetrical heating due to solar radiation.

REFERENCES

1. E.C.Sakshaug, J.S.Kresge and S.A.Miske, "A New Concept in Station Arrester Design", IEEE Transactions on Power Apparatus and Systems, Vol. PAS–96, No.2, pp. 647–656, March/April 1977.

2. M.V. Lat, "Thermal Properties of Metal Oxide Surge Arresters", IEEE Transactions on Power Apparatus and Systems, Vol. PAS–102, N0. 7, pp. 2194–2202, July 1983.

3. M.V. Lat, "Analytical Method for Performance of Metal Oxide Surge Arresters", IEEE Transactions on Power Apparatus and Systems, Vol. PAS–104, No.10, pp. 2665–2674, October 1985.

4. M.Mizuno, M.Hayashi and K.Mitani, "Thermal Stability and Life of the Gapless Surge Arrester", IEEE Transactions on Power Apparatus and Systems, Vol. PAS–100, No. 5, pp. 2664–2670, May 1981.

5. S.Nishiwaki, H.Kimura, T.Satoh, H.Mizoguchi and S.Yanabu, "Study of Thermal Runway/Equivalent Prorated Model of a ZnO Surge Arrester", IEEE Transactions on Power Apparatus and Systems, Vol. PAS–103, No.2, pp. 413–421, Feb. 1984.

6. Guy St–Jean and Andre Petit, "Metal–Oxide Surge Arrester Operating Limits Defined by a Temperature Margin Concept", IEEE Transactions on Power Delivery, Vol. PWRD–5, No.2, pp. 627–633, April 1990.

7. A.Bargigia, M. de Nigris, A Pigini and A. Sironi, "Comparison of Different Test Method to Assess the Thermal Stresses of Metal Oxide Surge Arresters Under Pollution Conditions" IEEE Transactions on Power Delivery, Vol. 8, No. 1, pp. 146–155, January 1993.

8. M.Kan, S.Nishiwaki, T.Sato, S.Kojima and S.Yanabu, "Surge Discharge Capability and Thermal Stability of a Metal Oxide Surge Arrester", IEEE Transactions on Power Apparatus and Systems, Vol. PAS–102, No.2 pp.282–288, February 1983.

9. S. Tominaga, Y. Shibuya, Y. Fujiwara, M. Imataki and T. Nitta, "Stability and Long Term Degradation of Metal Oxide Surge Arrester", IEEE Transactions on Power Apparatus and Systems, Vol. PAS–99, No.4, pp. 1548–1556, July/Aug. 1980.

10. V. Hinrichsen and R. Peiser, "Simulation of the AC–Performance of Gapless ZnO–Arresters", Fifth International Symposium on High Voltage Engineering, Braunschweig, paper 82.09, Aug. 1987.

11. V. Hinrichsen and R. Peiser, "Simulation of the Electrical and Thermal Behaviour of Metal Oxide Surge Arresters Under AC–Stress", Sixth International Symposium on High Voltage Engineering, New Oleans, LA, USA, paper 26.04, 1989.

12 Andre Petit, Xuan Dai Do and Guy St–Jean, "An experimental Method to Determine the Electro–Thermal Model Parameters of Metal Oxide Surge Arresters", IEEE Transactions on Power Delivery, Vol.6, No.2, pp. 715–721, April 1991.

13. F.R. Stockum, "Simulation of the Nonlinear Thermal Behavior of Metal Oxide Surge Arresters Using a Hybrid Finite Difference and Empirical Model", IEEE Transactions on Power Delivery, 1993.

14. K.Feser, W.Kohler, D.Qiu and K.Chrzan, "Behaviour of Zinc Oxide Surge Arresters Under Pollution", IEEE Transactions on Power Delivery, Vol. 6, No. 2, pp. 688–694, April 1991.

15. Peter Kirkby, C.C.Erven and O.Nigol, "Long–Term Stability and Energy Discharge Capacity of Metal Oxide Arresters", IEEE Transactions on Power Delivery, Vol. 3, No.4, pp. 1656–1662, October 1988.

16. M.Kobayashi, M.Mizuno, M.Hayashi and Y.Sughita, "Metal Oxide Surge Arrester", IEEE Transactions on Electrical Insulation Vol. EI–21 No.6, December 1986.

17. Kazuo Eda, "Destruction Mechanism of ZnO Varistors Due to High Currents", Journal of Applied Physics, Vol. 56, No. 10, pp. 2848–2955, November 1984.

18. A.Mizukoshi, "Influence of Uniformity on Energy Absorption Capability of Zinc Oxide Element as Applied in Arrester", IEEE Transactions on Power Apparatus and Systems, Vol. PAS–102, No. pp.1384–1390, May 1983.

19. T.K.Gupta, W.G.Carlson and P.L.Hower, "Current Instability Phenomena in ZnO Varistors Under a Continuous AC Stress", Journal of Applied Physics, Vol. 52, No. 6, pp. 4104–4110, June 1981.

20. S. Tominaga, K.Azumi, T.Nitta, N,Nagai, M.Tmataki and H.Kuwahara, " Reliability and Application of Metal Oxide Arrester", IEEE Transactions on Power Apparatus and Systems, Vol. PAS–98, No. 3, pp. 805–812, May/June 1979.

21. H.R.Philipp and Lionel M.Levinson, "High–Temperature Behavior of ZnO–Based Ceramic Varistors", Journal of Applied Physics, Vol. 50, No. 1, pp. 383–389, January 1979.

22. H.R.Philipp and Lionel M.Levinson, "Low–Temperature Electrical Studies on Metal–Oxide Varistors – A Clue to Conduction Mechanisms", Journal of Applied Physics, Vol. 48, No. 4, pp. 1621–1626, April 1977.

23. Lionel M.Levinson and H.R.Philipp, "The Physic of Metal Oxide Varistors", Journal of Applied Physics, Vol. 46, No. 3, pp. 1332–1341, March 1975.

24. P.P. Hebert and R.C.Steed, "A High Voltage Bushing Thermal Performance Computer Model", IEEE Transactions on Power Apparatus and Systems, Vol. PAS–97, No. 6, Nov/Dec 1978.

25 M.Kobayashi, M.Mizuno, T.Aizawa, M.Hayashi and K.Mitani, "Development of ZnO Non–Linear Resistors and Their Applications to Gapless Surge Arresters", IEEE Transactions on Power Apparatus and Systems, Vol. PAS–97, No. 4, pp. 1149–1157, July/Aug 1978.

26. Klaus Ragaller, "Surges In High–Voltage Networks", Plenum, New York, 1979.

27. B.V.Karlekar and R.M.Desmond, "Heat Transfer", 2th ed., West Publishing Co., U.S.A., 1982

28. Warren M.Rohsenow, James P.Hartnett and Ejup N.Ganic, "Handbook of Heat Transfer, Fundamentals", Second Edition, McGraw–Hill Book Company, 1985.

29. J.P.Holman, "Heat Transfer", 5th ed., New York: Mcgraw–Hill, 1981.

30. James P.Todd and Herbert B.Ellis, "Applied Heat Transfer", Harper & Raw, Publishers, New York, 1982.

31. R.Leuenberger and R.A.Person, "Complication of Radiation Shape Factors For Cylindrical Assemblies", ASME Paper 56–A–144, January 1957.

32. Ephraim M.Sparrow, "Radiation Heat Transfer", Washington: Hemisphere Pub. Corp., 1978

33. Frank M. White, "Heat Transfer", Addison–Wesley, 1984.

34. M.Necati Ozisik, "Boundary Value Problems of Heat Conduction", Scranton, International Textbook Co., 1968.

35. Vedat S.Arpaci, "Conduction Heat Transfer", Addison–Wesley Publishing Company, 1966

36. John H. Lienhard, "A Heat transfer Textbook", Prentice–Hall, Inc., Englewood Cliffs, 1981

37. M.Necati Ozisik, "Heat Conduction", New York: Wiley, 1980.

38. Tyn Myint–U and L.Debnath, "Partial Differential Equations for Scientists and Engineers", Third Edition, Elsevier Science Publishing Co., Inc., 1987

39. David R. Croft and David G. Lilley, "Heat Transfer Calculations Using Finite Difference Equations ", Applied Science Publications LTD, London

40. J.Alan Adams and David F.Roger, "Computer–Aided Heat Transfer Analysis", McGraw–Hill, Inc., 1973.

41. Leon Lapidus, "Numerical Solutions of Partial Differential Equations in Science and Engineering", Wiley, New York, 1982

42. Donald Q.Kern and Allan D., "Extended Surface Heat Transfer", McGraw–Hill, Inc., 1972.

43. W.A.Gray and R. Muller, "Engineering Calculation in Radiative Heat Transfer", Oxford, New York, 1974

44. James R.Welty", "Engineering Heat Transfer", John Wiley & Sons, Inc., 1974.

45. Louis C. Burmeister, "Convective Heat Transfer", John Wiley & Sons, Inc., 1983.

46. F.P. Incropera and D.P. Dewitt, "Fundamentals of Heat Transfer", John Wiley & Sons, Inc., 1981.

47. Alexander Goldsmith, Tbomas E. Waterman and Harry J. Hirscbborn, "Handbook of Thermo–physical Properties of Solid Materials", The Macmillan Company, New York, 1961.

48. P.A.Kinzie, "Thermocouple Temperature Measurement", John Wiley & Sons, Inc., 1973.

49. IEC Standard, "Surge Arresters, Part 3: Metal Oxide Surge Arresters Without Gaps for A.C. Systems", IEC TC 37 WG–4 (Secretary) 11, Revision Based on TC37 Gaithersburg Meeting, August 1988.

50. An American National Standard, IEEE Standard, "Metal–Oxide Surge Arresters for AC Power Circuits", ANSI/IEEE C62.11–1987, Institute of Electrical and Electronics Engineers, Inc., New York, USA, 1987.

51. National Standard of Canada, "Gapless Metal Oxide Surge Arresters for Alternating Current Systems", CAN/CSA– C233.1–87, 1987.

52. JEC–203–1978, "Surge Arresters", The Japanese Electrotechnical Committee, 1978

Appendix A

FORTRAN PROGRAM TO SIMULATE MOSA AND TEST SECTION

A.1 Nomenclature Used In FORTRAN Program

Variable	Definition
Ai(i=1,2...)	Area
B	Coefficient of cubical expansion
CL	Constant
CP	Specific heat of valve element
CP1	Specific heat of arrester housing
CP2	Specific heat of electrode
CPA	Specific heat of air
DEN	Density of valve element
DEN1	Density of arrester housing
DEN2	Density of electrode
DENA	Density of air
DR,DZ	Small increment of valve element in radial and axial directions
DR1,DZ1	Small increment of arrester housing in radial and axial directions
DT	Temperature difference
DTIME	Time step
E	Electric field
E(I)	Electric field at node (i,j=1,2,....m_1)
EE	Radiation emissivity on the surface of valve element
EEL	Radiation emissivity on the surface of electrode
EJO	Current density

EJR	Current flowing through the valve elements
EP	Radiation emissivity on the surface arrester housing
FIJ	Radiation shape factor between two small segment
G	Gravitational acceleration
GR	Grashof number
HIN	Enclosed convection heat transfer coefficient
HPO,H1	Convection heat transfer coefficient between housing and ambient (free and forced convection)
LE	Length of valve element
LP	Length of arrester housing
L1	Length of bottom electrode
L2	Length of top electrode
L3	Length of inside electrode at bottom
L4	Length of inside electrode at top
LF	shed length
LS	Length of arrester supporter
M	Number of nodes of valve element in radial direction
M1	=M+1
M2	Number of shed segments
N	Number of nodes of valve element in axial direction
N1	=N+1
NF	Number of sheds
NN	Number of nodes of arrester housing in radial direction
NN1	=NN+1
NP	Number of nodes of arrester housing in axial direction
NN2	=NP+1
NU	Nusselt number
PR	Prandtl number
QGEN	Heat Generation
QGEN1	Heat Generation per cubic volume (W/m^3)
QGEN1(I)	Heat Generation per cubic volume at node (I,J=1,2,...M1)
QCOND	Heat conduction
QCONV	Heat convection
QRAD	Heat radiation

QSUN	Energy input due to radiation of the sun
QSKY	Energy input due to radiation of the sky
RE	Radii of valve element
R(I)	Radial coordinate of valve element
RR(I)	Radial coordinate of arrester housing
RP1	Radii of inside cylinder of arrester housing
RP2	Radium of outside cylinder of arrester housing
RF	Radium of shed of arrester housing
RRA	Rayleigh number
SB	Stefan–Boltzmann constant
TAMB	Ambient temperature
TIME	Time
T(I,J)	Temperature of valve elements at the current time step
TO(I,J)	Temperature of valve elements at the previous time step
TK	Thermal conductivity of valve element
TK1	Thermal conductivity of arrester housing
TKAIR	Thermal conductivity of air
TT(I,J)	Temperature of arrester housing at the current time step
TTO(I,J)	Temperature of arrester housing at the previous time step
TTT1	Temperature of the bottom electrode
TTT2	Temperature of the top electrode
TF(II,J)	Temperature of the II^{th} shed at the current time step
TFO(II,J)	Temperature of the II^{th} shed at the previous time step
TS(I)	Supporter temperature at the current time step
TS(I)	Supporter temperature at the previous time step
U	Absolute viscosity
VL	Volume
VU	Kinematic viscosity of air
Z(II)	z coordinate of the II^{th} shed

A.2 FORTRAN Program

```
      REAL    LE, LP
      REAL    L1, L2 , LF, L3, L4
      COMMON / D1/ N, M, NN, NP, TAMB, TH/ D2/ RE, RP1, RP2, LE, LP
      COMMON / D/ T (50, 50), R (50), TT (50, 50), RR (50)
      COMMON   / D3/ CP, CP1, CP2, TK, TK1, DEN, DEN1, DEN2/ D4/ TKAIR, SB
      COMMON / D5/ EE, EP, EEL
      COMMON / D7/ ET, V, S/ D8/ DR, DZ, DR1, DZ1, DTIME/ D9/ VL, QGEN1
      COMMON N1, M1, NN1, NN2, I, J, RAT, RA1, RA2, RA3
      COMMON / D10/ TO (50, 50), TTO (50, 50), TF (20, 50), RF (50)
      COMMON / D12/ TSO (20), NS, DS
      COMMON / D13/ REL, REL1, L3, L4
      DATA  REL, REL1, L3, L4/
      DATA N, M, NN, NP, TAMB
      DATA RE, RP1, RP2, RP3, LE, LP/
      DATA CP, CP1, CP2, TK, TK1, DEN, DEN1, DEN2/
      DATA TKAIR, SB/
      DATA EE, EP, EEL/
      DATA ET, V/
      DATA L1, L2/
      DATA THI, NF/
      WRITE (80, 900)
900   FORMAT (1X, 'FORTRAN PROGRAM FOR THE SIMULATION OF THERMAL
  *   PROPERTIES OF MOSA')
C
C     CONSIDERING ELECTRODS, SET CS NOT TO BE EQUAL TO 0.0
C     CONSIDERING CONDUCTION IN METAL ELECTRODE, SET CS=1.
C     CONSIDERING shedS HEAT TRANSFER, SET CS1=1.
C     CONSIDERING ENERGY INPUT DUE TO SOLAR AND SKY RADIATION, SET
C     CS2=1., OTHERWISE SET CS2=0.
C
      CS=1.
      CS1=0.
      CS2=0.
      IF (CS2.EQ.1.) GO TO 97
      L=2000
      GO TO 441
97    L=1000
441   WRITE (80, 50) N, M, NN, NP, TAMB
      WRITE (80, 58) RE, RP1, RP2, LE, LP
      WRITE (80, 60) CP, CP1, CP2, TK, TK1, DEN, DEN1, DEN2
      WRITE (80, 65) TKAIR, SB
      WRITE (80, 70) EE, EP, EEL
50    FORMAT (/ 1X, 2HN:, I5, 2X, ' M:', I5, 2X, 3HNN:, I5, 2X, ' NP', I5, 3X,
  *   5HTAMB:, F10.4)
58    FORMAT (/ 1X, ' RE:', F10.4, ' RP1:', F10.4, ' RP2:', F10.4,
  *   ' LE:', F10.4, ' LP:', F10.4)
60    FORMAT (/ 1X, ' CP:', F10.4, ' CP1:', F10.4, ' CP2:', F10.4,
  *   ' TK:', F10.4, ' TK1:', F10.4, ' DEN:', F10.4, ' DEN1:', F10.4,
  *   ' DEN2', F10.4)
65    FORMAT (/ 1X, ' TKAIR:', F10.4, ' SB:', F10.4)
70    FORMAT (/ 1X, ' EE:', F10.4, ' EP', F10.4, ' EEL', F10.4)
      DZ=LE/ (0.0+N)
      DR=RE/ M
      DR1= (RP2-RP1)/ (0.0+NN)
      DZ1=LP/ (0.0+NP)
      WRITE (80, 620) DZ, DR, DZ1, DR1
```

```
620     FORMAT (/ 1X, ' DZ', F10.4, '  DR', F10.4, '  DZ1', F10.4, '  DR1',
     *  F10.4)
        N1=N+1
        M1=M+1
        NN1=NN+1
        NN2=NP+1
C
C
        R (1)=0.
        DO 11 J=2, M1
11      R (J)=R (J-1)+DR
        RR (1)=RP1
        DO 22 J=2, NN1
22      RR (J)=RR (J-1)+DR
C
C       ACCURATLY  RADIATION SHAPE FACTOR AND RA'
C
        CALL RSF (F25, F24, F17)
        CALL RAF (F25, F24, F17)
        WRITE (80, 399) F25, F24, F17, RAT, RA1, RA2, RA3
399     FORMAT (1X, 'F25=', F10.5, ' F24=', F10.5, ' F17=', F10.5, / 1X,
     *  ' RAT=', E10.5, ' RA1=', E10.5, ' RA=2', F10.5, ' RA3=', E10.5)
C
C       SET INITIAL TEMPERATURE
C
        DO 1 I=1, N1
        DO 1 J=1, M1
        TO (I, J)=TAMB
1       CONTINUE
        WRITE (80, 200)  ( (TO (I, J), J=1, M1), I=1, N1)
        DO 77 I=1, NN2
        DO 77 J=1, NN1
77      TTO (I, J)=TAMB
        TTT1=TAMB
        TTT2=TAMB
        DO 39 I=1, NS+1
39      TSO (I)=TAMB
C
C       SETTING INITIAL TEMPERATURE OF shedS
        LF=RP3-RP2
        M2=LF/ DR1
        DO 435 J=1, M2+1
        DO 435 II=1, NF
435     TF (II, J)=TAMB
C
C
C       SET COORDINATES OF shedS
        RF (1)=RP2
        DO 445 I=2, M2+1
445     RF (I)=RF (I-1)+DR1
C
        CALL CONVH (HTOP, HPO, HIN)
        WRITE (80, 640) HTOP, HPO, HIN
C
C       TIME STEP
C
        DT1=DEN*CP/ TK/  (2./ DZ**2+4./ DR**2)
        DT2=DEN1*CP1/ TK1/  (2./ DR1**2+2./ DZ1**2)
```

```
      DTIME=DT1
      IF (DT2.LT.DTIME) DTIME=DT2
      IF (CS2.EQ.1.) GO TO 19
      GO TO 91
19    DTIME=DTIME/ 500.
91    WRITE (80, 220) DTIME
C
C     HEAT INPUT DUE TO RADIATION OF SUN AND SKY
C
      CALL QSS (QSUN1, QSKY1, QSUN2, QSKY2)
      WRITE (80, 432) QSUN1, QSKY1, QSUN2, QSKY2
432   FORMAT (1X, 'QSUN & QSKY ON VERTICAL SURFACE  (W/ M**2):',
     * 1X, F10.4, 3X, F10.4, / 1X, 'QSUN & QSKY ON HORI. SURFACE',
     * ' (W/ M**2):', 1X, F10.4, 3X, F10.4)
      QSS1=QSUN1+QSKY1
      QSS2=QSUN2+QSKY2
      S=1.0
510   TIME=0.0
56    IC=0
55    TIME=TIME+DTIME
      IC=IC+1
C
C     CONVECTION COEFFICIENT:H
C
      CALL CONVH (HTOP, HPO, HIN)
C
C     POWER INPUT TO VALVE ELEMENT DUE TO LEAKAGE CURRENT
C
      CALL QQ (TIME, EJR)
C
C     ELECTRODE TEMPERATURE TTT
C
      IF (CS.EQ.0.) GO TO 910
      CALL TELEC (TTT1, TTT2, L1, L2, HTOP, HPO, CS2, QSS2, QSS1)
      DO 120 J=1, M1
      T (N1, J)=TTT2
120   T (1, J)=TTT1
      DO 122 J=1, NN1
      TT (1, J)=TTT1
122   TT (NN2, J)=TTT2
      GO TO 920
C
C     NOT CONSIDERING THE INFLUENCE  OF ELECDRODE
C     TOP AND BOTTOM ELEMENT TEMPERATURE
C
910   CALL TTB (HTOP)
      CALL TCORN (HIN, HTOP)
      CALL TCTOB (HTOP)
C
C     CONSIDERING ELECTRODE HEAT TRANSFER
C
C     VALVE ELEMENT ELEMENT TEMPERATURE
C
C     SURFACE TEMPERATURE
C
920   CALL TSE (HIN)
C
C     CENTERAL LINE TEMPERATURE  (R=0)
```

```
C
      CALL TCEN
C
C     NTERIAL TEMPERATURE
C
      CALL TINTE
C
C     HOUSING  TEMPERATURE
C
C     EXTERIOR SURFACE TEMPERATURE
C
      IF (CS1.EQ.1.) GO TO 930
      CALL TOSP (HPO, CS2, QSS1)
      GO TO 940
930   CALL TshedS (M2, NF, LF, THI, HTOP, HPO, CS2, QSS1)
C
C     INTERIOR TEMPERATURE
C
940   CALL TINP
C
C     INTERIOR SURFACE TEMPERATURE
C
      CALL TISP (HIN)
C
C*****************************************************************************
C
      DO 116 I=1, N1
      DO 116 J=1, M1
116   TO (I, J)=T (I, J)
      DO 118 I=1, NN2
      DO 118 J=1, NN1
118   TTO (I, J)=TT (I, J)
      IF (IC.LT.L) GO TO 55
      TIME1=TIME/ 3600.
      WRITE (6, 100) TIME1
      WRITE (80, 100) TIME1
C
C     HEAT LOSS
C
      QRAD=0.0
      QCOND=0.0
      QCONV=0.0
C
C     HEAT LOSS ON THE SURFACE OF ELEMENT AT TIME T
C
      I=1
      J=M1
      QRAD=QRAD+SB* ( ( (T (I, J)+273.)/ 100.)**4- ( (TT (I, 1)+273.)/ 100.)
     *  **4)/ RA1
      QRAD=QRAD+SB* ( ( (T (I, J)+273.)/ 100.)**4- ( (TT (I-1, 1)+273.)/ 100.)
     *  **4)/ RA2
      QRAD=QRAD+SB* ( ( (T (I, J)+273.)/ 100.)**4- ( (TTT2+273.)/ 100.)
     *  **4)/ RA3
      I=N1
      QRAD=QRAD+SB* ( ( (T (I, J)+273.)/ 100.)**4- ( (TT (I, 1)+273.)/ 100.)
     *  **4)/ RA1
      QRAD=QRAD+SB* ( ( (T (I, J)+273.)/ 100.)**4- ( (TT (I+1, 1)+273.)/ 100.)
     *  **4)/ RA2
```

```
      QRAD=QRAD+SB* ( ( (T (I, J)+273.)/ 100.)**4- ( (TTT1+273.)/ 100.)
     *      **4)/ RA3
      DO 88 I=2, N
      QRAD=QRAD+SB* ( ( (T (I, J)+273.)/ 100.)**4- ( (TT (I, 1)+273.)/ 100.)
     *      **4)/ RA1
      QRAD=QRAD+SB* ( ( (T (I, J)+273.)/ 100.)**4- ( (TT (I-1, 1)+273.)/ 100.)
     *      **4)/ RA2
      QRAD=QRAD+SB* ( ( (T (I, J)+273.)/ 100.)**4- ( (TT (I+1, 1)+273.)/ 100.)
     *      **4)/ RA2
 88   CONTINUE
      DO 89 I=1, N1
      QCOND=QCOND+TKAIR* (T (I, J)-TTO (I, 1))*2.*3.14/ ALOG (RP1/ RE)*DZ1
      QCONV=QCONV+HIN*2.*RR (1)* (T (I, J)-TT (I, 1))*3.14*DZ1
 89   CONTINUE
      QTOT1=QRAD+QCONV+QCOND
      WRITE (80, 660) QRAD, QCONV, QCOND, QTOT1
C
C     HEAT LOSS THROUGH ELECTRODES AT TIME T
C
      A=3.14159*RP2**2
      A1=2.*3.14159*RP2*L1
      A2=2.*3.14159*RP2*L2
      QRAD=EEL*SB* ( ( (TTT1+273.)/ 100.)**4- ( (TAMB+273.)/ 100.
     *      )**4)*A1
      QRAD=QRAD+EEL*SB* ( ( (TTT2+273.)/ 100.)**4- ( (TAMB+273.)/ 100.
     *      )**4)* (A+A2)
      QCONV=HPO* (TTT1-TAMB)*A1
      QCONV=QCONV+ (TTT2-TAMB)* (A*HTOP+A2*HPO)
      QCONS=TK1*A* (TTT1-TSO (NS))/ DS
      QTOT2=QRAD+QCONV
      WRITE (80, 640) HTOP, HPO, HIN
 640  FORMAT (/ 1X, 'HTOP', F10.4, ' HPO', F10.4, ' HIN', F10.4)
      WRITE (80, 600) QRAD, QCONV, QTOT2
C
C     HEAT LOSS FROM THE SURFACE OF HOUSING
C
      QRAD=0.0
      QCONV=0.0
      IF (CS1.EQ.1.) GO TO 950
      DO 99 I=1, NN2
      QRAD=-EP*SB*2*RR (NN1)* ( ( (TAMB+273.)/ 100.)**4- ( (TT (I, NN1)+273)
     *      / 100.)**4)*DZ1*3.14+QRAD
      QCONV=-HPO*2.*RR (NN1)*3.14* (TAMB-TT (I, NN1))*DZ1+QCONV
 99   CONTINUE
      QTOT=QRAD+QCONV
      GO TO 980
C     HEAT LOSS FROM shedS
C
 950  DO 960 II=1, NF
      DO 970 J=2, M2
      A3=3.14159*2.*RF (J)*DR1
      QCONV=QCONV-2.*HTOP* (TAMB-TF (II, J))*A3
      QRAD=QRAD-2.*EP*SB* ( ( (TAMB+273.)/ 100.)**4- ( (TF (II, J)+273.)
     *      / 100.)**4)*A3
 970  CONTINUE
      J=M2+1
      A=2*3.14159*RP3*THI
      QCONV=QCONV-HPO* (TAMB-TF (II, M2+1))*A
```

```
      A1=2.*3.14159* (RP3**2- (RP3-DR1/ 2.)**2)
      QCONV=QCONV-HTOP* (TAMB-TF (II, M2+1))*A1
      QRAD=QRAD-EP*SB* ( ( (TAMB+273.)/ 100.)**4- ( (TF (II, M2+1)+273.)
     *       / 100.)**4)* (A+A1)
960   CONTINUE
      A=2.*3.141569*RP2* (LP-NF*THI)
      QCONV=QCONV+HPO* (TT (2, NN1)-TAMB)*A
      QRAD=QRAD-EP*SB* ( ( (TAMB+273.)/ 100.)**4- ( (TT (2, NN1)+273.)
     *       / 100.)**4)*A
      QTOT=QCONV+QRAD
980   WRITE (80, 630) QRAD, QCONV, QTOT
      VL=3.14159*RE**2*LE*10.**6
      QUNI= (QTOT+QTOT2)/ VL
      WRITE (80, 968) QUNI
968   FORMAT (/ 1X, 'QUNI=', E10.4, '  W/ CM**3')
C
C*************************************************************************************
C
      IF (S.EQ.1.) GO TO 540
      QDIF=0.-QTOT-QTOT2+CS2* (QSS1*2.*3.14159*RP2*LP+
     *    QSS2*3.14159*RP2**2)
      WRITE (80, 625) QDIF
      GOTO 550
C
C     HEAT INPUT TO VALVE ELEMENT DUE TO LEAKAGE CURRENT
C      (E: V/ CM; QGEN2:W/ CM**3)
C
540   E=E/ 100.
      QGEN2=QGEN1 (I)/ 10.**6
      VL=3.14159*RE**2*LE
      QGEN=QGEN1 (I)*VL
      WRITE (80, 605) E, EJR, QGEN2, QGEN
      QDIF=QGEN-QTOT-QTOT2+CS2* (QSS1*2.*3.14159*RP2*LP+
     *    QSS2*3.14159*RP2**2)
      WRITE (80, 625) QDIF
625   FORMAT (/ 1X, '  QDIFFERENCE=', F10.5/ )
660   FORMAT (/ 1X, 'ELEMENT:', / 1X, 5HQRAD=, F10.4, 2X, 6HQCONV=, F10.4, 2X,
     *    6HQCOND=, F10.4, 2X, 8H QTOTAL=, F10.4)
600   FORMAT (1X, 'ELECTRODE:', / 1X, 5HQRAD=, F10.4, 2X, 7H QCONV=, F10.4,
     *    2X, 7HQTOTAL=, F10.4)
630   FORMAT (1X, 'HOUSING :', / 1X, ' QRAD=', F10.4, ' QCONV=', F10.4,
     *    ' QTOTAL=', F10.4)
605   FORMAT (/, 1X, ' E=', F10.2, 'V/ CM', '   EJR=', F10.4,
     *    ' QGEN1 (I)=', F12.5, 'W/ CM**3',  QGEN=', F10.4, 'W')
550   WRITE (80, 200)  ( (T (I, J), J=1, M1), I=1, N1)
      WRITE (80, 477)  (TSO (I), I=1, NS+1)
477   FORMAT (/ 1X, 'TS', 6 (1X, F10.4))
      IF (CS1.EQ.1.) GO TO 492
      GO TO 499
492   WRITE (80, 482)  ( (TF (II, J), II=1, NF), J=1, M2+1)
482   FORMAT (/ 1X, 'TF (II, J)', 4F10.4)
400   FORMAT (1X/ 3H TT, 4 (2X, F12.4))
100   FORMAT (1X// 6H TIME=, F13.4)
200   FORMAT (1X, 1HT, 4 (2X, F10.4))
220   FORMAT (1X, 6HDTIME=, F9.6)
499   IF (S.EQ.0.) GO TO 560
      DER=ABS (QDIF-QDIFO)
      IF (T (1, 1).GT.200.) GO TO 250
```

```
      IF (DER.LT.0.1) GO TO 250
      QDIFO=QDIF
      GO TO 56
560   IF (TIME.GT.TMAX) GO TO 530
      GO TO 56
250   S=0.
      TMAX=TIME
      GO TO 510
530   CONTINUE
      STOP
      END
C
C*********************************************************************************
C
C     VALVE ELEMENT SURFACE TEMPERATURE
C
      SUBROUTINE TSE (H)
      REAL LE, LP
      COMMON  / D1/ N, M, NN, NP, TAMB, TH/ D2/ RE, RP1, RP2, LE, LP
      COMMON  / D/ T (50, 50), R (50), TT (50, 50), RR (50)
      COMMON  / D3/ CP, CP1, CP2, TK, TK1, DEN, DEN1, DEN2/ D4/ TKAIR, SB
      COMMON  / D5/ EE, EP, EEL
      COMMON  / D7/ ET, V, S/ D8/ DR, DZ, DR1, DZ1, DTIME/ D9/ VL, QGEN1
      COMMON  N1, M1, NN1, NN2, I, J, RAT, RA1, RA2, RA3
      COMMON  / D10/ TO (50, 50), TTO (50, 50), TF (20, 50), RF (50)
      J=M1
      DO 2 I=2, N
      A1=3.14159* (R (J)**2– (R (J)–DR/ 2.)**2)
      A2=3.14159* (R (J)–DR/ 2.)*2*DZ
      QCON1=TK* (TO (I, J–1)–TO (I, J))/ DR*A2
      QCON2=TK* (TO (I+1, J)–TO (I, J))/ DZ*A1
      QCON3=TK* (TO (I–1, J)–TO (I, J))/ DZ*A1
      QCON4=TKAIR* (TTO (I, 1)–TO (I, J))*2*3.14159*DZ/ ALOG (RP1/ R (J))
      QCONV=H*2*3.14159*R (J)*DZ* (TTO (I, 1)–TO (I, J))
      QRAD=SB* ( ( (TTO (I, 1)+273.)/ 100.)**4– ( (TO (I, J)+273.)/ 100.)**4)
     *   / RA1
      QRAD=QRAD+SB* ( ( (TTO (I–1, 1)+273.)/ 100.)**4– ( (TO (I, J)+273.)/ 100.)
     *   **4)/ RA2
      QRAD=QRAD+SB* ( ( (TTO (I+1, 1)+273.)/ 100.)**4– ( (TO (I, J)+273.)/ 100.)
     *   **4)/ RA2
      VL=A1*DZ
      QGEN=QGEN1 (I)*VL
      T (I, J)=DTIME/ DEN/ CP/ VL* (QCON1+QCON2+QCON3+QCON4+QCONV+QRAD
     *   +QGEN)+TO (I, J)
2     CONTINUE
      RETURN
      END
C
C     CONSIDERING HEAT CONDUCTION IN MEATAL ELECTRODE
C     SURFACE TEMPERATURE OF ELEMENT AND ELECTRODE INSIDE
C
      SUBROUTINE TSE (H)
      REAL    LE, LP
      COMMON  / D1/ N, M, NN, NP, TAMB, TH/ D2/ RE, RP1, RP2, LE, LP
      COMMON  / D/ T (80, 80), R (80), TT (80, 80), RR (80)
      COMMON  / D3/ CP, CP1, CP2, TK, TK1, DEN, DEN1, DEN2/ D4/ TKAIR, SB
      COMMON  / D5/ EE, EP, EEL, TK2
      COMMON  / D7/ ET, V, S/ D8/ DR, DZ, DR1, DZ1, DTIME/ D9/ VL, QGEN1
```

```
      COMMON  N1, M1, NN1, NN2, I, J, RAT, RA1, RA2, RA3
      COMMON  / D10/ TO (80, 80), TTO (80, 80), TF (20, 80), RF (80)
      J=M1
      A1=3.14159* (R (J)**2- (R (J)-DR/ 2.)**2)
      A2=3.14159* (R (J)-DR/ 2.)*2*DZ
C
C     BOTTOME ELECTRODE
C
      DO 2 I=2, L3/ DZ
      QCON1=TK2* (TO (I, J-1)-TO (I, J))/ DR*A2
      QCON2=TK2* (TO (I+1, J)-TO (I, J))/ DZ*A1
      QCON3=TK2* (TO (I-1, J)-TO (I, J))/ DZ*A1
      QCON4=TKAIR* (TTO (I, 1)-TO (I, J))*2*3.14159*DZ/ ALOG (RP1/ R (J))
      QCONV=H*2*3.14159*R (J)*DZ* (TTO (I, 1)-TO (I, J))
      QRAD=SB* ( ( (TTO (I, 1)+273.)/ 100.)**4- ( (TO (I, J)+273.)/ 100.)**4 / RA1
      QRAD=QRAD+SB* ( ( (TTO (I-1, 1)+273.)/ 100.)**4- ( (TO (I, J)+273.)/ 100.)
     *  **4)/ RA2
      QRAD=QRAD+SB* ( ( (TTO (I+1, 1)+273.)/ 100.)**4- ( (TO (I, J)+273.)/
     *  100.)**4)/ RA2
      VL=A1*DZ
      T (I, J)=DTIME/ DEN2/ CP2/ VL* ( (QCON1+QCON2+QCON3+QCON4
     *  +QCONV+QRAD)/ 4.)+TO (I, J)
 2    CONTINUE
C
C     VALVE ELEMENT
C
      DO 12 I=L3/ DZ+1, L3/ DZ+N
      QCON1=TK* (TO (I, J-1)-TO (I, J))/ DR*A2
      QCON2=TK* (TO (I+1, J)-TO (I, J))/ DZ*A1
      QCON3=TK* (TO (I-1, J)-TO (I, J))/ DZ*A1
      QCON4=TKAIR* (TTO (I, 1)-TO (I, J))*2*3.14159*DZ/ ALOG (RP1/ R (J))
      QCONV=H*2*3.14159*R (J)*DZ* (TTO (I, 1)-TO (I, J))
      QRAD=SB* ( ( (TTO (I, 1)+273.)/ 100.)**4- ( (TO (I, J)+273.)/ 100.)**4)
     *  / RA1
      QRAD=QRAD+SB* ( ( (TTO (I-1, 1)+273.)/ 100.)**4- ( (TO (I, J)+273.)/ 100.)
     *  **4)/ RA2
      QRAD=QRAD+SB* ( ( (TTO (I+1, 1)+273.)/ 100.)**4- ( (TO (I, J)+273.)/
     *  100.)**4)/ RA2
      VL=A1*DZ
      QGEN=QGEN1 (I)*VL
      T (I, J)=DTIME/ DEN/ CP/ VL* ( (QCON1+QCON2+QCON3+QCON4
     *  +QCONV+QRAD)/ 4.+QGEN)+TO (I, J)
 12   CONTINUE
C
C     TOP  ELECTRODE
C
      DO 22 I=L3/ DZ+N+1,  (L3+L4)/ DZ+N
      QCON1=TK2* (TO (I, J-1)-TO (I, J))/ DR*A2
      QCON2=TK2* (TO (I+1, J)-TO (I, J))/ DZ*A1
      QCON3=TK2* (TO (I-1, J)-TO (I, J))/ DZ*A1
      QCON4=TKAIR* (TTO (I, 1)-TO (I, J))*2*3.14159*DZ/ ALOG (RP1/ R (J))
      QCONV=H*2*3.14159*R (J)*DZ* (TTO (I, 1)-TO (I, J))
      QRAD=SB* ( ( (TTO (I, 1)+273.)/ 100.)**4- ( (TO (I, J)+273.)/ 100.)**4)
     *  / RA1
      QRAD=QRAD+SB* ( ( (TTO (I-1, 1)+273.)/ 100.)**4- ( (TO (I, J)+273.)/ 100.)
     *  **4)/ RA2
      QRAD=QRAD+SB* ( ( (TTO (I+1, 1)+273.)/ 100.)**4- ( (TO (I, J)+273.)/
     *  100.)**4)/ RA2
```

```
      VL=A1*DZ
      T (I, J)=DTIME/ DEN2/ CP2/ VL* ( (QCON1+QCON2+QCON3+QCON4
     * +QCONV+QRAD)/ 4.)+TO (I, J)
 22   CONTINUE
      RETURN
      END
C
C     INTERIAL TEMPERATURE OF ELEMENT
C
      SUBROUTINE TINTE
      REAL LE, LP
      COMMON  / D1/ N, M, NN, NP, TAMB, TH/ D2/ RE, RP1, RP2, LE, LP
      COMMON  / D/ T (50, 50), R (50), TT (50, 50), RR (50)
      COMMON  / D3/ CP, CP1, CP2, TK, TK1, DEN, DEN1, DEN2/ D4/ TKAIR, SB
      COMMON  / D5/ EE, EP, EEL
      COMMON  / D7/ ET, V, S/ D8/ DR, DZ, DR1, DZ1, DTIME/ D9/ VL, QGEN1
      COMMON  / D10/ TO (50, 50), TTO (50, 50), TF (20, 50), RF (50)
      COMMON  N1, M1, NN1, NN2, I, J, RAT, RA1, RA2, RA3
      DO 44 I=2, N
      DO 44 J=2, M
      VL=1.
      QGEN=QGEN1 (I)*VL
      T (I, J)=DTIME/ DEN/ CP* (TK* ( (TO (I, J+1)-2*TO (I, J)+TO (I, J-1))/ DR**2
     * + (TO (I+1, J)-2*TO (I, J)+TO (I-1, J))/ DZ**2+ (TO (I, J+1)-TO (I, J-1))/
     * (2.*DR*R (J)))+QGEN)+TO (I, J)
 44   CONTINUE
      RETURN
      END
C
C     CENTRAL LINE TEMPERATURE OF ELEMENT
C
      SUBROUTINE TCEN
      REAL LE, LP
      COMMON / D1/ N, M, NN, NP, TAMB, TH/ D2/ RE, RP1, RP2, LE, LP
      COMMON / D/ T (50, 50), R (50), TT (50, 50), RR (50)
      COMMON / D3/ CP, CP1, CP2, TK, TK1, DEN, DEN1, DEN2/ D4/ TKAIR, SB
      COMMON / D5/ EE, EP, EEL
      COMMON / D7/ ET, V, S/ D8/ DR, DZ, DR1, DZ1, DTIME/ D9/ VL, QGEN1
      COMMON N1, M1, NN1, NN2, I, J, RAT, RA1, RA2, RA3
      COMMON / D10/ TO (50, 50), TTO (50, 50), TF (20, 50), RF (50)
      J=1
      DO 35 I=2, N
      VL=1.0
      QGEN=QGEN1 (I)*VL
      T (I, J)=DTIME/ DEN/ CP* (TK* ( (TO (I-1, J)-TO (I, J))/ DZ**2+
     * (TO (I+1, J)-TO (I, J))/ DZ**2+4* (TO (I, J+1)-TO (I, J))/ DR**2)+QGEN)
     * +TO (I, J)
 35   CONTINUE
      RETURN
      END
C
C
C     ELECTRODE   TEMPERATURE
C
C
      SUBROUTINE TELEC (TTT1, TTT2, L1, L2, HTOP, H1, CS2, QSS2, QSS1)
      REAL LE, LP
      REAL L1, L2, LS, L3, L4
```

```
      DIMENSION TS (20)
      COMMON / D1/ N, M, NN, NP, TAMB, TH/ D2/ RE, RP1, RP2, LE, LP
      COMMON / D/ T (50, 50), R (50), TT (50, 50), RR (50)
      COMMON / D3/ CP, CP1, CP2, TK, TK1, DEN, DEN1, DEN2/ D4/ TKAIR, SB
      COMMON / D5/ EE, EP, EEL
      COMMON / D7/ ET, V, S/ D8/ DR, DZ, DR1, DZ1, DTIME/ D9/ VL, QGEN1
      COMMON / D10/ TO (50, 50), TTO (50, 50), TF (20, 50), RF (50)
      COMMON / D12/ TSO (20), NS, DS
      COMMON N1, M1, NN1, NN2, I, J, RAT, RA1, RA2, RA3
      COMMON / D13/ REL, REL1, L3, L4
      DATA LS, NS, TS (1)/ 0.465, 5, 22./
      QCON=0.
      I=N1
      II=NN2
      DO 59 J=2, M
      A1=2*3.14159*R (J)*DR
      QCON=QCON+TK* (TO (I-1, J)-TTT2)/ DZ*A1
59    CONTINUE
      DO 41 J=2, NN
      A2=2*3.14159*RR (J)*DR1
      QCON=QCON+TK1* (TTO (II-1, J)-TTT2)/ DZ1*A2
41    CONTINUE
      J=M1
      A3=3.14159* (R (J)**2- (R (J)-DR/ 2.)**2)
      QCON=QCON+TK* (TO (I-1, J)-TTT2)/ DZ*A3
      J=NN1
      A4=3.14159* (RR (J)**2- (RR (J)-DR1/ 2.)**2)
      QCON=QCON+TK1* (TTO (II-1, J)-TTT2)/ DZ1*A4
      A5=3.14159* (DR/ 2.)**2
      QCON=QCON+TK* (TO (I-1, 1)-TTT2)/ DZ*A5
      A6=3.14159* ( (RR (1)+DR1/ 2.)**2-RR (1)**2)
      QCON=QCON+TK1* (TTO (II-1, 1)-TTT2)/ DZ1*A6
      A7=3.14159*RR (NN1)**2
      A8=3.14159*2.*RR (NN1)*L2
      VL=A7*L2
      QCONV= (TAMB-TTT2)* (HTOP*A7+H1*A8)
      QRAD=EEL*SB* ( ( (TAMB+273.0)/ 100.)**4- ( (TTT2+273.)/ 100.)**4)*
     *      (A7+A8)+CS2*QSS2*A7
      TTT2=DTIME/ DEN2/ CP2/ VL* (QCON+QCONV+QRAD)+TTT2
C
C     SUPPORTER TEMPERATURE
C
      DS=LS/ (NS+0.)
      A1=3.14159*RP2**2
      A2=2.*3.14159*RP2*DS
      VL=A1*DS
      DO 75 I=2, NS
      QCOND1=TK1* (TSO (I+1)-TSO (I))*A1/ DS
      QCOND2=TK1* (TSO (I-1)-TSO (I))*A1/ DS
      QCONV=H1* (TAMB-TS (I))*A2
      QRAD=EP*SB* ( ( (TAMB+273.0)/ 100.)**4- ( (TSO (I)+273.)/ 100.)**4)*
     *      A2+QSS1*A2*CS2
75    TS (I)=DTIME/ DEN1/ CP1/ VL* (QCOND1+QCOND2+QCONV+QRAD)+TSO (I)
C
C     BOTTOM ELECTRODE
C
      I=1
      QCON=0.
```

```
      DO 77 J=2, M
      A1=2*3.14159*R (J)*DR
      QCON=QCON+TK* (TO (I+1, J)–TTT1)/ DZ*A1
77    CONTINUE
      DO 74 J=2, NN
      A2=2*3.14159*RR (J)*DR1
      QCON=QCON+TK1* (TTO (I+1, J)–TTT1)/ DZ1*A2
74    CONTINUE
      J=M1
      QCON=QCON+TK* (TO (I+1, J)–TTT1)/ DZ*A3
      J=NN1
      QCON=QCON+TK1* (TTO (I+1, J)–TTT1)/ DZ1*A4
      QCON=QCON+TK* (TO (I+1, 1)–TTT1)/ DZ*A5
      QCON=QCON+TK1* (TTO (I+1, 1)–TTT1)/ DZ1*A6
      VL=A7*L1
      A8=2.*3.14159*RR (NN1)*L1
      QCONV=H1* (TAMB–TTT1)*A8
      QRAD=EEL*SB* ( ( (TAMB+273.0)/ 100.)**4– ( (TTT1+273.)/ 100.)**4)*
     * A8+QSS1*A8*CS2
      QCON=QCON+TK1* (TSO (NS)–TTT1)/ DS*3.14159*RP2**2
      TTT1=DTIME/ DEN2/ CP2/ VL* (QCON+QCONV+QRAD)+TTT1
      DO 774 II=2, NS
774   TSO (II)=TS (II)
      TS (NS+1)=TTT1
      TSO (NS+1)=TTT1
      RETURN
      END
C
C     EXTERIOR SURFACE TEMPERATURE OF HOUSING
C
      SUBROUTINE TOSP (H1, CS2, QSS1)
      REAL LE, LP
      COMMON / D1/ N, M, NN, NP, TAMB, TH/ D2/ RE, RP1, RP2, LE, LP
      COMMON / D/ T (50, 50), R (50), TT (50, 50), RR (50)
      COMMON / D3/ CP, CP1, CP2, TK, TK1, DEN, DEN1, DEN2/ D4/ TKAIR, SB
      COMMON / D5/ EE, EP, EEL
      COMMON / D7/ ET, V, S/ D8/ DR, DZ, DR1, DZ1, DTIME/ D9/ VL, QGEN1
      COMMON / D10/ TO (50, 50), TTO (50, 50), TF (20, 50), RF (50)
      COMMON N1, M1, NN1, NN2, I, J, RAT, RA1, RA2, RA3
      J=NN1
      A1= (RR (J)**2– (RR (J)–DR1/ 2.)**2)*3.14159
      VL=A1*DZ1
      A2=2*3.14159* (RR (J)–DR1/ 2.)*DZ1
      A3=2*3.14159*RR (J)*DZ1
      DO 800 I=2, NP
      QCON1=TK1* (TTO (I, J–1)–TTO (I, J))*A2/ DR1
      QCON2=TK1* (TTO (I+1, J)–TTO (I, J))*A1/ DZ1
      QCON3=TK1* (TTO (I–1, J)–TTO (I, J))*A1/ DZ1
      QRAD=EP*A3*SB* ( ( (TAMB+273.)/ 100.)**4– ( (TTO (I, J)+273.)
     * / 100.)**4)+CS2*QSS1*A3
      QCONV=H1*A3* (TAMB–TTO (I, J))
      TT (I, J)=DTIME/ DEN1/ CP1/ VL* (QCON1+QCON2+QCON3+QRAD+QCONV)
     * +TTO (I, J)
800   CONTINUE
      RETURN
      END
C
C     INTERIOR TEMPERATURE OF HOUSING
```

```
C
      SUBROUTINE TINP
      REAL LE, LP, L3, L4
      COMMON / D1/ N, M, NN, NP, TAMB, TH/ D2/ RE, RP1, RP2, LE, LP
      COMMON / D/ T (50, 50), R (50), TT (50, 50), RR (50)
      COMMON / D3/ CP, CP1, CP2, TK, TK1, DEN, DEN1, DEN2/ D4/ TKAIR, SB
      COMMON / D5/ EE, EP, EEL
      COMMON / D7/ ET, V, S/ D8/ DR, DZ, DR1, DZ1, DTIME/ D9/ VL, QGEN1
      COMMON / D10/ TO (50, 50), TTO (50, 50), TF (20, 50), RF (50)
      COMMON N1, M1, NN1, NN2, I, J, RAT, RA1, RA2, RA3
      COMMON / D13/ REL, REL1, L3, L4
      DO 46 I=2, NP
      DO 46 J=2, NN
      TT (I, J)=DTIME/ DEN1/ CP1*TK1* ( (TTO (I, J+1)–2*TTO (I, J)+TTO (I, J–1)
     * )/ DR1**2+ (TTO (I+1, J)–2*TTO (I, J)+TTO (I–1, J))/ DZ1**2+
     * (TTO (I, J+1)–TTO (I, J–1))/ (2.*DR1*RR (J)))+TTO (I, J)
 46   CONTINUE
      RETURN
      END
C
C     INTERIOR SURFACE TEMPERATURE OF HOUSING
C
      SUBROUTINE TISP (H1)
      REAL LE, LP
      COMMON / D1/ N, M, NN, NP, TAMB, TH/ D2/ RE, RP1, RP2, LE, LP
      COMMON / D/ T (50, 50), R (50), TT (50, 50), RR (50)
      COMMON / D3/ CP, CP1, CP2, TK, TK1, DEN, DEN1, DEN2/ D4/ TKAIR, SB
      COMMON / D5/ EE, EP, EEL
      COMMON / D7/ ET, V, S/ D8/ DR, DZ, DR1, DZ1, DTIME/ D9/ VL, QGEN1
      COMMON / D10/ TO (50, 50), TTO (50, 50), TF (20, 50), RF (50)
      COMMON N1, M1, NN1, NN2, I, J, RAT, RA1, RA2, RA3
      J=1
      A1=3.14159* ( (RR (J)+DR1/ 2.)**2–RR (J)**2)
      A2=2*3.14159* (RR (J)+DR1/ 2.)*DZ1
      DO 830 I=2, NP
      QCON1=TK1* (TTO (I, J+1)–TTO (I, J))*A2/ DR1
      QCON2=TK1* (TTO (I+1, J)–TTO (I, J))/ DZ1*A1
      QCON3=TK1* (TTO (I–1, J)–TTO (I, J))/ DZ1*A1
      QCON4=TKAIR* (TO (I, M1)–TTO (I, J))*2*3.14159*DZ1/ ALOG (RP1/ RE)
      QCONV=H1*2.*3.14159*RR (J)*DZ1* (TO (I, M1)–TTO (I, J))
      QRAD=SB* ( ( (TO (I, M1)+273.)/ 100.)**4– ( (TTO (I, J)+273.)/ 100.)
     * **4)/ RA1
      QRAD=QRAD+SB* ( ( (TO (I–1, M1)+273.)/ 100.)**4– ( (TTO (I, J)+273.
     * )/ 100.)**4)/ RA2
      QRAD=QRAD+SB* ( ( (TO (I+1, M1)+273.)/ 100.)**4– ( (TTO (I, J)+273.)
     * / 100.)**4)/ RA2
      VL=A1*DZ1
      TT (I, J)=DTIME/ DEN1/ CP1/ VL* (QCON1+QCON2+QCON3+QCON4+QCONV+
     * QRAD)+TTO (I, J)
830   CONTINUE
      RETURN
      END
C
C*****************************************************************************************
C
C     CONSIDERING shedE HEAT TRANSFER
C
C     EXTENDED SURFACE TEMPERATURE OF ARRESTER HOUSING
```

```
C
      SUBROUTINE TshedS (M2, NF, LF, THI, HTOP, H1, CS2, QSS1)
      REAL LE, LP, LF
      REAL Z (4)
      DIMENSION TFO (20, 50)
      COMMON / D1/ N, M, NN, NP, TAMB, TH/ D2/ RE, RP1, RP2, LE, LP
      COMMON / D/ T (50, 50), R (50), TT (50, 50), RR (50)
      COMMON / D3/ CP, CP1, CP2, TK, TK1, DEN, DEN1, DEN2/ D4/ TKAIR, SB
      COMMON / D5/ EE, EP, EEL
      COMMON / D7/ ET, V, S/ D8/ DR, DZ, DR1, DZ1, DTIME/ D9/ VL, QGEN1
      COMMON / D10/ TO (50, 50), TTO (50, 50), TF (20, 50), RF (50)
      COMMON N1, M1, NN1, NN2, I, J, RAT, RA1, RA2, RA3
      DATA Z/
C
C     shedS TEMPERATURE
C
      DO 465 II=1, NF
      DO 465 J=1, M2+1
465   TFO (II, J)=TF (II, J)
      DO 430 II=1, NF
      DO 425 J=2, M2
      A1=2.*3.14159* (RF (J)-DR1/ 2.)*THI
      A2=2.*3.14159* (RF (J)+DR1/ 2.)*THI
      A3=3.14159*2.*RF (J)*DR1
      QCON1=TK1* (TFO (II, J-1)-TFO (II, J))*A1/ DR1
      QCON2=TK1* (TFO (II, J+1)-TFO (II, J))*A2/ DR1
      QCONV=2.*HTOP* (TAMB-TFO (II, J))*A3
      QRAD=2.*EP*SB* ( ( (TAMB+273.)/ 100.)**4- ( (TFO (II, J)+273.)
     * / 100.)**4)*A3
C
      QRAD=QRAD+2.*QSS1*A3*CS2
      VL=A3*THI
      TF (II, J)=DTIME/ DEN1/ CP1/ VL* (QCON1+QCON2+QCONV+QRAD)
     * +TFO (II, J)
425   CONTINUE
C
C     TEMPERATURE OF shedS TIP
C
      RP3=RF (M2+1)
      A= (RP3-DR1/ 2.)*2.*3.14159*THI
      QCON=TK1* (TFO (II, M2)-TFO (II, M2+1))/ DR1*A
      A=2*3.14159*RP3*THI
      QCONV=H1* (TAMB-TFO (II, M2+1))*A
      A1=3.14159* (RP3**2- (RP3-DR1/ 2.)**2)
      QCONV=QCONV+HTOP* (TAMB-TFO (II, M2+1))*A1*2.
      QRAD=EP*SB* ( ( (TAMB+273.)/ 100.)**4- ( (TFO (II, M2+1)+273.)
     * / 100.)**4)* (A+A1)+CS2*QSS1* (A+2.*A1)
      VL=A1*THI
      TF (II, M2+1)=DTIME/ DEN1/ CP1/ VL* (QCON+QCONV+QRAD)+
     * TFO (II, M2+1)
430   CONTINUE
C
C     TEMPERATURE OF shedS BASE AND THE OTHER SURFACE OF HOUSING
C
      J1=Z (1)/ DZ1
      J=NN1
      A1=2.*3.14159* (RP2-DR1/ 2.)*DZ1
      A2=3.14159* (RP2**2- (RP2-DR1/ 2.)**2)
```

```
      A3=3.14159*RP2*2.*DZ1
      VL=A2*DZ1
      DO 450 I=2, J1
      QCON1=TK1* (TTO (I, NN)–TTO (I, J))*A1/ DR1
      QCON2=TK1* (TTO (I+1, J)–TTO (I, J))*A2/ DZ1
      QCON3=TK1* (TTO (I–1, J)–TTO (I, J))*A2/ DZ1
      QCONV=H1* (TAMB–TTO (I, J))*A3
      QRAD=EP*SB* ( ( (TAMB+273.)/ 100.)**4– ( (TTO (I, J)+273.)
     * / 100.)**4)*A3+CS2*QSS1*A3
      TT (I, J)=DTIME/ DEN1/ CP1/ VL* (QCON1+QCON2+QCON3+QCONV+QRAD)
     * +TTO (I, J)
450   CONTINUE
      I=J1+1
      A4=2.*3.14159* (RP2+DR1/ 2.)*DZ1
      QCON4=TK1* (TFO (1, 2)–TTO (I, J))/ DR1*A4
      QCON1=TK1* (TTO (I, NN)–TTO (I, J))*A1/ DR1
      QCON2=TK1* (TTO (I+1, J)–TTO (I, J))*A2/ DZ1
      QCON3=TK1* (TTO (I–1, J)–TTO (I, J))*A2/ DZ1
      TT (I, J)=DTIME/ DEN1/ CP1/ (VL*2.)* (QCON1+QCON2+QCON3+QCON4)
     * +TTO (I, J)
      TF (1, 1)=TT (I, J)
      DO 460 II=2, NF
      J1= (Z (II)–Z (II–1))/ DZ1
      I1=I+1
      I2=I+J1–1
      DO 455 I=I1, I2
      QCON1=TK1* (TTO (I, NN)–TTO (I, J))*A1/ DR1
      QCON2=TK1* (TTO (I+1, J)–TTO (I, J))*A2/ DZ1
      QCON3=TK1* (TTO (I–1, J)–TTO (I, J))*A2/ DZ1
      QCONV=H1* (TAMB–TTO (I, J))*A3
      QRAD=EP*SB* ( ( (TAMB+273.)/ 100.)**4– ( (TTO (I, J)+273.)
     * / 100.)**4)*A3+CS2*QSS1*A3
      TT (I, J)=DTIME/ DEN1/ CP1/ VL* (QCON1+QCON2+QCON3+QCONV+QRAD)
     * +TTO (I, J)
455   CONTINUE
      I=I2+1
      QCON4=TK1* (TFO (II, 2)–TTO (I, J))/ DR1*A4
      QCON1=TK1* (TTO (I, NN)–TTO (I, J))*A1/ DR1
      QCON2=TK1* (TTO (I+1, J)–TTO (I, J))*A2/ DZ1
      QCON3=TK1* (TTO (I–1, J)–TTO (I, J))*A2/ DZ1
      TT (I, J)=DTIME/ DEN1/ CP1/ (VL*2.)* (QCON1+QCON2+QCON3+QCON4)
     * +TTO (I, J)
460   TF (II, 1)=TT (I, J)
      I1=I+1
      DO 469 I=I1, NP
      QCON1=TK1* (TTO (I, NN)–TTO (I, J))*A1/ DR1
      QCON2=TK1* (TTO (I+1, J)–TTO (I, J))*A2/ DZ1
      QCON3=TK1* (TTO (I–1, J)–TTO (I, J))*A2/ DZ1
      QCONV=H1* (TAMB–TTO (I, J))*A3
      QRAD=EP*SB* ( ( (TAMB+273.)/ 100.)**4– ( (TTO (I, J)+273.)
     * / 100.)**4)*A3+CS2*QSS1*A3
      TT (I, J)=DTIME/ DEN1/ CP1/ VL* (QCON1+QCON2+QCON3+QCONV+QRAD)
     * +TTO (I, J)
469   CONTINUE
      RETURN
      END
C
C     HEAT GENERATION DUE TO LEAKAGE CURREN
```

```
C
C
      SUBROUTINE QQ (TIME, EJR)
      REAL LE, LP
      REAL E (50), V (50), R (50)
      COMMON / D1/ N, M, NN, NP, TAMB, TH/ D2/ RE, RP1, RP2, LE, LP
      COMMON / D/ T (50, 50), R (50), TT (50, 50), RR (50)
      COMMON / D3/ CP, CP1, CP2, TK, TK1, DEN, DEN1, DEN2/ D4/ TKAIR, SB
      COMMON / D5/ EE, EP, EEL
      COMMON / D7/ ET, V, S/ D8/ DR, DZ, DR1, DZ1, DTIME/ D9/ VL, QGEN1
      COMMON / D10/ TO (50, 50), TTO (50, 50), TF (20, 50), RF (50)
      COMMON N1, M1, NN1, NN2, I, J, RAT, RA1, RA2, RA3
      IF (S.EQ.0.) GO TO 750
      TMEAN=0.
      DO 700 I=1, N1
      DO 700 J=1, M1
 700  TMEAN=TMEAN+TO (I, J)
      TMEAN=TMEAN/ (1.*M1*N1)
      IF (TIME.EQ.0.) GO TO 710
      EJOM=0.
      DO 705 I=1, N1
      E=E (I)
      CALL LAGR12 (E, EJ0)
 705  EJ0M=EJOM+EJ0
      EJO=EJOM/ N1
      EJR=EJ0*EXP (-2400.0/ (TMEAN+273.))
      DO 760 I=1, N1
      TMEAN=0.
      DO 730 J=1, M1
      TMEAN=TMEAN+TO (I, J)
 730  TMEAN=TMEAN/ M1
      EJO==EJR*EXP (-2400.0/ (TMEAN+273.))
      CALL LAGR13 (E, EJO)
      E (I)=E
      V (I)=E (I)*DZ
      R (I)=V (I)/ (EJR*3.14159*RE*RE)
      QGEN1 (I) (I)=S*ET*E (I)*EJR
 760  CONTINUE
      GO TO 750
 710  E=V/ LE
      CALL LAGR12 (E, EJ0)
      EJR=EJ0*EXP (-2400.0/ (TAMB+273.))
      QGEN1 (I)=S*ET*E*EJR
 750  RETURN
      END
C
C     J0 (E), J0{E (I)}
C
      SUBROUTINE LAGR12 (X, Y)
      REAL Y0 (26)
      DATA Y0/ 51.286, 54.325, 57.544, 60.954, 66.069, 70.795, 78.523,
     * 85.114, 92.257, 100.0, 110.918, 116.145, 125.893, 136.458,
     * 151.356, 164.059, 177.828, 208.93, 231.74, 257.04, 281.838,
     * 316.228, 389.045, 501.187, 676.083, 954.993/
      AA=80000.
      BB=205000.
      AL=0.
      N3=26
```

```
      RN= (0.+N3)
      HH= (BB-AA)/ (RN-1.0)
      II= (X-AA)/ HH+0.5
      IF (II-1) 315, 325, 325
325   IF (II- (N3-2)) 318, 328, 328
328   II=N3-2
      GO TO 318
315   II=1
318   UI=II
      U= (X-AA)/ HH-UI
      IF (AL.EQ.1) GO TO 338
      C0=0.5*U* (U-1.0)
      C1=1.0-U*U
      C2=0.5*U* (U+1.0)
      Y=C0*Y0 (II)+C1*Y0 (II+1)+C2*Y0 (II+2)
      RETURN
338   C0=0.5* (2.0*U-1.0)
      C1=-2.0*U
      C2=0.5* (2.0*U+1.0)
      Y= (C0*Y0 (II)+C1*Y0 (II+1)+C2*Y0 (II+2))/ HH
      RETURN
      END
C
C     RADIATIONSHAPE FACTOR F12
C
      SUBROUTINE RSF (F25, F24, F17)
      COMMON / D1/ N, M, NN, NP, TAMB, TH/ D2/ RE, RP1, RP2, LE, LP
      COMMON / D/ T (50, 50), R (50), TT (50, 50), RR (50)
      COMMON / D3/ CP, CP1, CP2, TK, TK1, DEN, DEN1, DEN2/ D4/ TKAIR, SB
      COMMON / D5/ EE, EP, EEL
      COMMON / D7/ ET, V, S/ D8/ DR, DZ, DR1, DZ1, DTIME/ D9/ VL, QGEN1
      COMMON / D10/ TO (50, 50), TTO (50, 50), TF (20, 50), RF (50)
      COMMON N1, M1, NN1, NN2, I, J, RAT, RA1, RA2, RA3
      DL=DZ
      F52=RE/ RP1* (1.- (ACOS ( (DL*DL-RP1*RP1+RE*RE)/ (DL*DL+RP1*RP1-
 *    RE*RE))- (SQRT ( (DL*DL+RP1*RP1+RE*RE)**2-4* (RE*RP1)**2)*ACOS (
 *    RE* (DL*DL-RP1*RP1+RE*RE)/ RP1/ (DL*DL+RP1*RP1-RE*RE))+ (DL*DL-
 *    RP1*RP1+RE*RE)*ASIN (RE/ RP1)-3.14159* (DL*DL+RP1*RP1-RE*RE)/ 2.
 *    )/ 2./ RE/ DL)/ 3.14159)
      A5=2.*3.14159*RP1*DL
      A2=2.*3.14159*RE*DL
      F25=A5*F52/ A2
      F55=1-RE/ RP1+ (2.*RE/ RP1*ATAN (2.*SQRT (RP1*RP1-RE*RE)/ DL)-DL/
 *    2./ RP1* (SQRT (4.*RP1**2+DL**2)/ DL*ASIN (  (4* (RP1*RP1-RE*RE)+
 *    DL*DL/ RP1/ RP1* (RP1*RP1-2.*RE*RE))/ (DL*DL+4.* (RP1**2-RE**2)))
 *    -ASIN ( (RP1*RP1-2.*RE*RE)/
 *    RP1**2)+3.14159/ 2.* (SQRT (4.*RP1**2+DL**2)/ DL-1.)))/ 3.14159
      F47= (1.-F52-F55)/ 2.
      F17= (1.-F25)/ 2.
      A7=3.14159* (RP1**2-RE**2)
      F74=F47*A5/ A7
      F71=A2*F17/ A7
      DL=DL*2.
      F4512=RE/ RP1* (1.- (ACOS ( (DL*DL-RP1*RP1+RE*RE)/ (DL*DL+RP1*RP1-
 *    RE*RE))- (SQRT ( (DL*DL+RP1*RP1+RE*RE)**2-4* (RE*RP1)**2)*ACOS (
 *    RE* (DL*DL-RP1*RP1+RE*RE)/ RP1/ (DL*DL+RP1*RP1-RE*RE))+ (DL*DL-
 *    RP1*RP1+RE*RE)*ASIN (RE/ RP1)-3.14159* (DL*DL+RP1*RP1-RE*RE)/ 2.
 *    )/ 2./ RE/ DL)/ 3.14159)
```

```
      A45=2.*3.14159*RP1*DL
      A12=2.*3.14159*RE*DL
      F1245=A45*F4512/ A12
      F4545=1-RE/ RP1+ (2.*RE/ RP1*ATAN (2.*SQRT (RP1*RP1-RE*RE)/ DL)-DL/
     *   2./ RP1* (SQRT (4.*RP1**2+DL**2)/ DL*ASIN ( (4* (RP1*RP1-RE*RE)+
     *   DL*DL/ RP1/ RP1* (RP1*RP1-2.*RE*RE))/ (DL*DL+4.* (RP1**2-RE**2)))
     *   -ASIN ( (RP1*RP1-2.*RE*RE)/
     *   RP1**2)+3.14159/ 2.* (SQRT (4.*RP1**2+DL**2)/ DL-1.)))/ 3.14159
      F457= (1.-F4512-F4545)/ 2.
      F127= (1.-F1245)/ 2.
      F712=F127*A12/ A7
      F2456=1.- (RP1*RP1-RE*RE)/ RE*DL* (F712-F71)
      F24= (F2456-F25)/ 2.
      F745=F457*A45/ A7
      F72=F712-F71
      F75=F745-F74
      RETURN
      END
C
C     CALCULATE RA'
C
      SUBROUTINE RAF (F25, F24, F17)
      REAL LE, LP
      COMMON / D1/ N, M, NN, NP, TAMB, TH/ D2/ RE, RP1, RP2, LE, LP
      COMMON / D/ T (50, 50), R (50), TT (50, 50), RR (50)
      COMMON / D3/ CP, CP1, CP2, TK, TK1, DEN, DEN1, DEN2/ D4/ TKAIR, SB
      COMMON / D5/ EE, EP, EEL
      COMMON / D7/ ET, V, S/ D8/ DR, DZ, DR1, DZ1, DTIME/ D9/ VL, QGEN1
      COMMON / D10/ TO (50, 50), TTO (50, 50), TF (20, 50), RF (50)
      COMMON N1, M1, NN1, NN2, I, J, RAT, RA1, RA2, RA3
      RAT= (1-EE)/ (EE*2*3.14159*RE*DZ)+1/ (2*3.14159*RE*DZ)
     * + (1-EP)/ (EP*2*3.14159*RP1*DZ1)
      RA1= (1-EE)/ (EE*2*3.14159*RE*DZ)+1/ (F25*2*3.14159*RE*DZ)
     * + (1-EP)/ (EP*2*3.14159*RP1*DZ1)
      RA2= (1-EE)/ (EE*2*3.14159*RE*DZ)+1/ (F24*2*3.14159*RE*DZ)
     * + (1-EP)/ (EP*2*3.14159*RP1*DZ1)
      AE=3.14159* (RP1**2-RE**2)
      RA3= (1-EE)/ (EE*2*3.14159*RE*DZ)+1/ (F17*2*3.14159*RE*DZ)
     *    + (1-EEL)/ (EEL*AE)
      RETURN
      END
C
C     COEFICIENT: H
C
C--------ALF: TKAIR/ (DEN*CP)  (M*M/ S*S)
C     GR: GRASHOFS NUMBER
C     PR: PRANDTL NUMBER: U*CP/ KAIR
C     NU: NUSSELT NUMBER
C     VU: KINEMATIC VISCOSITY  (M*M/ S)
C     G:  GRAVITATIONAL ACCELERATION  (M/ S*S)
C     DENA: DENSITY OF AIR
C     VW: WIND VELOCITY  (KM/ HOUR)
C     REY: REYNODS NUMBE
C
      SUBROUTINE CONVH (HTOP, HPO, HIN)
      REAL LE, LP, NU, LL, NUT, NUP, NUC
      COMMON / D1/ N, M, NN, NP, TAMB, TH/ D2/ RE, RP1, RP2, LE, LP
      COMMON / D/ T (50, 50), R (50), TT (50, 50), RR (50)
```

```
      COMMON / D3/ CP, CP1, CP2, TK, TK1, DEN, DEN1, DEN2/ D4/ TKAIR, SB
      COMMON / D5/ EE, EP, EEL
      COMMON / D7/ ET, V, S/ D8/ DR, DZ, DR1, DZ1, DTIME/ D9/ VL, QGEN1
      COMMON / D10/ TO (50, 50), TTO (50, 50), TF (20, 50), RF (50)
      COMMON N1, M1, NN1, NN2, I, J, RAT, RA1, RA2, RA3
      DATA PR, G, ALF, VU, U/ 0.711, 9.8, 22.1E-6, 15.7E-6, 1.85E-5/
      DATA WIND, VW, DENA/ 0.0, 20.0, 1.18/
   B=1./ (TAMB+273.)
      TTMEAN=0.
      J=NN1
      DO 870 I=1, NN2
870   TTMEAN=TTMEAN+TTO (I, J)
      TTMEAN=TTMEAN/ (NN2+0.)
C
      IF (WIND.EQ.0.0) GO TO 840
      IF (REY.EQ.0.0) GO TO 872
      GO TO 855
C
C———FORCED CONVECTION
C
872  VW=VW*1000./ 3600.
      REY=DENA*VW*2.*RP2/ U
      IF (REY.LE.4.) GO TO 808
      IF (REY.LE.40.) GO TO 818
      IF (REY.LE.4000.) GO TO 828
      IF (REY.LE.4.E4) GO TO 838
      FN=0.805
      FB=0.0239
      GO TO 850
838   FN=0.618
      FB=0.174
      GO TO 850
828   FN=0.466
      FB=0.615
      GO TO 850
818   FN=0.385
      FB=0.821
      GO TO 850
808   FN=0.33
      FB=0.891
850   HPO=TKAIR*FB*REY**FN/ (2.*RP2)
      RECRIT=3.E5
      IF (REY.LT.3.E5) GO TO 890
      HTOP=0.0326*TKAIR/ (2.*RP2)* (REY*80.8-RECRIT**0.8+18.2*
     * RECRIT**0.5)
      GO TO 855
890   HTOP=0.592*TKAIR/ (2.*RP2)* (REY)**0.5
      GO TO 855
C
C     NATURAL CONVECTION
C
840   LL=RP2/ 2.
      DT=TO (N1, 1)-TAMB
      RRA=B*G*DT*LL**3/ VU/ ALF
      IF (RRA.LE.1.E7) GO TO 805
      NU=0.15*RRA** (1./ 3.)
      GO TO 810
805   NU=0.54*RRA**0.25
```

```
 810    HTOP=NU*TKAIR/ LL
C
        CL=4./ 3.*0.386
        DT=TTMEAN-TAMB
        RRA=G*B*DT*LP**3/ VU/ ALF
        IF (RRA.EQ.0.0) GO TO 880
        IF (RRA.LT.1.E5) GO TO 815
        NUT=CL*RRA**0.25
        SG=LP/ RP2/ NUT
        NUP=2.8/ ALOG (1.+2.8/ NUT)
        NUC=0.9*SG*NUP/ ALOG (1.+0.9*SG)
        GO TO 820
 815    RRA=B*G*DT* (2.*RP2)**4/ (VU*ALF*LP)
        NUC=1.8*LP/ (2.*RP2)/ ALOG (1.+1.8/ (CL*RRA**0.25))
 820    HPO=NUC*TKAIR/ LP
        GO TO 855
 880    HPO=0.
C
C———ENCLOSED CONVECTION
C
 855    TMEAN=0.
        J=M1
        DO 875 I=1, N1
 875    TMEAN=TMEAN+TO (I, J)
        TMEAN=TMEAN/ (N1+0.)
        DT=TMEAN-TTMEAN
        GR=DENA**2*B*G*DT*LP**3/ U/ U
        NU=0.55* (GR*PR)**0.25
        HIN=NU*TKAIR/ LP
        RETURN
        END
C
C       ENERGY INPUT DUE TO SUN AND SKY RADIATION
C
C       1: VERTICAL HOUSING
C       2: HORIZONTAL TOP ELECTRODE
C
        SUBROUTINE QSS (QSUN1, QSKY1, QSUN2, QSKY2)
        REAL LATI
        REAL Y01 (6), Y02 (6), Y03 (6), Y04 (6)
        DATA SI, ALFS1, ALFS2/ 1353.0, 0.04, 0.95/
        DATA ALTI, LATI, SN/ 0.3, 50., 210./
        DATA Y01/ 0.1283, 0.1742, 0.2195, 0.2582, 0.2915, 0.320/
        DATA Y02/ 0.7559, 0.7214, 0.6848, 0.6532, 0.6265, 0.602/
        DATA Y03/ 0.3876, 0.3436, 0.3139, 0.2910, 0.2745, 0.268/
        DATA Y04/ 0.22, 0.26, 0.32, 0.44, 0.71, 1.33/
        CALL LAGR (6, ALTI, A0, Y01, 0., 2.5)
        CALL LAGR (6, ALTI, A1, Y02, 0., 2.5)
        CALL LAGR (6, ALTI, AK, Y03, 0., 2.5)
        DLTS=23.45*SIN (2.*3.14159* (284.+SN)/ 365.)
        DLTS=DLTS*3.14159/ 180.
        HS=45.*3.14159/ 180.
        ALFS=SIN (LATI*3.14159/ 180.)*SIN (DLTS)+COS (LATI*3.14159
   *    / 180.)*COS (DLTS)*COS (HS)
        ALFS=ASIN (ALFS)
C
        ATM=A0+A1*EXP (-AK/ SIN (ALFS))
        SIB=SI*ATM
```

```
      QSUN2=ALFS2*SIB*SIN (ALFS)/ 4.
C
      VERI=COS (LATI*3.14159/ 180.)*SIN (DLTS)+
     *  +SIN (LATI*3.14159/ 180.)*COS (DLTS)*COS (HS)
      QSUN1=ALFS1*SIB*VERI
      VERI=ACOS (VERI)*180./ 3.1415
      HORI=SIN (ALFS)
      HORI=ACOS (HORI)*180./ 3.14159
      IF (VERI.LT.40) GO TO 443
      CALL LAGR (6, VERI, F1, Y04, 40., 90.)
      GO TO 463
443   F1=0.16+0.001*VERI
463   IF (VERI.LT.40) GO TO 453
      CALL LAGR (6, HORI, F2, Y04, 40., 90.)
      GO TO 473
453   F2=0.16+0.001*HORI
473   QSKY1=ALFS1*F1*SIB
      QSKY2=ALFS2*F2*SIB/ 4.
      RETURN
      END
C
      SUBROUTINE LAGR (N3, X, Y, Y0, AA, BB)
      REAL Y0 (N3)
      RN= (0.+N3)
      HH= (BB-AA)/ (RN-1.0)
      II= (X-AA)/ HH+0.5
      IF (II-1) 315, 325, 325
325   IF (II- (N3-2)) 318, 328, 328
328   II=N3-2
      GO TO 318
315   II=1
318   UI=II
      U= (X-AA)/ HH-UI
      C0=0.5*U* (U-1.0)
      C1=1.0-U*U
      C2=0.5*U* (U+1.0)
      Y=C0*Y0 (II)+C1*Y0 (II+1)+C2*Y0 (II+2)
      RETURN
      END
C
C*****************************************************************************
C
C     NO ELECTRODE HEAT TRANSFER
C
C     TOP AND BOTTOM ELEMENT TEMPERATURE
C
      SUBROUTINE TTB (H1)
      REAL LE, LP
      COMMON / D1/ N, M, NN, NP, TAMB, TH/ D2/ RE, RP1, RP2, LE, LP
      COMMON / D/ T (50, 50), R (50), TT (50, 50), RR (50)
      COMMON / D3/ CP, CP1, CP2, TK, TK1, DEN, DEN1, DEN2/ D4/ TKAIR, SB
      COMMON / D5/ EE, EP, EEL
      COMMON / D7/ ET, V, S/ D8/ DR, DZ, DR1, DZ1, DTIME/ D9/ VL, QGEN1
      COMMON N1, M1, NN1, NN2, I, J, RAT, RA1, RA2, RA3
      COMMON / D10/ TO (50, 50), TTO (50, 50), TF (20, 50), RF (50)
      I=N1
11    DO 4 J=2, M
      A1=2*3.14159*R (J)*DR
```

```
      A2= (R (J)-DR/ 2.)*3.14159*DZ
      A3= (R (J)+DR/ 2.)*3.14159*DZ
      IF (I.EQ.1) GOTO 19
      QCON1=TK* (TO (I-1, J)-TO (I, J))/ DZ*A1
      GOTO 20
19    QCON1=TK* (TO (I+1, J)-TO (I, J))/ DZ*A1
20    QCON2=TK* (TO (I, J-1)-TO (I, J))/ DR*A2
      QCON3=TK* (TO (I, J+1)-TO (I, J))/ DR*A3
      QCONV=H1*A1* (TAMB-TO (I, J))
      RA=1./ EE/ A1
      QRAD=SB* ( ( (TAMB+273.)/ 100.)**4- ( (TO (I, J)+273.)/ 100.)**4)/ RA
      VL=A1*DZ/ 2.
      QGEN=QGEN1 (I)*VL
      T (I, J)=DTIME/ DEN/ CP/ VL* (QCON1+QCON2+QCON3+QCONV+QRAD+QGEN)
     * +TO (I, J)
4     CONTINUE
      IF (I.EQ.1) GOTO 12
      I=1
      GOTO 11
12    RETURN
      END
C
      SUBROUTINE TCORN (H, H1)
      REAL LE, LP
      COMMON / D1/ N, M, NN, NP, TAMB, TH/ D2/ RE, RP1, RP2, LE, LP
      COMMON / D/ T (50, 50), R (50), TT (50, 50), RR (50)
      COMMON / D3/ CP, CP1, CP2, TK, TK1, DEN, DEN1, DEN2/ D4/ TKAIR, SB
      COMMON / D5/ EE, EP, EEL
      COMMON / D7/ ET, V, S/ D8/ DR, DZ, DR1, DZ1, DTIME/ D9/ VL, QGEN1
      COMMON N1, M1, NN1, NN2, I, J, RAT, RA1, RA2, RA3
      COMMON / D10/ TO (50, 50), TTO (50, 50), TF (20, 50), RF (50)
      J=M1
      I=N1
      A1=3.14159* (R (J)**2- (R (J)-DR/ 2.)**2)
      A2=3.14159* (R (J)-DR/ 2.)*DZ
16    IF (I.EQ.1) GOTO 21
      QCON1=TK* (TO (I-1, J)-TO (I, J))/ DZ*A1
      GOTO 24
21    QCON1=TK* (TO (I+1, J)-TO (I, J))/ DZ*A1
24    QCON2=TK* (TO (I, J-1)-TO (I, J))/ DR*A2
      QCONV1=H*3.14159*R (J)*DZ* (TTO (I, 1)-TO (I, J))
      QCONV2=H1* (TAMB-TO (I, J))*A1
      DZ=DZ/ 2.
      QRAD1=SB* ( ( (TTO (I, 1)+273.)/ 100.)**4- ( (TO (I, J)+273.)/ 100.
     * )**4)/ RAT
      RA=1/ EE/ A1
      QRAD2=SB* ( ( (TAMB+273.)/ 100.)**4- ( (TO (I, J)+273.)/ 100.)**4)/ RA
      VL=A1*DZ/ 2.
      QGEN=QGEN1 (I)*VL
      T (I, J)=DTIME/ DEN/ CP/ VL* (QCON1+QCON2+QCONV1+QRAD1+QCONV2+QRAD2
     * +QGEN)+TO (I, J)
      IF (I.EQ.1) GOTO 18
      I=1
      GOTO 16
18    RETURN
      END
C
C     CENTRAL LINE TEMPERATURE OF ELEMENT ON TOP AND BOTTOM
```

```
C
      SUBROUTINE TCTOB (H1)
      REAL LE, LP
      COMMON / D1/ N, M, NN, NP, TAMB, TH/ D2/ RE, RP1, RP2, LE, LP
      COMMON / D/ T (50, 50), R (50), TT (50, 50), RR (50)
      COMMON / D3/ CP, CP1, CP2, TK, TK1, DEN, DEN1, DEN2/ D4/ TKAIR, SB
      COMMON / D5/ EE, EP, EEL
      COMMON / D7/ ET, V, S/ D8/ DR, DZ, DR1, DZ1, DTIME/ D9/ VL, QGEN1
      COMMON / D10/ TO (50, 50), TTO (50, 50), TF (20, 50), RF (50)
      COMMON N1, M1, NN1, NN2, I, J, RAT, RA1, RA2, RA3
      J=1
      I=1
      A1=3.14159* (DR/ 2.)**2
      A2=3.14159*DR*DZ/ 2.
      QCON1=TK* (TO (I+1, J)-TO (I, J))*A1/ DZ
      GOTO 39
37    QCON1=TK* (TO (I-1, J)-TO (I, J))*A1/ DZ
39    QCON2=TK* (TO (I, J+1)-TO (I, J))*A2/ DR
      QRAD=EE*SB* ( ( (TAMB+273.)/ 100.)**4- ( (TO (I, J)+273.)/ 100.
     * )**4)*A1
      QCONV=H1* (TAMB-TO (I, J))*A1
      VL=A1*DZ/ 2.
      QGEN=QGEN1 (I)*VL
      T (I, J)=DTIME/ DEN/ CP/ VL* (QCON1+QCON2+QRAD+QCONV+QGEN)
     * +TO (I, J)
      IF (I.EQ.N1) GOTO 38
      I=N1
      GOTO 37
38    RETURN
      END
C
C*****************************************************************
C     SIMULATE TEST SECTIONS
C
C*****************************************************************
C
      REAL LE, LP
      COMMON / D1/ M, NN, TAMB/ D2/ RE, RP1, RP2, LE, LP
      COMMON / D/ T (50), R (50), TT (50), RR (50)
      COMMON / D3/ CP, CP1, TK, TK1, DEN, DEN1/ D4/ TKAIR, SB
      COMMON / D5/ EE, EP
      COMMON / D7/ ET, V, S/ D8/ DR, DR1, DTIME/ D9/ VL, QGEN, QGEN1
      COMMON M1, NN1, J, RA
      COMMON / D10/ TO (50), TTO (50)
      DATA M, NN, TAMB/
      DATA RE, RP1, RP2, LE, LP/
      DATA CP, CP1, TK, TK1, DEN, DEN1/
      DATA TKAIR, SB/ 0.026, 5.668/
      DATA EE, EP/ 0.9, 0.9/
      DATA ET, V/ 0.5, 3200.0/
      CALL RAF (RA)
      L=1000
      WRITE (8, 50) M, NN, TAMB
      WRITE (8, 58) RE, RP1, RP2, LE, LP
      WRITE (8, 60) CP, CP1, TK, TK1, DEN, DEN1
      WRITE (8, 65) TKAIR, SB
      WRITE (8, 70) EE, EP
50    FORMAT (/ 1X, 2HM:, I5, 2X, ' NN:', I5, 2X,
```

```
     *      5HTAMB:, F10.4)
    58      FORMAT (/ 1X, ' RE:', F10.4, ' RP1:', F10.4, ' RP2:', F10.4,
     *       ' LE:', F10.4, ' LP:', F10.4)
    60      FORMAT (/ 1X, ' CP:', F10.4, ' CP1:', F10.4,
     *      ' TK:', F10.4, ' TK1:', F10.4, ' DEN:', F10.4, ' DEN1:', F10.4)
    65      FORMAT (/ 1X, ' TKAIR:', F10.4, ' SB:', F10.4)
    70      FORMAT (/ 1X, ' EE:', F10.4, ' EP', F10.4)
            DR=RE/ M
            DR1= (RP2-RP1)/ (0.0+NN)
            WRITE (8, 620) DR, DR1
   620      FORMAT (/ 1X, ' DR', F10.4, ' DR1', F10.4)
            M1=M+1
            NN1=NN+1
            R (1)=0.
            DO 11 J=2, M1
    11      R (J)=R (J-1)+DR
            RR (1)=RP1
            DO 22 J=2, NN1
    22      RR (J)=RR (J-1)+DR
            DO 1 J=1, M1
            TO (J)=TAMB
     1      CONTINUE
            WRITE (8, 200)  (TO (J), J=1, M1)
            DO 77 J=1, NN1
    77      TTO (J)=TAMB
C
C           TIME STEP: DTIME
C
            S=1.0
   510      TIME=0.0
    56      IC=0
    55      TIME=TIME+DTIME
            IC=IC+1
C
C           CONVECTION COEFFICIENT:H
C
            CALL CONVH (HPO, HIN)
C
C           ELEMENT TEMPERATURE
C
C           SURFACE TEMPERATURE
C
            CALL TSE (HIN)
C
C           CENTERAL LINE TEMPERATURE  (R=0)
C
            CALL TCEN
C
C           INTERIAL TEMPERATURE
C
            CALL TINTE
C
C           HOUSING  TEMPERATURE
            CALL TOSP (HPO)
   940      CALL TINP
            CALL TISP (HIN)
C
C***************************************************************************
```

```
C
        DO 116 J=1, M1
116     TO (J)=T (J)
        DO 118 J=1, NN1
118     TTO (J)=TT (J)
        IF (IC.LT.L) GO TO 55
        WRITE (6, 100) TIME
        TIME1=TIME/ 3600.
        WRITE (8, 100) TIME1
C
C       HEAT LOSS
C
        QRAD=0.0
        QCOND=0.0
        QCONV=0.0
C
C       HEAT LOSS FROM THE SURFACE OF ELEMENT AT TIME T
C
        J=M1
        QRAD=QRAD+SB* ( ( (T (J)+273.)/ 100.)**4- ( (TT (1)+273.)/ 100.)
   *    **4)/ RA
        QCOND=QCOND+TKAIR* (T (J)-TTO (1))*2.*3.14/ ALOG (RP1/ RE)*LE
        QCONV=QCONV+HIN*2.*RR (1)* (T (J)-TT (1))*3.14*LE
        QTOT1=QRAD+QCONV+QCOND
        WRITE (8, 660) QRAD, QCONV, QCOND, QTOT1
C
C       HEAT LOSS FROM THE SURFACE OF HOUSING
C
        QRAD=0.0
        QCONV=0.0
        QRAD=-EP*SB*2*RR (NN1)* ( ( (TAMB+273.)/ 100.)**4- ( (TT (NN1)+273)
   *    / 100.)**4)*LE*3.14+QRAD
        QCONV=-HPO*2.*RR (NN1)*3.14* (TAMB-TT (NN1))*LE+QCONV
        QTOT=QRAD+QCONV
        WRITE (8, 630) QRAD, QCONV, QTOT
        VL=3.14159*RE**2*LE*10.**6
        QUNI= (QTOT+QTOT2)/ VL
        WRITE (8, 968) QUNI
968     FORMAT (/ 1X, 'QUNI=', E10.4, '  W/ CM**3')
C
        IF (S.EQ.1.) GO TO 540
        QDIF=0.-QTOT-QTOT2+CS2* (QSS1*2.*3.14159*RP2*LP+
   *    QSS2*3.14159*RP2**2)
        WRITE (8, 625) QDIF
        GO TO 550
540     E=V/ LE
        QGEN1=QGEN1/ 10.**6
        VL=3.14159*RE**2*LE
        QGEN=QGEN*VL
        WRITE (8, 605) E, EJR, TMEAN, QGEN1, QGEN
        QDIF=QGEN-QTOT-QTOT2+CS2* (QSS1*2.*3.14159*RP2*LP+
   *    QSS2*3.14159*RP2**2)
        WRITE (8, 625) QDIF
625     FORMAT (/ 1X, '  QDIFFERENCE=', F10.5/ )
660     FORMAT (/ 1X, 'ELEMENT:', / 1X, 5HQRAD=, F10.4, 2X, 6HQCONV=, F10.4, 2X,
   *    6HQCOND=, F10.4, 2X, 8H QTOTAL=, F10.4)
600     FORMAT (1X, 'ELECTRODE:', / 1X, 5HQRAD=, F10.4, 2X, 7H QCONV=, F10.4,
   *    2X, 7HQTOTAL=, F10.4)
```

```
630     FORMAT (1X, 'HOUSE:', / 1X, ' QRAD=', F10.4, ' QCONV=', F10.4,
 *      ' QTOTAL=', F10.4)
605     FORMAT (/ , 1X, ' E=', F10.2, 'V/ CM', '   EJR=', F10.4, ' TMEAN',
 *      F10.4, / 1X, ' QGEN1=', F12.5, 'W/ CM**3', 'QGEN=', F10.4, 'W')
550     WRITE (8, 200)  (T (J), J=1, M1)
        WRITE (8, 400)  (TT (J), J=1, NN1)
        WRITE (8, 640) HPO, HIN
400     FORMAT (1X/ 3H TT, 4 (2X, F12.4))
100     FORMAT (1X/ / 6H TIME=, F13.4)
200     FORMAT (1X, 1HT, 4 (2X, F10.4))
220     FORMAT (1X, 6HDTIME=, F9.6)
        IF (S.EQ.0.) GO TO 560
        DER=ABS (QDIF–QDIFO)
        IF (T (1).GT.100.) GO TO 250
        IF (DER.LT.0.001) GO TO 250
        QDIFO=QDIF
        GO TO 56
560     IF (TIME.GT.TMAX) GO TO 530
        GO TO 56
250     S=0.
        TMAX=TIME/
        GO TO 510
530     CONTINUE
        STOP
        END
C
C       ELEMENT  SURFACE  TEMPERATURE
C
        SUBROUTINE TSE (H)
        REAL LE, LP
        COMMON / D1/ M, NN, TAMB/ D2/ RE, RP1, RP2, LE, LP
        COMMON / D/ T (50), R (50), TT (50), RR (50)
        COMMON / D3/ CP, CP1, TK, TK1, DEN, DEN1/ D4/ TKAIR, SB
        COMMON / D5/ EE, EP
        COMMON / D7/ ET, V, S/ D8/ DR, DR1, DTIME/ D9/ VL, QGEN, QGEN1
        COMMON M1, NN1, J, RA
        COMMON / D10/ TO (50), TTO (50)
        A1=3.14159* (R (M1)**2– (R (M1)–DR/ 2.)**2)
        A2=3.14159* (R (M1)–DR/ 2.)*2*LE
        QCON1=TK* (TO (M1–1)–TO (M1))/ DR*A2
        QCON4=TKAIR* (TTO (1)–TO (M1))*2*3.14159*LE/ ALOG (RP1/ RE)
        QCONV=H*2*3.14159*R (M1)*LE* (TTO (1)–TO (M1))
        QRAD=SB* ( ( (TTO (1)+273.)/ 100.)**4– ( (TO (M1)+273.)/ 100.)**4)
 *      / RA
        VL=A1*LE
        CALL QQ (E, EJR)
        T (M1)=DTIME/ DEN/ CP/ VL* (QCON1+QCON4+QCONV+QRAD
 *      +QGEN)+TO (M1)
        RETURN
        END
C
C       CENTRAL LINE TEMPERATURE OF ELEMENT
C
        SUBROUTINE TCEN
        REAL LE, LP
        COMMON / D1/ M, NN, TAMB/ D2/ RE, RP1, RP2, LE, LP
        COMMON / D/ T (50), R (50), TT (50), RR (50)
        COMMON / D3/ CP, CP1, TK, TK1, DEN, DEN1/ D4/ TKAIR, SB
```

```
      COMMON / D5/ EE, EP
      COMMON / D7/ ET, V, S/ D8/ DR, DR1, DTIME/ D9/ VL, QGEN, QGEN1
      COMMON M1, NN1, J, RA
      COMMON / D10/ TO (50), TTO (50)
      J=1
      VL=1.0
      CALL QQ (E, EJR)
      T (J)=DTIME/ DEN/ CP* (TK* (4* (TO (J+1)-TO (J))/ DR**2)+QGEN)
     *      +TO (J)
 35   CONTINUE
      RETURN
      END
C
C
C     INTERIAL TEMPERATURE OF ELEMENT
C
      SUBROUTINE TINTE
      REAL LE, LP
      COMMON / D1/ M, NN, TAMB/ D2/ RE, RP1, RP2, LE, LP
      COMMON / D/ T (50), R (50), TT (50), RR (50)
      COMMON / D3/ CP, CP1, TK, TK1, DEN, DEN1/ D4/ TKAIR, SB
      COMMON / D5/ EE, EP
      COMMON / D7/ ET, V, S/ D8/ DR, DR1, DTIME/ D9/ VL, QGEN, QGEN1
      COMMON / D10/ TO (50), TTO (50)
      COMMON M1, NN1, J, RA
      DO 44 J=2, M
      VL=1.
      CALL QQ (E, EJR)
      T (J)=DTIME/ DEN/ CP* (TK* ( (TO (J+1)-2*TO (J)+TO (J-1))/ DR**2
     *      + (TO (J+1)-TO (J-1))/
     *      (2.*DR*R (J)))+QGEN)+TO (J)
 44   CONTINUE
      RETURN
      END
C
C     TEMPERATURE ON THE EXTERIOR SURFACE OF HOUSING
C
      SUBROUTINE TOSP (H1)
      REAL LE, LP
      COMMON / D1/ M, NN, TAMB/ D2/ RE, RP1, RP2, LE, LP
      COMMON / D/ T (50), R (50), TT (50), RR (50)
      COMMON / D3/ CP, CP1, TK, TK1, DEN, DEN1/ D4/ TKAIR, SB
      COMMON / D5/ EE, EP
      COMMON / D7/ ET, V, S/ D8/ DR, DR1, DTIME/ D9/ VL, QGEN, QGEN1
      COMMON / D10/ TO (50), TTO (50)
      COMMON M1, NN1, J, RA
      J=NN1
      A1= (RR (J)**2- (RR (J)-DR1/ 2.)**2)*3.14159
      VL=A1*LE
      A2=2*3.14159* (RR (J)-DR1/ 2.)*LE
      A3=2*3.14159*RR (J)*LE
      QCON1=TK1* (TTO (J-1)-TTO (J))*A2/ DR1
      QRAD=EP*A3*SB* ( ( (TAMB+273.)/ 100.)**4- ( (TTO (J)+273.)
     *      / 100.)**4)
      QCONV=H1*A3* (TAMB-TTO (J))
      TT (J)=DTIME/ DEN1/ CP1/ VL* (QCON1+QRAD+QCONV)
     *      +TTO (J)
      RETURN
```

```
      END
C
C     INTERIOR TEMPERATURE OF HOUSING
C
      SUBROUTINE TINP
      REAL LE, LP
      COMMON / D1/ M, NN, TAMB/ D2/ RE, RP1, RP2, LE, LP
      COMMON / D/ T (50), R (50), TT (50), RR (50)
      COMMON / D3/ CP, CP1, TK, TK1, DEN, DEN1/ D4/ TKAIR, SB
      COMMON / D5/ EE, EP
      COMMON / D7/ ET, V, S/ D8/ DR, DR1, DTIME/ D9/ VL, QGEN, QGEN1
      COMMON / D10/ TO (50), TTO (50)
      COMMON M1, NN1, J, RA
      DO 46 J=2, NN
      TT (J)=DTIME/ DEN1/ CP1*TK1* ( (TTO (J+1)–2*TTO (J)+TTO (J–1)
     * )/ DR1**2+ (TTO (J+1)–TTO (J–1))/  (2.*DR1*RR (J)))+TTO (J)
 46   CONTINUE
      RETURN
      END
C
C     TEMPERATURE ON INTERIOR SURFACE OF HOUSING
C
      SUBROUTINE TISP (H1)
      REAL LE, LP
      COMMON / D1/ M, NN, TAMB/ D2/ RE, RP1, RP2, LE, LP
      COMMON / D/ T (50), R (50), TT (50), RR (50)
      COMMON / D3/ CP, CP1, TK, TK1, DEN, DEN1/ D4/ TKAIR, SB
      COMMON / D5/ EE, EP
      COMMON / D7/ ET, V, S/ D8/ DR, DR1, DTIME/ D9/ VL, QGEN, QGEN1
      COMMON / D10/ TO (50), TTO (50)
      COMMON M1, NN1, J, RA
      J=1
      A1=3.14159* ( (RR (J)+DR1/ 2.)**2–RR (J)**2)
      A2=2*3.14159* (RR (J)+DR1/ 2.)*LE
      QCON1=TK1* (TTO (J+1)–TTO (J))*A2/ DR1
      QCON4=TKAIR* (TO (M1)–TTO (J))*2*3.14159*LE/ ALOG (RP1/ RE)
      QCONV=H1*2.*3.14159*RR (J)*LE* (TO (M1)–TTO (J))
      QRAD=SB* ( ( (TO (M1)+273.)/ 100.)**4– ( (TTO (J)+273.)/ 100.)
     * **4)/ RA
      VL=A1*LE
      TT (J)=DTIME/ DEN1/ CP1/ VL* (QCON1+QCON4+QCONV+
     * QRAD)+TTO (J)
      RETURN
      END
C
C     HEAT GENERATION
C
      SUBROUTINE QQ (E, EJR)
      REAL LE, LP
      COMMON / D1/ M, NN, TAMB/ D2/ RE, RP1, RP2, LE, LP
      COMMON / D/ T (50), R (50), TT (50), RR (50)
      COMMON / D3/ CP, CP1, TK, TK1, DEN, DEN1/ D4/ TKAIR, SB
      COMMON / D5/ EE, EP
      COMMON / D7/ ET, V, S/ D8/ DR, DR1, DTIME/ D9/ VL, QGEN, QGEN1
      COMMON / D10/ TO (50), TTO (50)
      COMMON M1, NN1, J, RA
      E=V/ LE
      TMEAN=0.
```

```
      DO 730 J=1, M1
      TMEAN=TMEAN+TO (J)
730   TMEAN=TMEAN/ M1
      CALL LAGR12 (E, EJ0)
      EJR=EJ0*EXP (-2400.0/ (TAMB+273.))
      QGEN1=S*ET*E*EJR
      QGEN=S*VL*QGEN1
      RETURN
      END
C
C     RA'
C
      SUBROUTINE RAF (RA)
      REAL LE, LP
      COMMON / D1/ M, NN, TAMB/ D2/ RE, RP1, RP2, LE, LP
      COMMON / D/ T (50), R (50), TT (50), RR (50)
      COMMON / D3/ CP, CP1, TK, TK1, DEN, DEN1/ D4/ TKAIR, SB
      COMMON / D5/ EE, EP
      COMMON / D7/ ET, V, S/ D8/ DR, DR1, DTIME/ D9/ VL, QGEN, QGEN1
      COMMON / D10/ TO (50), TTO (50)
      RA= (1-EE)/ (EE*2*3.14159*RE*LE)+1/ (2*3.14159*RE*LE)
     * + (1-EP)/ (EP*2*3.14159*RP1*LE)
      RETURN
      END



C
C*****************************************************************
C
C     ARRESTER  NO  HOUSING
C
C*****************************************************************
C
      REAL LE
      REAL L1, L2
      COMMON / D1/ N, M, TAMB/ D2/ RE, LE
      COMMON / D/ T (50, 50), R (50)
      COMMON / D3/ CP, CP2, TK, DEN, DEN2/ D4/ TKAIR, SB
      COMMON / D5/ EE, EEL, TK2
      COMMON / D7/ ET, V, S/ D8/ DR, DZ, DTIME/ D9/ VL, QGEN
      COMMON N1, M1, I, J
      COMMON / D10/ TO (50, 50)
      COMMON / D12/ TSO (20), NS, DS
      DATA N, M, TAMB/
      DATA RE, LE/
      DATA CP, CP2, TK, DEN, DEN2/
      DATA TKAIR, SB/
      DATA EE, EEL, TK2/
      DATA ET, V/
      DATA L1, L2/
C
      CP=836.
      TK=5.685
      CS=1.
      CS1=0.
      L=3000
```

```
50      FORMAT (/ 1X, 2HN:, I5, 2X, ' M:', I5, 2X, 3HNN:, I5, 2X, ' NP', I5, 3X,
  *      5HTAMB:, F10.4)
58      FORMAT (/ 1X, ' RE:', F10.4, ' RP1:', F10.4, ' RP2:', F10.4,
  *      ' LE:', F10.4, ' LP:', F10.4)
60      FORMAT (/ 1X, ' CP:', F10.4, ' CP1:', F10.4, ' CP2:', F10.4,
  *      ' TK:', F10.4, ' TK1:', F10.4, ' DEN:', F10.4, ' DEN1:', F10.4,
  *      ' DEN2', F10.4)
65      FORMAT (/ 1X, ' TKAIR:', F10.4, ' SB:', F10.4)
70      FORMAT (/ 1X, ' EE:', F10.4, ' EP', F10.4, ' EEL', F10.4)
        DZ=LE/ (0.0+N)
        DR=RE/ M
620     FORMAT (/ 1X, ' DZ', F10.4, ' DR', F10.4, ' DZ1', F10.4, ' DR1',
  *     F10.4)
        N1=N+1
        M1=M+1
C
        R (1)=0.
        DO 11 J=2, M1
11      R (J)=R (J-1)+DR
C
        DO 1 I=1, N1
        DO 1 J=1, M1
        TO (I, J)=TAMB
1       CONTINUE
        WRITE (10, 200) ( (TO (I, J), J=1, M1), I=1, N1)
        TTT1=TAMB
        TTT2=TAMB
        DO 39 I=1, NS+1
39      TSO (I)=TAME
C       TIME STEP
C
        DTIME=DEN*CP/ TK2/ (2./ DZ**2+4./ DR**2)
        WRITE (10, 220) DTIME
        S=1.0
510     TIME=0.0
56      IC=0
55      TIME=TIME+DTIME
        IC=IC+1
C
        IF (CS.EQ.0.) GO TO 910
        CALL TELEC (TTT1, TTT2, L1, L2, HTOP, HPO)
        DO 120 J=1, M1
        T (N1, J)=TTT2
120     T (1, J)=TTT1
        DO 122 J=1, NN1
        TT (1, J)=TTT1
122     TT (NN2, J)=TTT2
C
        CALL TOSP (HPO)C
        CALL TCEN
        CALL TINTE
        DO 116 I=1, N1
        DO 116 J=1, M1
116     TO (I, J)=T (I, J)
        IF (IC.LT.L) GO TO 55
        WRITE (10, 100) TIME
C
C       HEAT LOSS
```

```
C————
      QRAD=0.0
      QCOND=0.0
      QCONV=0.0
      A=3.14159*RP2**2
      A1=2.*3.14159*RP2*L1
      A2=2.*3.14159*RP2*L2
      QRAD=EEL*SB* ( ( (TTT1+273.)/ 100.)**4– ( (TAMB+273.)/ 100.
     * )**4)*A1
      QRAD=QRAD+EEL*SB* ( ( (TTT2+273.)/ 100.)**4– ( (TAMB+273.)/ 100.
     * )**4)* (A+A2)
      QCONV=HPO* (TTT1–TAMB)*A1
      QCONV=QCONV+ (TTT2–TAMB)* (A*HTOP+A2*HPO)
      QCONS=TK1*A* (TTT1–TSO (NS))/ DS
      QTOT2=QRAD+QCONV+QCONS
      WRITE (10, 640) HTOP, HPO, HIN
 640  FORMAT (/ 1X, 'HTOP', F10.4, ' HPO', F10.4, ' HIN', F10.4)
      WRITE (10, 600) QRAD, QCONV, QCONS, QTOT2
C
      QRAD=0.0
      QCONV=0.0
      DO 99 I=1, N1
      QRAD=–EE*SB*2*R (M1)* ( ( (TAMB+273.)/ 100.)**4– ( (T (I, M1)+273)
     * / 100.)**4)*DZ*3.14+QRAD
      QCONV=–HPO*2.*R (M1)*3.14* (TAMB–T (I, M1))*DZ+QCONV
 99   CONTINUE
      QTOT=QRAD+QCONV
 980  WRITE (10, 630) QRAD, QCONV, QTOT
      VL=3.14159*RE**2*LE*10.**6
      QUNI= (QTOT+QTOT2)/ VL
      WRITE (10, 968) QUNI
 968  FORMAT (/ 1X, ' QTOTAL/ S*Le =', E10.4, ' W/ CM**3')
C
      IF (S.EQ.1.) GO TO 540
      GO TO 550
 540  E=V/ LE
      MEAN=0.
      DO 700 I=1, N1
      DO 700 J=1, M1
 700  TMEAN=TMEAN+T (I, J)
      TMEAN=TMEAN/ (1.*M1*N1)
      EJR=0.1283*EXP (0.0431*TMEAN)+0.1460
      QGEN=S*ET*E*EJR
      E=E/ 100.
      QGEN1=QGEN/ 10.**6
      VL=3.14159*RE**2*LE
      QGEN=QGEN*VL
      QDIF=QGEN–QTOT–QTOT2
 625  FORMAT (1X, '  QDIFFERENCE=', F10.5)
 660  FORMAT (/ 1X, 'ELEMENT:', / 1X, 5HQRAD=, F10.4, 2X, 6HQCONV=, F10.4, 2X,
     * 6HQCOND=, F10.4, 2X, 8H QTOTAL=, F10.4)
 600  FORMAT (1X, 'ELECTRODE:', / 1X, 5HQRAD=, F10.4, 2X, 7H QCONV=, F10.4,
     * 2X, ' QCONS=', F10.4, 2X, 7HQTOTAL=, F10.4)
 630  FORMAT (1X, 'PORCELAIN:', / 1X, ' QRAD=', F10.4, ' QCONV=', F10.4,
     * ' QTOTAL=', F10.4)
 605  FORMAT (/ , 1X, 'E=', F10.2, 'V/ CM', 2X, ' EJR=', F10.4, 'A/ M**2', / 2X,
     * ' TMEAN', F10.4, ' DEGREE', 2X, ' QGEN1=', F12.5, ' W/ CM**3', 2X,
     * ' QGEN=', F10.4, ' W')
```

```
      TTIME=TIME/ 3600.
      EJR1=EJR*1000.*3.14159*RE**2
      K1=N1/ 2.
C
      WRITE (15, 220) TTIME
550   WRITE (15, 200) ( (T (I, J), J=1, M1), I=1, N1)
477   FORMAT (/ 1X, 'TS', 5F10.4)
400   FORMAT (1X/ 3H TT, 6 (2X, F12.4))
100   FORMAT (1X/ / 6H TIME=, F13.4)
200   FORMAT (1X, 1HT, 6 (2X, F10.4))
220   FORMAT (1X, 6HDTIME=, F9.6)
      CALL CONVH (HTOP, HPO, HIN)
      IF (T (1, 1).GT.65) GO TO 560
      IF (T (1, 1).GE.60.) DTIME=DTIME/ 2.
560   IF (TIME.GT.20941.0) GO TO 530
      GO TO 56
250   S=0.
      TMAX=TIME/ 3.
      GO TO 510
530   CONTINUE
      STOP
      END
C
C     SURFACE TEMPERATURE OF ELEMENT ANS ELECTRODE
C     *CONSIDERING HEAT CONDUCTION IN ELECTRODESC
      SUBROUTINE TSE (H)
      REAL LE, L1, L2
      COMMON / D1/ N, M, TAMB/ D2/ RE, LE
      COMMON / D/ T (50, 50), R (50)
      COMMON / D3/ CP, CP2, TK, DEN, DEN2/ D4/ TKAIR, SB
      COMMON / D5/ EE, EEL, TK2
      COMMON / D7/ ET, V, S/ D8/ DR, DZ, DTIME/ D9/ VL, QGEN
      COMMON N1, M1, I, J
      COMMON / D10/ TO (50, 50)
      J=M1
      A1=3.14159* (R (J)**2– (R (J)–DR/ 2.)**2)
      A2=3.14159* (R (J)–DR/ 2.)*2*DZ
C
C     BOTTOM  ELECTRODE
C
      I1=L1/ DZ
      DO 2 I=2, I1
      QCON1=TK2* (TO (I, J–1)–TO (I, J))/ DR*A2
      QCON2=TK2* (TO (I+1, J)–TO (I, J))/ DZ*A1
      QCON3=TK2* (TO (I–1, J)–TO (I, J))/ DZ*A1
      QCON4=TKAIR* (TTO (I, 1)–TO (I, J))*2*3.14159*DZ/ ALOG (RP1/ R (J))
      QCONV=H*2*3.14159*R (J)*DZ* (TTO (I, 1)–TO (I, J))
      QRAD=SB* ( ( (TTO (I, 1)+273.)/ 100.)**4– ( (TO (I, J)+273.)/ 100.)**4)
 *    / RA1
      QRAD=QRAD+SB* ( ( (TTO (I–1, 1)+273.)/ 100.)**4– ( (TO (I, J)+273.)/ 100.)
 *    **4)/ RA2
      QRAD=QRAD+SB* ( ( (TTO (I+1, 1)+273.)/ 100.)**4– ( (TO (I, J)+273.)/ 100.)
 *    **4)/ RA2
      VL=A1*DZ
      T (I, J)=DTIME/ DEN2/ CP2/ VL* (QCON1+QCON2+QCON3+QCON4+QCONV+QRAD
 *    )+TO (I, J)
2     CONTINUE
C
```

```
C        ELEMENT
C
         I2= (L1+LE)/ DZ
         DO 3 I=I1+1, I2
         QCON1=TK* (TO (I, J-1)-TO (I, J))/ DR*A2
         QCON2=TK* (TO (I+1, J)-TO (I, J))/ DZ*A1
         QCON3=TK* (TO (I-1, J)-TO (I, J))/ DZ*A1
         QCON4=TKAIR* (TTO (I, 1)-TO (I, J))*2*3.14159*DZ/ ALOG (RP1/ R (J))
         QCONV=H*2*3.14159*R (J)*DZ* (TTO (I, 1)-TO (I, J))
         QRAD=SB* ( ( (TTO (I, 1)+273.)/ 100.)**4- ( (TO (I, J)+273.)/ 100.)**4)
     *   / RA1
         QRAD=QRAD+SB* ( ( (TTO (I-1, 1)+273.)/ 100.)**4- ( (TO (I, J)+273.)/ 100.)
     *   **4)/ RA2
         QRAD=QRAD+SB* ( ( (TTO (I+1, 1)+273.)/ 100.)**4- ( (TO (I, J)+273.)/ 100.)
     *   **4)/ RA2
         VL=A1*DZ
         CALL QQ (E, EJR)
         T (I, J)=DTIME/ DEN/ CP/ VL* (QCON1+QCON2+QCON3+QCON4+QCONV+QRAD
     *   +QGEN)+TO (I, J)
 3       CONTINUE
         DO 4 I=I2+1, I2+L2/ DZ
         QCON1=TK2* (TO (I, J-1)-TO (I, J))/ DR*A2
         QCON2=TK2* (TO (I+1, J)-TO (I, J))/ DZ*A1
         QCON3=TK2* (TO (I-1, J)-TO (I, J))/ DZ*A1
         QCON4=TKAIR* (TTO (I, 1)-TO (I, J))*2*3.14159*DZ/ ALOG (RP1/ R (J))
         QCONV=H*2*3.14159*R (J)*DZ* (TTO (I, 1)-TO (I, J))
         QRAD=SB* ( ( (TTO (I, 1)+273.)/ 100.)**4- ( (TO (I, J)+273.)/ 100.)**4)
     *   / RA1
         QRAD=QRAD+SB* ( ( (TTO (I-1, 1)+273.)/ 100.)**4- ( (TO (I, J)+273.)/ 100.)
     *   **4)/ RA2
         QRAD=QRAD+SB* ( ( (TTO (I+1, 1)+273.)/ 100.)**4- ( (TO (I, J)+273.)/ 100.)
     *   **4)/ RA2
         VL=A1*DZ
         T (I, J)=DTIME/ DEN2/ CP2/ VL* (QCON1+QCON2+QCON3+QCON4+QCONV+QRAD
     *   )+TO (I, J)
 4       CONTINUE
         RETURN
         END
C
C        CENTRAL LINE TEMPERATURE OF ELEMENT & ELECTRODE
C        *CONSIDERING HEAT CONDUCTION IN ELECTRODES
C
         SUBROUTINE TCEN
         REAL LE
         COMMON / D1/ N, M, TAMB/ D2/ RE, LE
         COMMON / D/ T (50, 50), R (50)
         COMMON / D3/ CP, CP2, TK, DEN, DEN2/ D4/ TKAIR, SB
         COMMON / D5/ EE, EEL, TK2
         COMMON / D7/ ET, V, S/ D8/ DR, DZ, DTIME/ D9/ VL, QGEN
         COMMON N1, M1, I, J
         COMMON / D10/ TO (50, 50)
         J=1
         VL=1.0
         I1=L1/ DZ
         I2=L2/ DZ
C
C        BOTTOM ELECTRODE
C
```

```
      DO 35 I=2, I1
      T (I, J)=DTIME/ DEN2/ CP2* (TK2* ( (TO (I-1, J)-TO (I, J))/ DZ**2+
   *  (TO (I+1, J)-TO (I, J))/ DZ**2+4* (TO (I, J+1)-TO (I, J))/ DR**2))
   *  +TO (I, J)
35    CONTINUE
C
C     ELEMENT
      DO 36 I=I1+1, I1+N
      CALL QQ (E, EJR)
      T (I, J)=DTIME/ DEN/ CP* (TK* ( (TO (I-1, J)-TO (I, J))/ DZ**2+
   *  (TO (I+1, J)-TO (I, J))/ DZ**2+4* (TO (I, J+1)-TO (I, J))/ DR**2)+QGEN)
   *  +TO (I, J)
36    CONTINUE
C
C     TOP ELECTRODE
C
      DO 37 I=I1+N+1, I1+N+I2
      T (I, J)=DTIME/ DEN2/ CP2* (TK2* ( (TO (I-1, J)-TO (I, J))/ DZ**2+
   *  (TO (I+1, J)-TO (I, J))/ DZ**2+4* (TO (I, J+1)-TO (I, J))/ DR**2))
   *  +TO (I, J)
37    CONTINUE
      RETURN
      END
C
C     INTERIAL ELEMENT TEMPERATURE & ELECTRODE
C     *CONSIDERING HEAT CONDUCTION IN ELECTRODES
C
      SUBROUTINE TINTE
      REAL LE
      COMMON / D1/ N, M, TAMB/ D2/ RE, LE
      COMMON / D/ T (50, 50), R (50)
      COMMON / D3/ CP, CP2, TK, DEN, DEN2/ D4/ TKAIR, SB
      COMMON / D5/ EE, EEL, TK2
      COMMON / D7/ ET, V, S/ D8/ DR, DZ, DTIME/ D9/ VL, QGEN
      COMMON / D10/ TO (50, 50)
      COMMON N1, M1, I, J
      VL=1.0
      I1=L1/ DZ
      I2=L2/ DZ
C
C     BOTTOM ELECTRODE
C
      DO 44 I=2, I1
      DO 44 J=2, M
      T (I, J)=DTIME/ DEN2/ CP2* (TK2* ( (TO (I, J+1)-2*TO (I, J)
   *  +TO (I, J-1))/ DR**2
   *  + (TO (I+1, J)-2*TO (I, J)+TO (I-1, J))/ DZ**2+ (TO (I, J+1)-TO (I, J-1))/
   *  (2.*DR*R (J))))+TO (I, J)
44    CONTINUE
C
C     ELEMENT
C
      DO 45 I=I1+1, I1+N
      DO 45 J=2, M
      CALL QQ (E, EJR)
      T (I, J)=DTIME/ DEN/ CP* (TK* ( (TO (I, J+1)-2*TO (I, J)+TO (I, J-1))/ DR**2
   *  + (TO (I+1, J)-2*TO (I, J)+TO (I-1, J))/ DZ**2+ (TO (I, J+1)-TO (I, J-1))/
   *  (2.*DR*R (J)))+QGEN)+TO (I, J)
```

```
 45     CONTINUE
C
C       TOP ELECTRODE
C
        DO 46 I=I1+N+1, I1+N+I2
        DO 46 J=2, M
        T (I, J)=DTIME/ DEN2/ CP2* (TK2* ( (TO (I, J+1)-2*TO (I, J)
   *    +TO (I, J-1))/ DR**2
   *    + (TO (I+1, J)-2*TO (I, J)+TO (I-1, J))/ DZ**2+ (TO (I, J+1)-TO (I, J-1))/
   *    (2.*DR*R (J))))+TO (I, J)
 46     CONTINUE
        RETURN
        END
```

Appendix B

TEMPERATURE OF THE ENCLOSED AIR IN HOUSING

Valve element temperature of the single element test section shown in Fig. 5.3 was increased until it reached the same steady state max temperature of complete arrester by applying a suitable voltage to in it. The temperature variation of the valve element and the enclosed air in the test section housing were measured. The values are shown in Fig. B.1 and Table B.1.

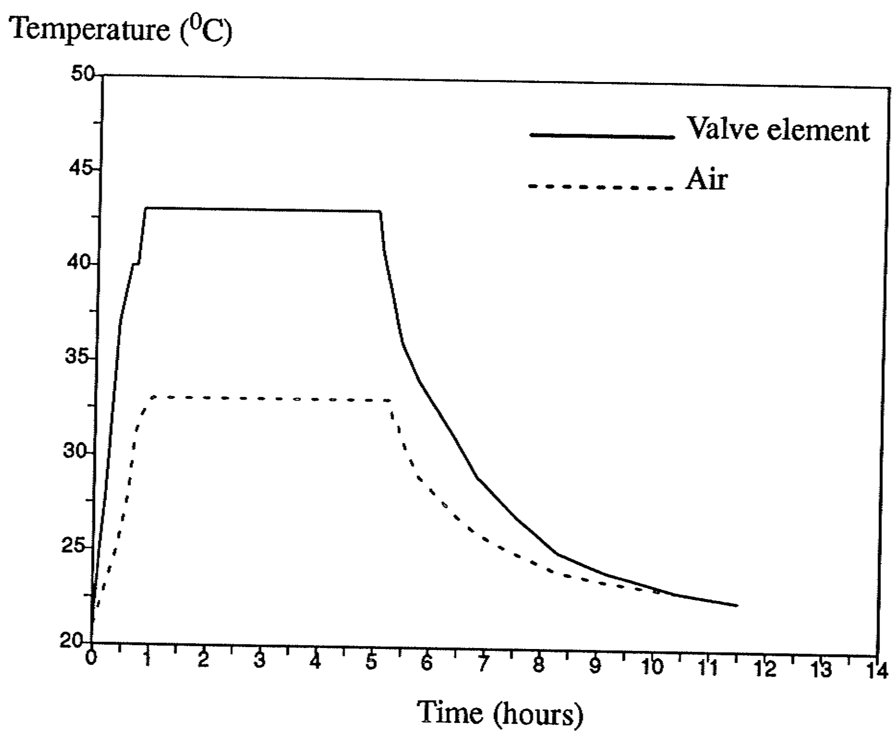

Figure B.1. Temperature variation with time (Measured)

Table B.1. Temperature of valve element and enclosed air in the test section housing (Measured)

Time (hours)	Applied voltage (kV)	Valve element temperature (^0C)	Air gap temperature between the element and housing (^0C)
(Heating)	3.2	21	21
0.1	3.3	25	22
0.2	3.4	28	23
0.4	3.4	37	25
0.6	3.1	40	28
0.7	3.2	40	31
0.8	3.02	43	32
1.	3.07	43	33
5 (Cooling begins)	0	43	33
5.08		41	33
5.15		40	33
5.23		39	33
5.3		38	32
5.37		37	32
5.45		36	31
5.77		34	29
6.43		31	27
6.83		29	26
7.5		27	25
8.3		25	24
9.15		24	23.5
10.4		23	23
11.5		22.5	22.5